TARGETED AUGER ELECTRON RADIOTHERAPY OF HER2-AMPLIFIED BREAST CANCER

By

DANNY L. COSTANTINI

A THESIS SUBMITTED IN CONFORMITY WITH THE REQUIREMENTS FOR THE DEGREE OF DOCTOR OF PHILOSOPHY
GRADUATE DEPARTMENT OF PHARMACEUTICAL SCIENCES
UNIVERSITY OF TORONTO

Your file Votre référence
ISBN: 978-0-494-59062-1
Our file Notre référence
ISBN: 978-0-494-59062-1

Abstract

Targeted Auger Electron Radiotherapy of HER2-Amplified Breast Cancer

Danny L. Costantini
Doctor of Philosophy, 2009
Graduate Department of Pharmaceutical Sciences
University of Toronto

Monoclonal antibodies (mAbs) conjugated to nuclear localization sequences (NLS) and labeled with Auger electron-emitters have great potential for targeted radiotherapy of cancer. This approach may be especially appropriate for the 25-30% of patients with breast cancer whose tumors display overexpression of HER2. Trastuzumab (Herceptin) is a humanized anti-HER2 mAb approved for immunotherapy of HER2-amplified breast cancer. The goal of this research was to radiolabel trastuzumab with ^{111}In, and to modify it with peptides harboring the NLS (CGYG*PKKKRKV*GG) of the simian virus 40 large-T antigen (*italicized*) for targeted radiotherapy of breast cancer. It was hypothesized that the NLS-peptides would mediate the translocation of covalently linked ^{111}In-trastuzumab molecules into the nuclei of HER2-overexpressing breast cancer cells where subcellular-range Auger electrons are most damaging to DNA and lethal to cells.

Trastuzumab was derivatized with sulfosuccinimidyl-4-(N-maleimidomethyl)-cyclohexane-1-carboxylate for reaction with NLS-peptides and labeled with ^{111}In using diethylenetriaminepentaacetic acid. The dissociation constant for binding of ^{111}In-NLS-trastuzumab to HER2-overexpressing SK-BR-3 human breast cancer cells was reduced < 3-fold compared to ^{111}In-trastuzumab, demonstrating relatively preserved receptor-binding affinity. The NLS-peptides did not affect the biodistribution of ^{111}In-trastuzumab, but promoted its nuclear uptake in HER2-overexpressing MDA-MB-361 xenografts. The cytotoxicity of ^{111}In-NLS-trastuzumab on breast cancer cells correlated with their HER2 expression. Moreover, ^{111}In-NLS-trastuzumab was 2-fold and 5-fold more potent at killing MDA-MB-361 and SK-BR-3 cells compared to ^{111}In-trastuzumab, and nearly 3-fold and 6-fold more effective than unlabeled

trastuzumab, respectively. Methotrexate is a known radiosensitizer that can amplify the lethal effects of ionizing radiation on tumor cells. Non-cytotoxic, but radiosensitizing doses of methotrexate were therefore combined with ^{111}In-NLS-trastuzumab; this enhanced the sensitivity of HER2-overexpressing breast cancer cells to ^{111}In-NLS-trastuzumab. The blood $t_{1/2}$ of ^{111}In-NLS-trastuzumab in non-tumor bearing BALB/c mice was 23-34 h when administered intravenously or intraperitoneally. The maximum tolerated dose was 9.2-18.5 MBq; doses >18.5 MBq caused decreased leukocyte and platelet counts. ^{111}In-NLS-trastuzumab exhibited strong anti-tumor effects against HER2-overexpressing MDA-MB-361 xenografts, reducing their growth rate 2-fold and 3-fold compared to mice administered ^{111}In-trastuzumab or unlabeled trastuzumab, respectively.

These promising results suggest that ^{111}In-NLS-trastuzumab may be a useful Auger electron radioimmunotherapeutic agent for HER2-positive breast cancer in humans.

Acknowledgments

First and foremost, I want to extend my utmost appreciation to Dr. Raymond Reilly for allowing me to pursue my PhD studies in his laboratory. Only my own father has shown me the same support and guidance that Ray has provided throughout the past four years, and for this I remain sincerely grateful to Ray. It is my hope that in the future, I will have the opportunity to collaborate further with Ray and the Laboratory of Medical Imaging and Targeted Radiopharmaceutics. I also want to extend my appreciation to Dr. Katherine Vallis for being able to serve on my supervisory committee, even after moving back to the UK. I am especially indebted to Dr. Vallis for recruiting me in the Excellence in the Radiation Research for the 21st Century strategic training program, and to Dr. Fei-Fei Liu for providing me with the valuable opportunity to benefit from this program. I also remain thankful to Dr. Christine Allen for her support and service on my supervisory committee, to Dr. Jean Gariépy for his valuable comments in committee meetings, and to Dr. Gerald DeNardo from the University of California, Davis, for coming to Toronto in January to serve as my external reader and examiner.

I am especially grateful to my many friends and colleagues for providing a stimulating and fun environment in which to learn and grow, especially Kristin McLarty, Conrad Chan, Deborah Scollard, Shaun Ramdhany, Emma Bahroos, Bart Cornelissen and Verlee Kersemans. Our times together were truly memorable. My studies were supported by the Canadian Institutes of Health Research, the Canadian Breast Cancer Foundation and the Leslie Dan Faculty of Pharmacy. They are gratefully acknowledged.

My deepest gratitude is to my parents Frank and Carla for their continuous love and support. They believed in me, supported me, and always encouraged me to pursue my dreams. To them I remain eternally grateful. My brother Frank (Jr.) definitely helped to make my skin a little thicker, and for that I am actually thankful. Finally, I want to thank the love of my life Daniela, for being my best friend, for listening to me as I thought out loud, and for providing comfort in both the good and hard times. Your love and caring made this endeavor worthwhile.

In Loving Memory of My Mother

Table of Contents

List of Tables

List of Figures

List of Abbreviations

% ID/g	Percent Injected Dose per Gram of Tissue
^{125}IUdR	5-[^{125}I]iodo-2'-deoxyuridine
^{18}FDG	2-[^{18}F]-fluoro-2-deoxy-D-glucose
5-FU	5-Fluorouracil
AC	Anthracycline-Cyclophosphamide
ADCC	Antibody-Dependent Cellular Cytotoxicity
ahx	Aminohexyl
ALT	Alanine Transaminase
AML	Acute Myeloid Leukemia
AMU	Atomic Mass Unit
ANOVA	Analysis of Variance
AUC	Area Under the Curve
BCIRG	Breast Cancer International Research Group
BCS	Breast Conserving Surgery
BMT	Bone Marrow Transplant
Bq	Becquerel
BRCA	Breast Cancer gene
BSA	Bovine Serum Albumin
BUN	Blood Urea Nitrogen
BWI	Body Weight Index
CD	Cluster of Differentiation
CDC	Complement-Dependent Cytotoxicity
CDK	Cyclin-Dependent Kinase
CDR	Complementary Determining Region
CEA	Carcinoembryonic Antigen
Ci	Curies
CMF	Cyclophosphamide, Methotrexate, 5-Fluorouracil
cpm	Counts Per Minute
CR	Complete Remission

Cr	Creatinine
CT	Computer Tomography
CTA	Clinical Trial Application
DAPI	4,6-diamidino-2-phenylindole
DCIS	Ductal Carcinoma *In Situ*
DFS	Disease Free Survival
DHFR	Dihydrofolate Reductase
DNA	Deoxyribose Nucleic Acid
DOTA	1,4,7,10-tetraazacyclododecane-1,4,7,10-tetraacetic acid
dTMP	Deoxythymidine-5′-monophosphate
DTPA	Diethylenetriaminepentaacetic Acid
EC	Electron Capture
EC_{50}	Effective Concentration 50%
ECD	Extracellular Domain
EGFR	Epidermal Growth Factor Receptor
EGP	Epithelial Glycoprotein
ELISA	Enzyme-Linked Immunosorbent Assay
ErbB	Erythroblastosis oncogene
eV	Electron Volt
Fab	IgG Fragment: Antigen-Binding Region
FBS	Fetal Bovine Serum
Fc	IgG Fragment: Constant Region
FDA	Food and Drug Administration
FdUrd	5-fluoro-2'-deoxyuridine
FISH	Fluorescence *In Situ* Hybridization
γH2AX	Gamma Histone 2AX
GMP	Good Manufacturing Practices
H&E	Hematoxylin and Eosin
HAMA	Human Anti-Mouse Antibody
HER	Human Epidermal Growth Factor Receptor

HERA	HERceptin Adjuvant
hIgG	Human IgG
HIV	Human Immunodeficiency Virus
HRP	Horse Radish Peroxidase
HU	Hydroxyurea
IHC	Immunohistochemistry
IGF-I	Insulin-like Growth Factor I
IGF-IR	Insulin-like Growth Factor I Receptor
IGFBP-3	Insulin-like Growth Factor Binding Protein 3
IgG	Immunoglobulin Gamma
IMP	Importin
i.p.	Intraperitoneal
ITLC-SG	Instant Thin-Layer Chromatography Silica-Gel
i.v.	Intravenous
Kd	Equilibrium Dissociation Constant
kDa	Kilo Dalton
LCIS	Lobular Carcinoma *In Situ*
LET	Linear Energy Transfer
mAb	Monoclonal Antibody
MAPK	Mitogen-Activated Protein Kinase
MDR	Multi-Drug Resistant
MTD	Maximum Tolerated Dose
MTX	Methotrexate
NADH	Nicotinamide Adenine Dinucleotide
NHL	Non-Hodgkin Lymphoma
NK	Natural Killer
NLS	Nuclear Localizing Sequence
NPC	Nuclear Pore Complex
NSABP	National Surgical Adjuvant Breast and Bowel Project
ORR	Objective Response Rate

OS	Overall Survival
PAGE	Polyacrylamide Gel Electrophoresis
PAS	Periodic-Acid Schiff
PASM	Periodic Acid Silver Methenamine
PBS	Phosphate Buffered Saline
pCR	Pathologic Complete Response
PDK	Phosphoinositide-Dependent Kinase
PDSA	Pyridyl Disulfide Acrylate
PET	Positron Emission Tomography
p.i.	Post Injection
PI3K	Phosphatidylinositol 3' kinase
PIP2	Phosphatidylinositol-4,5-bisphosphate
PIP3	Phosphatidylinositol-3,4,5-trisphosphate
PKB	Protein Kinase B
PR	Partial Remission
PTEN	Phosphatase and Tensin Homolog
RBC	Red Blood Cells
RER	Radiation Enhancement Ratio
RIT	Radioimmunotherapy
RNA	Ribonucleic acid
RNAi	RNA interference
RTK	Receptor Tyrosine Kinase
s.c.	Subcutaneous
scFv	Single Chain Variable Region Fragment
SDS	Sodium Dodecyl Sulfate
SEM	Standard Error of the Mean
SMCC	Succinimidyl-4-(N-maleimidomethyl)-cyclohexane-1-carboxylate
SSTR	Somatostatin Receptor
SV-40	Simian Virus 40
T/B	Tumor-to-Blood ratio

T/N	Tumor-to-Normal Tissue ratio
TAT	Transactivator of Transcription
TCH	Taxane-Carboplatin-Herceptin
TDLU	Terminal Ductal-Lobular Unit
TFO	Triplex-Forming Oligodeoxynucleotides
TGF	Transforming Growth Factor
TGI	Tumor Growth Index
TNM	Tumor, Node, Metastasis
TOC	Tyr_3-Octreotide
UdR	Deoxyuridine
VEGF	Vascular Endothelial Growth Factor
VH	Variable region of the immunoglobulin, Heavy chain
VL	Variable region of the immunoglobulin, Light chain
WBC	White Blood Cells

CHAPTER 1

INTRODUCTION

1.1 The incidence, diagnosis and management of breast cancer

1.1.1 Breast cancer epidemiology and etiology

Breast cancer is the most common epithelial cancer diagnosed in North American women and is second only to lung cancer as the cause of cancer-related deaths. It is estimated that over 200,000 women in the U.S. and 20,000 women in Canada are diagnosed with breast cancer each year (*1,2*). Despite advances in early detection and intervention over the past few decades, about 20% of women diagnosed with breast cancer will eventually die from the disease. The chance of being diagnosed with breast cancer increases with age with an overall lifetime risk of approximately 1 in 8 for a woman by age 85 years. Other known risk factors for the development of the disease include ethnicity, estrogen exposure, radiation exposure, family history and genetic predisposition (e.g. mutations in BRCA1 and BRCA2 genes), and lifestyle factors, such as obesity, alcohol consumption, and lack of exercise (*3*).

The mammary gland is the functional structure of the female breast. In adults, each mammary gland is composed of fifteen to twenty lobes, divided by adipose tissue. Each lobe is subdivided into lobules, which contain the glandular alveoli that secrete the milk of a lactating female. The clustered alveoli secrete milk into a series of secondary tubules. These tubules converge to form a series of mammary ducts, which in turn converge to form a lactiferous duct that drains at the tip of the nipple. It is generally believed that most breast cancers (approximately 75%) occur within the terminal ductal-lobular unit (TDLU), consisting of the lobule and its adjacent ducts (*3*). However, there is still not complete agreement as to whether breast cancer originates as a disease of a single cell, whose progeny spread through a single duct system and accumulate multiple genetic changes toward malignant transformation, or as a cluster of genetically unstable cells and ducts that are simultaneously involved (*4*). Although the vast majority of invasive breast cancers are sporadic in nature, the risk of developing the disease does appear to increase when atypical ductal hyperplasia, atypical lobular hyperplasia, lobular neoplasia, and lobular or ductal carcinoma *in situ* (LCIS or DCIS) are discovered (*5*).

1.1.2 Diagnosis and treatment of breast cancer

After a diagnosis of breast cancer is confirmed, the treatment chosen is primarily based on the stage of the disease and pathologic features such as receptor status and tumor grade.

Disease stage is determined using the TNM staging system that was established by the International Union against Cancer and accepted by the American Joint Commission on Cancer Staging. The TNM classification characterizes breast cancer by three criteria at diagnosis, including: tumor size (T), the number and location of lymph nodes involved (N), and the presence or absence of distant metastatic disease (M) (*6*). Stage 0 (T_{is}, N_0, M_0), the earliest stage, represents *in situ* cancer, and stage IV (any T, any N, and M_1) represents the most advanced form of breast cancer. The purposes of staging are to: i) plan a therapeutic strategy that is most appropriate for the patient, and ii) allow for more intelligent prognostication of the disease status of the patient (*6*). In patients without metastatic disease, prognosis is heavily dependent upon the number of axillary lymph nodes involved, the size of the primary tumor, and pathologic features such as its histological grade (*7*). The grading system assesses the mitotic activity of the cell population, the level of differentiation of the cells, their pleomorphism, and their architectural differention (*8*).

Management of breast cancer involves multiple disciplines such as diagnostic imaging, pathology, surgery, radiation therapy and medical oncology (*3*). For an individual patient, the choice of treatment depends on the clinical stage of the disease, as well as factors such as the woman's age, general health, and personal preferences (*6*). In most situations, patients are treated with surgery followed by single or a combination of multiple adjuvant local and systemic therapies (*3*).

Ductal carcinoma *in situ* (DCIS) represents the earliest stage of breast cancer (stage 0). These lesions generally have a good prognosis and may be successfully treated with breast conserving surgery (BCS) with or without post-operative local radiotherapy (*6*). The addition of tamoxifen has also been shown to reduce recurrence in estrogen receptor (ER)-positive DCIS patients treated with lumpectomy with or without radiation therapy (*9*). For other early stage I and II breast cancers, the preferred treatment is BCS and dissection of the axillary lymph nodes. In some cases, however, a modified radical mastectomy may be necessary (*10*). To further reduce the risk of local recurrence, patients may receive radiation therapy to the remaining breast tissue or chest wall, and draining lymph nodes after definitive surgery (*10*). Adjuvant chemotherapy or hormonal therapy in these disease settings has been shown to reduce the risk of breast cancer recurrence by 30-50% (*3*).

For large operable breast tumors (stage IIIA, and operable stage IIIC), neoadjuvant doxorubicin-based or taxane-based chemotherapy is the preferred option for initial treatment (*11*). This permits observation for tumor responsiveness to the chosen regimen and allows some patients to subsequently undergo BCS. The sentinel lymph node is often sampled at surgery to determine if breast cancer has metastasized to axillary lymph nodes and whether further nodal dissection is required (*12*). For patients treated initially with mastectomy, adjuvant therapy using an anthracyline-based or taxane-based regimen is recommended (*11*). Another commonly used adjuvant chemotherapeutic regime includes a combination of cyclophosphamide, methotrexate and 5-fluorouracil (CMF) (*13*). Tamoxifen further improves the survival of ER-positive patients when combined with chemotherapy, however, this has largely been replaced by the new generation nonsteroidal aromatase inhibitors (i.e., anastrozole and letrozole) which are at least as effective as tamoxifen and better tolerated (*14*). Postoperative radiation therapy is also generally employed after the completion of chemotherapy, but it is preferable to delay breast reconstruction until after the completion of local radiation therapy for women treated with mastectomy (*11*).

When breast cancer is inoperable (stage IIIB, inoperable stage IIIC) but has not spread to distant sites, patients are treated with systemic chemotherapy with or without tamoxifen (*11*). In some cases, neoadjuvant chemotherapy may shrink the tumor and render it suitable for BCS or mastectomy. Patients with breast cancer metastasis to organ systems outside the breast and adjacent lymph nodes, such as the bones, lungs, liver, or brain, carry the diagnosis of stage IV or advanced breast cancer (*6*). Advanced breast cancer is associated with a median survival of 2-3 years after diagnosis, and the prognosis is dependent on the site of organ metastasis, with visceral involvement carrying a worse prognosis (*3*). Treatment of the majority of patients with advanced breast cancer is considered palliative in nature. Systemic therapy is the primary treatment, using chemotherapy, endocrine therapy, or both, depending upon the hormone responsiveness of the tumor. Surgery is occasionally used in conjunction with radiotherapy, chemotherapy and hormone therapy to improve local control and provide relief from symptoms. Therapy with trastuzumab alone or in combination with chemotherapy is an option for women whose cancer cells have high levels of the HER2 protein. Trastuzumab has been shown to

prolong time-to-progression as well as survival in this group of patients when used in combination with chemotherapy or endocrine therapy (*15*).

1.2 Treatment of HER2-overexpressing breast cancer with trastuzumab (Herceptin)

1.2.1 The biology of HER2 and its importance in breast cancer

The importance of the HER2 proto-oncogene in cancer was established when it was discovered that 25-30% of human breast cancers have overexpression of HER2, and that these cancers have worse biologic behavior and prognosis (*16*). HER2 is a member of the ErbB protein family of receptors which consists of three other receptor tyrosine kinases (RTKs) with similar homology: HER1 (also referred to as epidermal growth factor receptor [EGFR], or ErbB1), HER3 (ErbB3) and HER4 (ErbB4) (*16*). The HER receptors are located at the cell membrane and share similar structure, comprising of an extracellular ligand-binding domain, a lipophilic transmembrane region, and cytoplasmic domain with tyrosine kinase activity. HER2 itself is a 185 kDa RTK, and is encoded by a gene that is located on the long arm of chromosome 17 (17q21) (*16*). In foetal tissues, HER2 is widely expressed and is critically important for normal development (*17*). In adult tissue, however, HER2 is minimally expressed in breast epithelium and in the ovaries, endometrium, central nervous system, skin, bone, muscle, heart, kidney, and gastrointestinal tract (*17*). The normal physiological role of HER2 in adult tissues is not completely understood, but it appears to have a role in normal cell function by regulating growth and proliferation in epithelial cells (*18*).

Ligand binding induces either homodimer formation between two identical HER receptors, or heterodimer formation between two different HER family receptors (*16*). HER2, unlike the other HER-family receptors, is considered an “orphan receptor” as it lacks an endogenous ligand, but it preferentially partners with the other members of the family to enhance ligand-induced signaling (*19*). Dimerization activates the tyrosine kinase activity of the intracellular domain, which subsequently triggers the signaling cascades leading to cell proliferation and growth (*19*).

The importance of HER2 in cancer was realized in the early 1980s when a mutationally activated form of its rodent homolog *neu* was identified in a search for oncogenes in a carcinogen-induced rat tumorigenesis model (*20*). *Neu* was found to be mutated in transforming cDNAs derived from rat neuroglioblastomas following exposure to ethylnitrosurea (*20*). A single point mutation (valine to glutamic acid) in neu caused the tyrosine kinase domain of the receptor to become constitutively activated, and subsequently conferred oncogenic transformation (*21*). Although such mutations in the transmembrane domain have not been found in the *HER2* gene in human tumors (*21*), HER2 was later found to be amplified in numerous breast cancer cell lines (*22*). Overexpression of HER2 is a combined result of increased transcription and protein translation. Indeed, breast cancer cells may have as many as 100 copies of the gene per cell compared with two copies of the HER2-gene in normal cells (*23*). Moreover, there are approximately 20 thousand receptors per cell on normal cells, but breast cancer cells may contain as many as 500 thousand to 2 million HER2 receptors per cell (*24*). At this high level of HER2 receptor expression, the kinase activity of HER2 becomes constitutively activated which appears to exert potent mitogenic and transforming effects on cells (*24*). Histopathologically, overexpression of HER2 in breast cancer is associated with large tumor size, lymph node involvement, high histologic grade, high S-phase fraction, and lack of hormone receptors (*25*). Clinically, overexpression of HER2 is directly associated with increased risk of relapse and poor long-term survival in breast cancer (*25*).

1.2.2 Natural immunoglobulins and recombinant antibodies

Antibodies that target antigens on the surface of cancer cells have been used to treat patients with a variety of malignancies, including breast cancer. Antibodies, or immunoglobulins (Ig), are complex proteins that are produced by plasma B-lymphocytes, and occur naturally as part of the immune system of mammals by recognizing antigens in a “lock and key” fitting model (*26*). When activated, lymphocytes will proliferate and differentiate into plasma cells, and the resulting antibody response is polyclonal. The most prevalent antibody isotype in humans is Ig gamma (IgG), which comprises approximately 85% of the immunoglobulin in serum. Human IgG is comprised of two antigen-binding fragments (Fab’s) and a constant region (Fc), linked via a flexible disulfide-bridged hinge region. These regions are part of two pairs of polypeptide chains - two identical heavy chains (H) and two identical

light chains (L) - held together by the disulfide linkages and folded into compact globular domains forming a "Y" shaped molecule. Two light chain (e.g. κ or λ) and four heavy chain variants (e.g. 1, 2, 3 and 4) exist in humans, each with a molecular weight of approximately 25 kDa and 55 kDa, respectively. Each heavy and light chain has a similar structure, and each contain constant and variable regions. The main differences observed in the variable regions are located in three small hyper-variable sequences that are located in the N-terminal regions of the light and heavy chains (i.e. Fab domain). These regions are responsible for antigen binding and are referred to as the complementary determining regions (CDR) (*27*).

Since the development of hybridoma technology, it is possible to generate antibodies specifically directed against tumor-associated antigens by immunizing mice with these target proteins, isolating the B-lymphocytes and fusing these with murine myeloma cells. Following selection of the hybridoma of interest, murine monoclonal antibodies (mAbs) can then be expressed into the cell culture and purified for subsequent use (*28*). Murine mAbs were thus the first clinically applied antibodies. A major disadvantage was the production of human antimouse antibodies (HAMAs) that could mediate the humoral immune response (*28*). The HAMA response can create problems such as an allergic-like reaction to the mouse antibody and rapid clearance of the mouse antibody from circulation (*28*). Re-treatment is also less likely to be successful with murine mAbs because of the higher likelihood of developing an immune response when receiving the mouse antibody for the second time (*28*). In order to reduce the immunogenicity of murine mAbs, recombinant DNA techniques were applied to produce chimeric and humanized mAbs (*26*). In chimeric mAbs, the variable regions of heavy and light chains are of murine origin, and these are then fused with the constant regions of human origin. In humanized mAbs, only the CDR of the murine origin is grafted into a human antibody framework. To improve *in vivo* targeting properties, new antibody constructs have been produced using recombinant DNA techniques (e.g. scFv, minibodies, diabodies and affibodies) (*26*). However, the high renal uptake and low tumor accumulation of these molecules does not make them suitable for radiotherapeutic applications (*29*).

1.2.3 Recombinant monoclonal antibody trastuzumab (Herceptin)

Given the critical importance of HER2 in some forms of breast cancer, extensive research has focused on HER2 inhibitors as potential anticancer agents. Trastuzumab

(Herceptin®, Genentech, Inc., San Francisco, CA), for example, is currently the only HER2-targeted therapeutic agent that has received marketing clearance from the U.S. Food and Drug Administration (FDA) and Health Canada for use in the treatment of patients with HER2-overexpressing breast cancer (*24*). Trastuzumab is a humanized mAb that binds specifically to HER2 on the C-terminal portion of the extracellular domain (ECD) near the juxtamembrane region in domain IV of the receptor (*30*). Trastuzumab was constructed by grafting the complementary-determining regions (CDRs) from the murine mAb 4D5 into a human kappa IgG_1 to avoid eliciting a human anti-mouse antibody (HAMA) response in patients (*31*).

1.2.4 Clinical trials with trastuzumab

The efficacy and safety of trastuzumab as a single agent were evaluated in two phase II clinical trials in women with HER2-overexpressing metastatic breast cancer who had progressed after one or two chemotherapeutic regimens (*32,33*). In these trials, trastuzumab was administered intravenously as a loading dose of 4 mg/kg, followed by weekly doses of 2 mg/kg. The objective response rate (ORR) was defined as the total percentage of complete and partial remissions (CR and PR, respectively), and were 11.6% (*32*) and 15% (*32,33*) in these two trials, whereas the median duration of response was 9.1 months (*33*). The most serious adverse effect was cardiac dysfunction. This was an unexpected finding that occurred in 4.7% of treated patients, many of whom had previously received doxorubicin, suggesting that trastuzumab may have exacerbated pervious myocardial damage induced by the anthracycline treatment (*32,33*). The efficacy of trastuzumab was therefore evaluated in another trial in HER2-positive metastatic breast cancer patients who had not been treated previously with chemotherapy (*34*). Breast cancer specimens were assayed by immunohistochemical (IHC) staining for HER2 protein, or by fluorescence *in situ* hybridization (FISH) for HER2-gene amplification. Strong IHC staining (i.e. a score of 3^+) was defined as complete membrane staining in more than 10% of tumor cells with either 4D5 or CB11 anti-HER2 mAbs. The ORR was 35% for patients with HER2-overexpressing tumors at the 3^+ level, and 34% for those with HER2-gene amplification. This was nearly double than the ORR that was reported in previous trials (*32,33*), possibly because patients with moderate (score 2^+) staining tumors, which generally do not respond well to trastuzumab, were included in the earlier studies (*35*). Cardiac dysfunction occurred in two

patients (2%) (*34*). However, both had histories of cardiac disease and did not require additional intervention after discontinuation of trastuzumab (*34*).

In a pivotal randomized phase III trial, Slamon et al. (*36*) showed that the addition of trastuzumab to chemotherapy (doxorubicin plus cyclophosphamide [AC] or single-agent paclitaxel) for patients with HER2-overexpressing metastatic breast cancer (ICH score 2^+ and 3^+) produced a longer time to disease progression, a higher ORR, and a longer median overall survival (OS) compared to chemotherapy alone (OS; 25.1 months versus 20.3 months, respectively). However, cardiotoxicity was more common with the combined treatment, especially in women treated previously or concurrently with AC. These results led to the recommendation that concomitant anthracyclines and trastuzumab be avoided, and clinical trials are currently under way to evaluate the safety and efficacy of trastuzumab combined with other non-anthracycline containing trastuzumab-based regimes (*35*). For example, combination therapies with trastuzumab and cisplatin, paclitaxel/carboplatin, docetaxel, vinorelbine or gemcitabine have shown promising results in various clinical studies (*35*).

The efficacy of trastuzumab has also been evaluated in the adjuvant setting. For example, investigators from the National Surgical Adjuvant Breast and Bowel Project (NSABP)-31 and the North American Intergroup randomized node-positive, HER2-positive breast cancer patients to adjuvant chemotherapy (AC plus paclitaxel) with or without trastuzumab (*37*). The absolute difference in disease-free survival (DFS) between the trastuzumab group and the control group was 12% at 3 years (87.1% versus 75.4%, respectively), and the addition of trastuzumab reduced the mortality rate by one third (*37*). The HERceptin Adjuvant (HERA) trial is an ongoing study comparing one or two-year trastuzumab with observation alone after standard neoadjuvant or adjuvant locoregional therapy in women with HER2-positive, node-positive or high-risk node negative breast cancer (*38*). DFS at 3 years was higher for the trastuzumab group compared to observation alone (87% versus 81%, respectively), however, longer follow-up is needed for a definitive result for OS (*38*). The Breast Cancer International Research Group trial (BCIRG 006) is also currently investigating the role of docetaxel with or without trastuzumab after adjuvant AC, versus the taxane-carboplatin-herceptin (TCH) regime (*15*). In a preliminary report (*15*), DFS was significantly better in both the trastuzumab-containing arms in comparison to AC followed by docetaxel, but

a significant difference between the two trastuzumab-containing arms was not detected. Notably, there were fewer severe cardiac events with TCH compared to either of the AC-containing regimens (*15*).

Several studies have also evaluated the role of neo-adjuvant trastuzumab therapy in patients with early-stage HER2-positive breast cancer. In the study by Buzdar et al. (*38*), HER2-positive breast cancer patients were preoperatively assigned to chemotherapy (four cycles of paclitaxel followed by four cycles of fluorouracil, epirubicin and cyclophosphamide) with or without trastuzumab. The pathologic complete response (pCR) rates were 25% and 65% for chemotherapy and trastuzumab plus chemotherapy, respectively. This study was stopped early because of the clear superiority of trastuzumab plus chemotherapy (*39*). Although no cardiac related side-effects have been detected (*40*), long-term safety and efficacy data are needed before trastuzumab is applied widely to patients with early-stage disease.

1.3 The mechanisms of action of trastuzumab

The effectiveness of trastuzumab appears to correlate with the level of HER2 expression in breast cancer, and with the accessibility of tumors to the drug (*35*). To date, however, the mechanism by which trastuzumab induces regression of HER2-overexpressing tumors is not completely understood, but several molecular and cellular effects have been observed in experimental *in vitro* and *in vivo* models.

1.3.1 Immune-mediated response

One of the proposed mechanisms of trastuzumab anti-tumor action is through antibody-dependent cellular cytotoxicity (ADCC) (*41-43*). Specifically, the natural killer (NK) cell is important for the ADCC response to trastuzumab (*24*). These cells express the Fc_{γ} receptor that bind the Fc domain of the IgG_1 trastuzumab antibody, and promote lyses of trastuzumab-bound cancer cells. The importance of this immunological effect was revealed by Clynes et al. (*39*), who achieved a tumor regression rate of 96% in mice bearing HER2-overexpressing BT-474 xenografts treated with trastuzumab, but only a 26% reduction in tumor growth in mice lacking the Fc_{γ} receptor. Nonetheless, the fact that there was still a response in mice lacking the Fc_{γ} receptor indicates that mechanisms in addition to activating ADCC are likely responsible for

trastuzumab anti-tumor effects. Preoperative administration of trastuzumab has also been reported to increase tumor infiltration by lymphoid cells, and enhance ADCC activity in patients with HER2-positive breast tumors (*40*). Thus, an active immune response may contribute significantly to trastuzumab efficacy.

1.3.2 Inhibition of angiogenesis

Both primary and metastatic breast cancer are dependent on angiogenesis for tumor growth (*41*). Trastuzumab can modulate different pro- and antiangiogenic factors to achieve angiogenesis suppression. For example, HER2-positive mouse mammary tumors treated with trastuzumab showed increased expression of the antiangiogenic factor thrombospondin-1, and reduced expression of vascular endothelial growth factor (VEGF) and transforming growth factor-α (TGF-α) which normally act to promote angiogenesis (*42-44*). A further finding from the study by Izumi et al. (*42*) was that trastuzumab caused the tumor vasculature of human breast cancer xenografts to revert to a more normal appearance. For example, vessels in control tumors were dilated and leaky, whereas those in trastuzumab-treated tumors had diameters and vascular permeability closer to those of normal vessels. Klos et al. (*43*) further demonstrated in mice bearing HER2-transfected MDA-MB-435 (435.eB) breast cancer xenografts, that combined trastuzumab plus paclitaxel treatment more effectively inhibited HER2-mediated angiogenesis than either treatment alone, which resulted in more pronounced tumoricidal effects. Trastuzumab-induced normalization of the tumor vasculature might also enhance the killing of cancer cells by improving the delivery and efficacy of other therapeutic agents (*43*).

1.3.3 Inhibition of HER2-ECD cleavage

The extracellular domain (ECD) of HER2 can be released by proteolytic cleavage from the full-length receptor, yielding a 110-kDa fragment that can be detected *in vitro* in cell culture medium, and a 95-kDa amino-terminally truncated membrane-associated fragment with increased kinase activity (*30*). The HER2-ECD can also be detected *in vivo* in serum, and is currently measured in the clinic with an FDA approved ELISA-based test to follow-up and monitor patients with metastatic breast cancer (*45*). Molina et al. (*46*) demonstrated in HER2-overexpressing SK-BR-3 and BT-474 human breast cancer cells that trastuzumab can block metalloprotease-mediated cleavage of the HER2-ECD. Moreover, several clinical studies have

demonstrated that a decline in serum HER2-ECD during trastuzumab treatment correlates with improved tumor responsiveness and progression-free survival (*47,48*), which indirectly supports the hypothesis that trastuzumab may act by inhibiting HER2 cleavage (*49*) .

1.3.4 Inhibition of the PI3K pathway

Overexpression of HER2 receptor tyrosine kinases leads to ligand-independent homodimerization and autophosphorylation of tyrosine residues on the cytoplasmic domain of the receptors (*50*). Phosphatidylinositol 3' kinase (PI3K) associates with these phosphorylated tyrosine residues and activates downstream effectors, such as phosphoinositide-dependent kinase (PDK) and protein kinase B (PKB), by phosphorylating phosphatidylinositol-4,5-bisphosphate (PIP2) to form phosphatidylinositol-3,4,5-trisphosphate (PIP3), which ultimately leads to enhanced protein synthesis, cell proliferation, survival and motility (*50*). The lipid phosphatase and tensin homolog (PTEN) is a key tumor suppressor protein that can translocate to the plasma membrane and oppose the activation of the PI3K-PKB pathway by dephosphorylating PIP3. The non-receptor tyrosine kinase Src is also recruited to the plasma membrane by phosphorylated tyrosines, and can inhibit the phosphatase activity and growth-inhibitory effects of PTEN. A proposed mechanism of action of trastuzumab was described by Nagata et al. (*50*), who demonstrated that the interaction between HER2 and Src tyrosine kinase is disrupted in response to trastuzumab treatment, leading to inactivation of Src with subsequent activation of PTEN. This in turn leads to rapid PKB dephosphorylation and inhibition of cell proliferation.

1.3.5 Inducing G1 arrest by modulating the expression of $p27^{kip1}$

Cyclin-D/cyclin-dependent kinase (Cdk)-4 and cyclin-E/Cdk2 complexes are regulated by a group of proteins known as Cdk inhibitors, and are pivotal in regulating the progression of cells though the G1-S phase of the cell-cycle (*51*). Lane et al. (*52*), demonstrated that treatment of HER2-overexpressing SK-BR-3 and BT-474 cell lines with trastuzumab caused a reduction in the expression of proteins involved in the intracellular sequestration of the Cdk inhibitor $p27^{kip1}$, including cyclin D1. Trastuzumab has also been shown to inhibit the ubiquitin-mediated degradation of $p27^{kip1}$ (*53*). These processes promote the release and accumulation of $p27^{kip1}$,

allowing it to bind and inhibit cyclin E/Cdk2 complexes, resulting in G1 cell-cycle arrest (*52,53*).

1.4 The development of resistance to trastuzumab

The majority of patients who achieve an initial response to trastuzumab generally become refractory within a year, due to the emergence of resistance (*33,34*). Elucidating the molecular mechanisms by which tumors escape trastuzumab-mediated cytotoxicity is critical to improving the survival of women with HER2-positive metastatic breast cancer. Multiple mechanisms contributing to trastuzumab resistance have been proposed.

1.4.1 Disrupted interaction between HER2 and trastuzumab

Although somatic mutations in the region of the *HER2* gene encoding the ECD of the receptor have not been reported (*24*), such mutations and deletions might potentially result in a decreased ability of trastuzumab to bind HER2. Indeed, Anido et al. (*54*) demonstrated that trastuzumab was ineffective *in vivo* for controlling tumor growth in mice inoculated with T47D breast cancer cells stably transfected with a C-terminal truncated form of HER2. Alternatively, the lack of epitope accessibility for trastuzumab on HER2 due to masking may limit its effectiveness. For example, Nagy et al. (*55*) demonstrated that elevated levels of MUC4, a membrane-associated mucin which consists of several highly glycosylated proteins that form protective barriers on epithelial cells, contributes to trastuzumab resistance in JIMT-1 breast cancer cells by masking the trastuzumab binding epitopes of HER2. The JIMT-1 cell line was established from a patient with trastuzumab-refractory HER2-positive breast cancer (*55*). The cell-surface expression level of MUC4 was inversely correlated with the ability of trastuzumab to bind HER2. However, downregulation of MUC4 expression by RNA interference (RNAi) restored trastuzumab binding and increased the sensitivity of JIMT-1 cells to trastuzumab (*55*).

HER2-targeted mAbs have been shown to bind to circulating HER2-ECD and decrease the level of antibodies available to bind to membrane-bound HER2, suggesting that elevated levels of HER2-ECD in the serum of patients may also limit the efficacy of trastuzumab (*56*). Indeed, one study demonstrated improved disease-free survival in patients with at least a 20% decline in circulating HER2-ECD levels within the first few weeks of trastuzumab-based therapy compared to those whose ECD levels did not drop (*57*). Thus, monitoring circulating

HER2-ECD levels may be a very useful tool in predicting early and overall response to trastuzumab-based therapies (*57*).

1.4.2 Increased ErbB-receptor signaling

Although trastuzumab reduces HER2-mediated signaling, it might not reduce signaling mediated through other HER receptors (*24*). For example, heterodimerisation of HER2 with other receptors of the erbB2-family can be induced by ligands of HER1, HER3 and HER4, and in the presence of an excess of ligands, the resulting heterodimers may initiate mitogenic signaling even in the presence of trastuzumab (*24*). Indeed, increased levels of the ErbB family ligands EGF and heregulin blocked trastuzumab-mediated growth inhibition of HER2-overexpresssing breast cancer cell lines, and this inhibition was associated with increased signaling from HER2/HER1(EGFR) and HER2/HER3 complexes (*58,59*). Valabrega et al. (*60*) compared tumor tissue from patients with advanced HER2-positive breast cancer before and after trastuzumab treatment, and observed a strong increase in TGF-α production upon disease progression, suggesting a possible role of EGFR signaling by TGF-α as mediator of acquired resistance to trastuzumab. Indeed, these authors found that trastuzumab was less efficient at inhibiting the growth of HER2-positive SK-BR-3 cells engineered to overexpress TGF-α compared to the parental cells (*60*). Trastuzumab-resistant variants of BT-474 cells isolated from tumor xenografts in mice similarly exhibited increased mRNA for TGF-α, EGF and EGFR, and upregulated total and phosphorylated EGFR levels, whereas HER2 expression was unchanged (*61*). Interestingly, the EGFR tyrosine kinase inhibitors erlotinib and gefitinib, and the dual EGFR/HER2 inhibitor, lapatinib, were able to induce apoptosis in cultured trastuzumab-resistant cells, suggesting that EGFR amplification is a plausible mechanism of acquired resistance to trastuzumab (*61*). Indeed, EGFR overexpression has been correlated clinically with disease progression in patients receiving trastuzumab (*62*).

1.4.3 Increased insulin-like growth factor-I (IGF-I) receptor signaling

The insulin-like growth factor I (IGF-I) receptor (IGF-IR) is a transmembrane tyrosine kinase receptor that is frequently overexpressed in human breast cancers. IGF-IR activation stimulates mitogenic signaling pathways involved in cell proliferation and metastasis (*63*). Overexpression of IGF-IR has also been shown to confer resistance to the growth-inhibitory

actions of trastuzumab. For example, Lu et al. (*64*) demonstrated that trastuzumab activity was significantly reduced in HER2-overxpressing SK-BR-3 human breast cancer cells transfected with the *IGF-IR* gene (SK-BR-3/IGF-IR) compared to non-transfected cells. However, resistance to trastuzumab in SK-BR-3/IGF-1R cells was reversed in the presence of the IGF-IR antagonist IGF-binding protein-3 (IGFBP-3), which binds and sequesters IGF-I ligands. Similar results were obtained with HER2-transfected MCF-7 human breast cancer cells (MCF-7/HER2-18) that naturally overexpress IGF-IR; these cells were growth-inhibited by trastuzumab only if IGF-IR were blocked by anti-IGF-IR (α-IR3) mAbs or IGF-I was sequestered by IGFBP-3 (*64*).

In another study, exposure of trastuzumab-resistant MCF-7/HER2-18 and SK-BR-3/IGF-IR cells to recombinant human IGFBP-3 inhibited IGF-IR phosphorylation and enhanced killing by trastuzumab (*65*). Moreover, BT-474 cells with trastuzumab resistance (BT-474/HerR) acquired through serial passage in the presence of the drug, displayed elevated IGF-IR levels (3- to 5-fold) when compared with their trastuzumab-sensitive counterparts (BT-474) (*70*). Importantly, this study showed that inhibition of IGF-IR signaling *in vivo* by administration of IGFBP-3 improved the anti-tumor effects of trastuzumab in athymic mice bearing subcutaneous MCF-7/HER2-18 xenografts. While 56% of mice treated with trastuzumab and IGFBP-3 exhibited no tumor growth or regression, only 6% receiving trastuzumab alone responded (*65*).

Crosstalk between IGF-IR and HER2 has also been shown to occur uniquely in trastuzumab-resistant cells (*22*). For example, Nahta et al. (*65*), developed an *in vitro* model of trastuzumab-resistance by chronic exposure of SK-BR-3 cells to trastuzumab, and found that these cells exhibited a more rapid IGF-I mediated stimulation of downstream PI3K/PKB and mitogen-activated protein kinase (MAPK) pathways relative to parental cells. Moreover, IGF-IR was shown to physically interact and promote the phosphorylation and activation of HER2 in trastuzumab-resistant SK-BR-3 cells (*65*). This could be inhibited, however, by the IGF-IR neutralizing mAb α-IR3, or by the IGF-IR tyrosine kinase inhibitor I-OMe-AG538. IGF-IR signaling has also been shown to antagonize the trastuzumab-induced increase of the Cdk inhibitor $p27^{kip1}$, which results in a loss of cell growth arrest, even in the presence of

trastuzumab (*66*). Thus, increased IGF-IR expression, or reduced $p27^{kip1}$ levels, may serve as predictive markers for trastuzumab resistance (*22*).

The importance of IGF-IR in mediating resistance of breast cancer to trastuzumab in patients nevertheless remains unresolved. One study found no relationship between IGF-IR expression and patient outcome in trastuzumab-based therapies (*73*), whereas another (*62*) found a significant correlation between IGF-IR and S6 ribosomal protein phosphorylation in tumors with poor response to trastuzumab, despite HER2 amplification.

1.4.4 Loss of PTEN

Nagata et al. (*74*), suggested an important role for decreased expression of PTEN in conferring trastuzumab resistance. They demonstrated that a reduction of PTEN protein levels caused by exposure to antisense oligodeoxynucleotides rendered trastuzumab-sensitive SK-BR-3 and BT-474 breast cancer cells resistant to trastuzumab. This resistance could be overcome, however, with pharmacological inhibitors of PI3K. They further demonstrated in patients with HER2-overexpressing breast tumors that the absence of PTEN expression was associated with much poorer response to trastuzumab-based therapy than in those with normal PTEN (*74*). These results suggest that PTEN loss could serve as a predictor of trastuzumab resistance, and that PI3K-targeted therapies could overcome trastuzumab-resistance in patients with tumors expressing low levels of PTEN (*24*).

1.5 Targeted *in situ* radioimmunotherapy of malignancies

Radioimmunotherapy (RIT) is a branch of molecular medicine in which an antibody is used to deliver a therapeutic radionuclide to a tumor-associated antigen in order to selectively kill cancer cells. To achieve specific tumor uptake and minimize normal tissue accumulation, the antigenic epitope must be expressed uniquely, or at least preferentially, on cancer cells compared with normal cells (*29*). RIT differs from conventional external beam radiation in that RIT is a form of systemically delivered and targeted radiotherapy. The anti-tumor effect of RIT is primarily due to the radioactivity delivered by the antibody to tumor cells, which provides continuous, exponentially decreasing, low-dose-rate radiation that is sufficient to cause lethal DNA damage in cancer cells (*29*). One advantage of RIT is that the antibody itself may also

contribute to tumor cell killing by eliciting ADCC and/or CDC (*29*). Several factors that are critical in developing an effective RIT regimen include the selection of an optimal radionuclide; identification of a promising tumor-associated antigen; and the design of an antibody-radionuclide immunoconjugate with high specificity and low immunogenicity (*29*).

1.5.1 Radionuclides used for RIT

Radionuclides which may be conjugated to antibodies for RIT of malignancies include alpha (α)-emitters (e.g. ^{211}At, ^{213}Bi or ^{225}Ac), beta (β)-emitters (e.g., ^{131}I or ^{90}Y) or low-energy Auger and internal conversion (IC) electron emitters (e.g., ^{111}In, ^{123}I, ^{125}I, ^{99m}Tc and ^{67}Ga) (*67*). α-emitters are radionuclides that contain a proton to neutron ratio that exceeds that for stable elements of similar atomic number. Emission of an α-particle (i.e., two protons and two neutrons identical to a helium nucleus with a mass of two atomic mass units [AMU]) reduces the repulsive forces between the positively charged protons, and brings the decaying radionuclide to a more stable configuration. In β-decay, a neutron in an unstable atomic nucleus that has an excess of neutrons is converted to a proton, and a β-particle (i.e., an electron with a single negative charge and mass that is 1/1837th of an AMU) is emitted as well as an antineutrino. In some radionuclides that have an excess of protons (e.g., ^{11}C, ^{13}N, ^{15}O, ^{18}F, ^{64}Cu, ^{68}Ga, ^{124}I), a decay process can occur in which a proton is converted into a neutron by emission of a positron (i.e. an electron that has a single positive charge) and a neutrino. Auger electrons are emitted by radionuclides that decay by electron capture (EC). In EC, a proton in the nucleus captures an inner orbital electron, decreasing the number of protons by one, and creating a vacancy in the shell. An electron from a higher energy level may decay to fill the vacancy, resulting in a release of energy. Although sometimes this energy is released in the form of an emitted γ-photon, the energy can also be transferred to an outer orbital electron, which is ejected from the atom. This second ejected electron is called an Auger electron. The EC decay process causes the release of a shower of Auger electrons of discrete but low energies that travel nanometer to micrometer distances in tissues (i.e., less than one cell diameter) (*67*). Internal conversion (IC) electrons are created by collision of photons (from the nuclear decay) with inner shell electrons that are ejected.

The range of β-particles in tissue is much longer than for α-particles or Auger electrons, but is directly proportional to their energy. For example, the range in tissue of the β-particles emitted by ^{131}I ($E_\beta = 0.6$ MeV) is about 2 mm, while the range of the β-particles emitted by ^{90}Y ($E_\beta = 2.3$ MeV) is 12 mm (*67*). β-particles transfer their energy to the surrounding matter over a long distance (several millimeters). Moreover, β-particles deposit most of their energy at the end of their track length (Bragg peak), and are therefore considered to be low linear energy transfer (LET) radiation. This property makes them most suitable for treating tumors with a diameter of 2-12 mm (200-1200 cell diameters) since for smaller tumors, most of the radiation energy would be deposited outside the target volume due the Bragg peak phenomenon (*67*). Nevertheless, the long range β-particles addresses the issue of heterogeneity in tumor uptake of the radionuclides, since radioactivity targeted to tumor cells can also kill neighboring non-targeted cells within striking distance of the β-particles ("cross-fire" effect) (*67*). In contrast, the high energy emissions of α-particles (4 to 9 MeV) are directly deposited over a short distance in tissue (4 to 9 μm) resulting in high LET. Auger electrons have very low energies (<30 keV). However, because Auger electrons travel very short distances in tissue (nanometer-to-micrometer distances), their energy deposition approaches that of α-emitters (4-26 keV/μm) (*67*). Auger electrons are therefore considered to be high LET radiation. IC electrons have discrete energies in the keV range. This energy is higher than that of most Auger electrons, but lower than that of the β-particles, such as those emitted by ^{131}I or ^{90}Y. For therapeutic purposes the decay of an Auger electron-emitting radionuclide should ideally occur inside the cell nucleus to have the strongest lethal effect against cancer cells. The short path length and consequent high LET of α-particles and Auger electrons have therefore been proposed as ideal for the treatment of small tumor deposits, micrometastatic disease, and for eradication of malignant single cells (*67*).

1.5.2 Current status of radioimmunotherapy in the clinic

The only radiolabeled antibodies currently with FDA approval for the treatment of cancer are ^{90}Y-ibritumomab tiuxetan (Zevalin®, IDEC Pharmaceuticals Corporation, San Diego, CA, USA) and ^{131}I-tositumomab (Bexxar®, Corixa Corporation, Seattle, WA, USA) (*68*). Bexxar is the murine IgG_1 mAb B1 labeled ^{131}I, whereas Zevalin is the murine $IgG_1\kappa$ mAb Y2B8 covalently linked to the radiometal chelator isothiocyanatobenzyl MX-DTPA (tiuxetan)

and labeled with ^{90}Y (*67*). Each radioimmunoconjugate is approved for treatment of chemotherapy-refractory non-Hodgkin's lymphoma (NHL), and both agents target the CD20 antigen, a 35-kDa transmembrane glycoprotein that is abundantly expressed on a high percentage (>95%) of both normal and malignant B-cells, but not on early progenitor B cells in the bone marrow. Encouraging results have been reported at low radiation absorbed doses (25-45 cGy to the whole body), and at higher doses (65-75 cGy to the whole body) with bone marrow support (*69*). In several phase III clinical trials, the efficacy of Bexxar and Zevalin were evaluated in patients with chemo-refractory, low-grade or transformed NHL (Bexxar study), or with relapsed/refractory low-grade, follicular or transformed NHL (Zevalin study) (*70*). In the Bexxar study, the ORR was greater in patients receiving RIT with Bexxar (1.7-7.8 GBq; ORR: approximately 65%) whereas only 28% of patients responded to chemotherapy (*70*). In the Zevalin study, the ORR was significantly higher for patients receiving RIT with Zevalin (14.8 MBq/kg, maximum dose of 1.4 GBq; ORR: approximately 80%) than for patients treated with rituximab (Rituxan; Roche Pharmaceuticals) a non-radiolabeled chimeric anti-CD20 mAb or chemotherapy alone (ORR: approximately 56%), thus demonstrating that the response to immunotherapy of NHL may be enhanced by incorporation of a therapeutic radionuclide (*70*).

Zevalin and Bexxar represent the most successful forms of RIT described to date. However, other radioimmunoconjugates being tested clinically could potentially improve responses or expand indications in patients with NHL. For example, radiolabeled epratuzumab (humanized anti-CD22 IgG; Immunomedics, Inc., Morris Plains, NJ, USA) and Oncolym (anti-HLA-DR10; Peregrine Pharmaceuticals, Inc., Tustin, CA, USA) have shown promising anti-tumor effects in patients with aggressive forms of NHL (*71*). Encouraging results have also been achieved in the treatment of acute myeloid leukemia (AML) using ^{131}I- or ^{90}Y-labeled anti-CD33 mAb M195, or its humanized IgG_1 analogue, HuM195 (*72*). Indeed, RIT with myeloablative doses of ^{90}Y-HuM195 elicited potent antileukemic effects in patients, suggesting that RIT with ^{90}Y-HuM195 may be useful if incorporated into a bone marrow transplant (BMT) preparatory regimen (*72*).

1.5.3 Anti-HER2 RIT of breast cancer and other malignancies

HER2 is an attractive target for systemic RIT of breast cancer due to the high levels of expression of this receptor on tumor cells compared to normal cells, and because of the

promising results that have already been achieved with non-radiolabeled forms of anti-HER2 mAbs (i.e. trastuzumab) (*73*). DeSantes et al. (*82*) was the first to examine ^{131}I-labeled mAb 4D5 in beige/nude mice being subcutaneous NIH3T3/HER2 murine fibroblast allografts. Treatment with ^{131}I-4D5 was 20-fold more effective than a similarly radiolabeled control antibody in delaying tumor growth, and was 75-fold more effective than unlabeled 4D5. The main limitation found with ^{131}I-4D5, however, was its rapid intracellular dehalogenation by deiodinases, and the subsequent export of radioiodine from the cell (*75*). Due to the *in vivo* limitations of radioiodinated antibodies, Tsai et al. (*74*) used the bifunctional chelate DOTA to conjugate 4D5 to the radiometals ^{111}In or ^{90}Y. Compared to halogens, radiometals conjugated to biomolecules such as antibodies have a comparably longer intracellular retention, probably because of the formation of charged radio-catabolites that have difficulty in penetrating the cell membrane. Indeed, in distribution studies, ^{111}In-labeled 4D5 obtained a higher maximum tumor uptake compared to ^{131}I-4D5 in mice bearing MCF7/HER2 breast cancer xenografts (30% ID/g versus 17% ID/g) (*74*). Moreover, the radioactivity that was required to achieve maximum tumor growth inhibition was 4-fold lower for ^{90}Y-4D5 compared to ^{131}I -4D5 (100 μCi versus 400 μCi, respectively). However, tumor re-growth occurred within 20 days, suggesting that higher doses or multiple treatments may be needed in order to increase the therapeutic efficacy of these ^{90}Y-labeled HER2 antibodies (*74*).

Trastuzumab has also been conjugated with several short range α-emitting radionuclides. For example, Zhang et al. (*75*) and Akabani et al. (*76*) conjugated the α-emitter ^{213}Bi or ^{211}At to trastuzumab using the metal chelator DTPA that complexes ^{213}Bi, or by direct conjugation of N-succinimidyl-3-[^{211}At]astatobenzoate, respectively, and they demonstrated the ability of these agents to specifically target and kill HER2-overexpressing breast cancer cells *in vitro*. Interestingly, the cytotoxic effect of ^{213}Bi-trastuzumab has also been demonstrated for HER2-overexpressing LNCaP-LN3 and DU-145 human prostate cancer cells (*77*). Similarly, Milenic et al. (*87*) labeled trastuzumab with ^{213}Bi using the acyclic chelator CHX-A"-DTPA, and evaluated the effectiveness of this agent for treating mice bearing LS-174T human colon carcinoma xenografts that overexpress HER2. Median survival was increased from 20 days for saline-treated mice to 60 days for mice treated with a single intraperitoneal dose of ^{213}Bi-CHX-

A"-trastuzumab (750 μCi [27.8 MBq]). Doses >1 mCi (37 MBq) caused a significant reduction in body weight (> 20%), indicating that the maximum-tolerated dose (MTD) had been reached.

Ballangrud et al. (*78*), used trastuzumab labeled with the α-particle emitter, ^{225}Ac, and demonstrated its efficacy in killing HER2-positive human breast cancer spheroids (MCF7, MDA-MB-361 and BT-474 cell lines) with increasing receptor expression. ^{225}Ac emits four α-particles per decay, as well as daughter decay products that are themselves α-emitters (^{221}Fr, ^{217}At, ^{213}Bi, or ^{213}Po) or β-emitters (^{213}Bi, ^{209}Tl, or ^{209}Pb). The *in vivo* use of ^{225}Ac is therefore limited by the availability of a chelating agent able to stably bind these daughter radionuclides which tend to redistribute and cause significant normal tissue radiotoxicity following decay of the parent ^{225}Ac radionuclide (*89*).

Studies have also exploited ^{212}Pb as an *in vivo* generator of the α-emitter ^{212}Bi, and have clearly showed the feasibility of this radionuclide for targeted α-particle RIT of HER2-overexpressing malignancies (*79-81*). For example, Horak et al. (*79*) conjugated anti-HER2 AE1 mAbs to ^{212}Pb using a bifunctional derivative of tetraazacyclododecane tetraacetic acid (p-SCN-Bz-DOTA), and evaluated the efficacy of these radioimmunoconjugates in athymic mice bearing HER2-overexpressing SK-OV-3 human ovarian tumor xenografts growing within the peritoneal cavity. Prolongation of survival was obtained after intraperitoneal injection of ^{212}Pb-DOTA-AE1, whereas intravenous injection caused only a modest delay in the progression of small tumors (<15 mm^3). Dose-limiting hematopoietic toxicities associated with circulating large amounts of ^{212}Pb-AE1 mAbs in the blood limited the effectiveness of this agent in the therapy of larger tumors, suggesting that it may be most useful in the adjuvant setting for eradicating micrometastatic disease (*79*).

Milenic et al. (*81*) continued the evaluation of systemic RIT targeting HER2 with ^{212}Pb-trastuzumab in athymic mice bearing LS-174T colon cancer xenografts. Compared to the untreated control group, a single dose of ^{212}Pb-trastuzumab (10 μCi) increased the median survival of tumor-bearing mice from 3 to 8 weeks. More recently, the same group enhanced the efficacy of ^{212}Pb-trastuzumab RIT by combining the radiopharmaceutical with the chemotherapeutic agent gemcitabine or paclitaxel, suggesting that regimens combining chemotherapeutics with high-LET targeted therapy may have potential in the management and treatment of HER2-positive colon cancer patients (*80,82*).

1.5.4 Radioimmunotherapy of solid tumors

Despite the success of RIT in patients with advanced lymphohematopoietic malignancies (as discussed in section 1.5.2), the treatment of patients with solid tumors has been limited due to a 3-fold lower radiosensitivity of these malignancies compared to hematological cancers (*83*). RIT of solid tumors is also severely limited by the irradiation and killing of normal cells, such as bone marrow stem cells, by the moderate energy and long-range (2-10 mm) β-particles emitted by radionuclides such as ^{131}I or ^{90}Y that have been commonly conjugated to radiotherapeutic agents ("cross-fire" effect) (*83*). Studies of RIT in breast cancer have primarily been performed with antibodies specific for tumor-specific antigens such as L6 (a 24 kDa surface protein), carcinoembryonic antigen (CEA), and mucin-1 (MUC1) (*84*). Using ^{131}I or ^{90}Y-labeled antibodies to these antigens, doses of up to 20 to 40 Gy have been delivered to breast cancer metastases (*84*). Although these radiation doses have been high enough to cause tumor regressions, they have not been sufficient alone to consistently cause durable remissions (*84*). Moreover, the major dose-limiting side effect in these investigations has been myelotoxicity caused by the persistently high circulating levels of radiolabeled mAbs perfusing the bone marrow (*95,94*).

1.6 Auger electron radiotherapy

Auger electron-emitting radionuclides, such as ^{125}I and ^{111}In, represent an appealing alternative to β-particle emitters for targeted radiotherapy of cancer (*85*). These radionuclides emit low-energy Auger electrons that dissipate their energy within nanometer distances from the decaying atom (*85*). Most Auger electrons have an energy of < 30 keV and a very short, subcellular pathlength (2-12 μm) in tissues (*85*). These properties render Auger electron-emitting radionuclides highly cytotoxic and damaging to DNA when internalized into the cytoplasm and particularly when they are imported into the cell nucleus (*86*). Decay of an Auger electron-emitting radionuclide outside the cell or at the cell surface delivers an insufficient dose of radiation to cause radiotoxicity (*86*). The selective toxicity of Auger electron emitters toward cells that can bind and internalize the radionuclide could minimize, or even eliminate the non-

specific radiotoxicity against bone marrow stem cells that was previously observed with β-emitters in RIT (*87*).

One of the most widely studied Auger electron-emitting radiopharmaceuticals is ^{125}I-iododeoxyuridine (^{125}I-UdR), a radiolabeled thymidine analog that is transported into cells and incorporated directly into DNA during the synthesis phase of the cell cycle (*87*). *In vitro*, ^{125}I-UdR has been shown to be highly toxic in Chinese hamster V79 cells, and can produce extensive DNA damage in these cells (*88,89*). This is mainly due to the high LET associated with the emission of Auger electrons and the consequent efficient yield of double-strand breaks within DNA induced both by direct and indirect mechanisms (i.e. formation of reactive radicals such as $OH^{\cdot}$, $H^{\cdot}$ and e^{-} (aq) that bind and alter nucleotide structure in DNA) (*90*).

^{125}I-UdR has limitations as a *systemically* administered radiotherapeutic agent for several reasons (*91*). The first relates to the extremely short biological half-life ($t_{1/2}$) of ^{125}I-UdR in blood ($t_{1/2}$ of minutes in humans) (*91*). The second involves its extensive hepatic deiodination in the liver. The third concerns the apparent lack of specificity of ^{125}I-UdR for tumor cells, and its dependency on cell-cycle because the radiopharmaceutical is incorporated into DNA only during the S-phase of cell growth (*91*). Nevertheless, investigators have been examining the efficacy of direct introduction of ^{125}I-UdR into the targeted area. For example, loco-regional administration of ^{125}I-UdR has been examined in a rat intracerebral 9L gliosarcoma model (*92*) and a rat intrathecal TE671 human rhabdomyosarcoma model of neoplastic meningitis (*93*). In the rat intracerebral 9L gliosarcoma model, the median survival of animals infused for 34 hours with 6.9 MBq ^{125}I-UdR was significantly longer than that of control animals treated with the stable analog ^{127}I-UdR (approximately 80% survival versus 20% survival at 20 days after intracerebral injection of ^{125}I-UdR and ^{127}I-UdR, respectively) (*92*). In rats with the intrathecal human rhabdomyosarcoma model of neoplastic meningitis, the median time to onset of hind-leg paralysis is about 20 days (*95*). However, for tumor-bearing rats infused intrathecally with ^{125}I-UdR (7.4 MBq every other day, 6 administrations), the median time to onset of paralysis was 36 days (*104*). Within the cell, ^{125}I-UdR is phosphorylated by thymidine kinase to ^{125}I-UdR-monophosphate (^{125}I-dUMP) before being incorporated into DNA. Since MTX is an effective inhibitor of thymidylate synthetase (TS, dehalogenates ^{125}I-dUMP to dUMP), its presence is hypothesized to enhance ^{125}I-UdR uptake by DNA-synthesizing cells and augment its

cytotoxicity following loco-regional administration (*104*). Indeed, the co-administration of methotrexate (MTX, 31 μg) further enhanced the therapeutic potential of ^{125}I-UdR, and delayed the onset of hind-leg paralysis to 47 days, compared to 29.5 days for MTX alone (*104*).

^{125}I-UdR has also been administered to human patients with brain, breast, colorectal, or gastrointestinal cancers (intratumorally); ovarian cancer (intraperitoneally); bladder cancer (intravesically); or liver metastases from colorectal cancer (through the hepatic artery using a permanent intra-arterial catheter) (*91*). In patients with breast cancer, preliminary studies have shown that high values for tumor incorporation of ^{125}I-UdR can be achieved by direct intratumoral injection. For example, the mean fraction of injected dose (ID) incorporated by breast cancers is 0.025% ID/g, but this corresponds to an average tumor-to-non-tumor and tumor-to-blood ratios of 147 and 32.7, respectively (*91*). Nevertheless, direct intratumoral injection does not appear to be practible for therapy trials in humans with breast cancer, both because of inhomogeneous diffusion within the tumor mass (*91*) and the need for a systemic treatment to address occult metastatic disease.

1.6.1 Targets for Auger electron radiotherapy

Many different molecular targets overexpressed by cancer cells have been exploited for Auger electron radiotherapy using mAbs, peptides as well as small molecules labeled with ^{111}In, ^{99m}Tc, ^{123}I or ^{125}I (*67*).

1.6.1.1 Somatostatin receptors (SSTR)

The ^{111}In-labeled octapeptide somatostatin analog octreotide (^{111}In-DTPA^{0}-octreotide, pentetreotide; OctreoScan® Mallinckrodt Medical, Hazelwood, MO) is routinely used as an imaging agent for somatostatin receptor (SSTR)-positive tumors (*94*). *In vitro*, ^{111}In-DTPA^{0}-octreotide binds specifically and with high affinity to $SSTR_2$, a seven-membrane-spanning, G-protein-coupled receptor that is frequently overexpressed on the cell surface of certain neuroendocrine tumors, such as pituitary tumors, endocrine pancreatic tumors, carcinoids, paragangliomas, small-cell lung cancers, medullary thyroid carcinomas, and pheochromocytomas (*95*). ^{111}In-DTPA^{0}-octreotide has shown prolonged retention times in human carcinoid and gastrinoma cells, with approximately 50% of the internalized radioligand being retained by these cells after 42 hours (*96*). Interestingly, electron microscopic

autoradiographs of SSTR-positive tumor cells incubated with ^{111}In-DTPA^{0}-octreotide have revealed that the radioligand internalizes and accumulates in the cytoplasm as well as the nucleus (*96*). ^{111}In-DTPA^{0}-octreotide has shown extremely high tumor-to-normal tissue ratios of up to 1500:1 in patients with carcinoid and endocrine pancreatic tumors (*96*), and ultrastructural autoradiography of midgut carcinoid tumor specimens excised from patients who were administered the radiopharmaceutical has revealed the presence of internalized radioactivity in the nucleus of tumor cells (*99*). The close proximity of ^{111}In to the tumor-cell DNA, therefore, suggests that ^{111}In-DTPA^{0}-octreotide could also function as an Auger electron-emitting radiopharmaceutical for the treatment of SSTR-overexpressing tumors (*97*). Indeed, Slooter et al. (*98*) studied the radiotherapeutic effect of ^{111}In-DTPA^{0}-octreotide in a rat model of hepatic metastasis and found that the administration of 370 MBq of the radiopharmaceutical resulted in a significant reduction in the number of liver metastases in the SSTR-positive tumor model, but not in the SSTR-negative tumors.

Based on these promising results, clinical trials have been conducted to investigate ^{111}In-DTPA^{0}-octreotide for the systemic radionuclide therapy of neuroendocrine tumors (*99,100*). In one study, 50 patients with SSTR-positive neuroendocrine tumors were treated with multiple doses (6-7 GBq; 40-50 μg) of ^{111}In-DTPA-octreotide administered every 2 weeks up to a total amount of 20-160 GBq (*100*). Anti-tumor effects were achieved in 21 of 40 evaluated patients, with 1 partial remission, 6 minor remissions, and a stabilization of disease in 14 patients. Despite these encouraging results, further evaluation with ^{111}In-DTPA-octreotide showed only rare cases of tumor regression, possibly owing to the heterogenous uptake of the radioligand in tumor tissues, which may limit its therapeutic efficacy (*103*).

1.6.1.2 Epidermal Growth Factor Receptor (EGFR)

The internalization and nuclear translocation of the EGFR has been exploited as a means of introducing Auger electron-emitting ^{111}In-labeled EGF (^{111}In-DTPA-hEGF) to the nucleus of breast cancer cells (*101,87*). Chen et al. (*104*), found that ^{111}In-DTPA-hEGF possessed strong anti-tumor effects when administered to athymic mice bearing EGFR-positive MDA-MB-468 human breast cancer xenografts. The tumor growth rate was reduced approximately 3-fold in mice treated with ^{111}In-DTPA-hEGF (total, 92.5 MBq; 17 μg), compared to normal saline-treated mice (*104*). These results were attributed to the rapid translocation of ^{111}In-DTPA-hEGF

into the nucleus of breast cancer cells following its receptor-mediated endocytosis, where nearly 10% of internalized ^{111}In-DTPA-hEGF was bound by chromatin (*87*). On a molar concentration basis, the radiopharmaceutical was nearly 85 to 300 times more toxic to MDA-MB-468 cells (IC_{50} < 70 pM), compared to several chemotherapeutic agents commonly used for breast cancer, such as paclitaxel, methotrexate, or doxorubicin (IC_{50} 6 nM, 15 nM, and 20 nM, respectively), several logarithms more potent than 5-fluorouracil (IC_{50} 4 μM) and provided cytotoxic effects equivalent to those of 4 Gy of γ-radiation (*102*).

1.6.1.3 Human Epidermal Growth Factor Receptor 2 (HER2)

Michel et al. (*103*) demonstrated > 99% killing of HER2-overexpressing SK-BR-3 cells *in vitro* by incubation with increasing concentrations (up to 18.5 MBq/mL) of a mixture of ^{111}In-labeled anti-HER2 mAbs 21.1 and 4D5 (the murine analogue of trastuzumab) and mAbs against epithelial glycoprotein-2 (EGP-2). Use of a mixture of these mAbs increased the amount of ^{111}In bound to the cells compared to targeting with single mAbs. Cytotoxicity of the ^{111}In-labeled HER2 mAbs was similarly observed for SK-OV-3.ip3 human ovarian carcinoma cells with high HER2 density, but their survival could not be eliminated completely; this was attributed to partial radioresistance of these cells since a similar level of ^{111}In targeting as on SK-BR-3 cells was found (*103*). In contrast, minimal cytotoxic effects (surviving fraction, 77%–79%) were observed with ^{111}In-labeled non-specific MN-14 and MOPC-21 mAbs or with unlabeled mAb 4D5. Interestingly, 4D5 labeled with ^{131}I, was equally as effective at killing SK-OV-3.ip3 cells as ^{131}I-labeled non-specific Abs (MN-14 or MOPC-21) (*103*). These results illustrated that the crossfire effect from the β-particles substantially contributes to the cytotoxic effects; demonstration of the specificity of cell killing *in vitro* is thus much more difficult than for antibodies labeled with subcellular-range Auger electron-emitters. In a follow-up *in vivo* study, Mattes and Goldenberg (*104*) reported significantly prolonged survival in mice bearing s.c. SK-OV-3 tumor xenografts treated with 59 MBq of ^{111}In-4D5 compared to mice receiving the same dose of an irrelevant control mAb. At a slightly higher and more toxic dose (68 MBq) which caused death in 2 of 9 mice, cures were obtained in 5 of 7 surviving mice. No examination of the effects of treatment with these or lower amounts of ^{111}In-labeled HER2 mAbs on bone marrow, liver or kidney function was performed (*104*).

1.6.1.4 Estrogen Receptor (ER)

The ER can enter the cell nucleus and associate with distinct response elements in the DNA when ligand bound (*105*). Several studies have, therefore, investigated the possibility of targeting ER-positive breast cancer cells with ER-specific ligands (i.e., estrogen, 17-β-estradiol, or tamoxifen) labeled with ^{123}I or ^{125}I (*106-110*). For example, Beckmann et al. (*106*) showed that DNA strand breaks were produced in ER-positive MCF-7 breast cancer cells incubated *in vitro* with 16-α-^{125}I-iodo-17-β-estradiol (^{125}I-E2). The surviving fraction of the MCF-7 cells was decreased 5-fold by exposure to < 0.2 MBq/mL of ^{125}I-E2, whereas the surviving fraction of an ER-negative MCF-7 subclone was not effected (*106*). Similarly, DeSombre et al. (*108*) showed that the estradiol analogue, 2-^{123}I-iodo-1,1-bis-(4-hydroxyphenyl)-2-phenylethylene (^{123}I-BHPE) (8.9 MBq/pmole) was selectively toxic *in vitro* to Chinese hamster ovary (CHO) cells transfected with the ER gene after only a short incubation time of 30-60 minutes. In a subsequent study, a 2-logarithm decrease in the tumorigenicity of MCF-7 cells *in vivo* in athymic mice was found if the cells were pre-treated with the estradiol analogue, E-17-α-^{125}I-iodovinyl-11-β-methoxyestradiol (^{125}I-VME2) (*111*).

1.6.1.5 Other antigens or receptors in solid tumors

MAbs labeled with ^{125}I and recognizing other epithelial-derived antigens have been studied for Auger electron radiotherapy of colon cancer (*112,113*). MAbs A33 and CO17-1A, for example, recognize cell-surface epitopes and accumulate in cytoplasmic vesicles that traverse the cytoplasm and come into close proximity to the cell nucleus (*114,115*). Both ^{123}I-labeled A33 and CO17-1A effectively inhibited the growth of s.c. SW1222 or GW-39 colon cancer xenografts in athymic mice (*112,116*). The MTD for ^{125}I-A33 and ^{125}I-CO17-1A were 185 Mq and 111 MBq, respectively; these were approximately 10-to-20-fold higher than for ^{131}I-labled A33 and CO17-1A (11 MBq and 4 MBq, respectively) (*112,116*). At equitoxic doses (i.e. radioactivity required for an equivalent tumor growth delay), the ^{125}I-labeled mAbs were less toxic compared to the ^{131}I-labeled counterparts (*112,116*). The dose-limiting toxicity for ^{125}I- and ^{131}I-CO17-1A was myelosuppression, but no significant changes in blood urea nitrogen (BUN), serum creatinine or hepatic transaminases were found (*116*). Similarly, CO17-1A labeled with the Auger electron-emitter, ^{111}In was more effective at inhibiting the growth of

GW-39 colon cancer xenografts when administered at the MTD (85 MBq) than CO17-1A labeled with the β-emitter, ^{90}Y (MTD; 4 MBq), with CR achieved only with ^{111}In-CO17-1A (*128*).

In a Phase I/II clinical trial, 21 patients with chemotherapy-resistant colon cancer were administered increasing doses of ^{125}I-A33 up to 12,950 MBq/m^2 (*117*). Decreased carcinoembryonic antigen (CEA) levels were noted in 3 patients, while one patient demonstrated a mixed radiological response on CT. One patient who had prior exposure to mitomycin developed transient grade 3 thrombocytopenia. In another Phase I clinical trial, 28 patients with metastatic colorectal cancer were administered ^{125}I-CO17-1A in escalating single or multiple doses from 740 to 9,250 MBq (*118*). Although there were no major hematological toxicities, a few patients exhibited moderate decreases in platelet and white blood cell (WBC) counts at the higher administered doses. Unfortunately, there were no objective responses observed in this study, likely due to the poor penetration of the radiolabeled mAbs into large tumor deposits, and inefficient translocation of the radiolabeled mAbs into close enough proximity to the tumor cell nucleus (*118*).

1.6.1.6 DNA intercalating agents

Antigene radiotherapy is based on the principle of depositing localized radiation damage in specific genomic DNA sequences through the hybridization of radiolabeled triplex-forming oligodeoxynucleotides (TFOs) with selected gene sequences associated with disease (*119*). TFOs anneal in a sequence-specific manner to their target gene by forming noncanonical Hoogsteen hydrogen bonds with bases located in the major groove of the DNA duplex. TFOs radiolabeled with Auger electron-emitters capable of inducing lethal DNA-DSBs could provide a promising tool to selectively target and destroy specific oncogene sequences and thereby suppress the malignant phenotype or even kill cancer cells (*67*).

^{125}I-labeled TFOs directed against the human *mdr*-1 gene have been shown to induce DSBs in genomic DNA isolated from KB-V1 vinblastine-resistant human epidermoid cancer cells with *mdr*-1 gene amplification (0.5-0.7 breaks per decay of ^{125}I) (*120*). Gene specific strand breaks were also detected in DNA recovered from intact nuclei and in digitonin permeabilized cells incubated *in vitro* with ^{125}I-TFOs, although the efficiency of DNA damage diminished 10-fold (0.03-0.04 breaks per decay). Nevertheless, these results demonstrated that

^{125}I-TFOs were able to hybridize to their target DNA sequence, even in chromatin-compacted DNA (*120*).

1.7 Nuclear Localizing Sequences

Nuclear localizing sequences (NLS) have been conjugated to a variety of macromolecules that are typically excluded from the nucleus such as bovine serum albumin, ferritin, IgG and IgM proteins (*121-123*). These proteins undergo efficient nuclear translocation following conjugation to NLS. NLS sequences have also been shown to have the capability of inserting mAbs and peptide growth factors conjugated to nanometer-micrometer range Auger electron-emitting radionuclides (e.g. ^{111}In) into the nucleus of cancer cells following their receptor-mediated internalization, where these electrons are highly potent in causing lethal DNA strand breaks (Fig. 1.1; reviewed in (*124*)). Typical NLS peptide-motifs possess a cluster of four or more cationic residues (i.e. lysine - K, or arginine - R) and are categorized as either monopartite, containing a single cluster of basic amino acid residues, or bipartite, containing two clusters of basic amino acid residues separated by a linking sequence of 10-12 unconserved amino acids. The prototypical monopartite NLS is exemplified by the SV-40 large-T antigen NLS (^{126}PKKKRKV^{132}), whereas the NLS of the *Xenopus* phosphoprotein nucleoplasmin (KRPAATKKAGQAKKKKL^{170}) first defined the bipartite class. Mutagenesis studies have revealed that substituting one lysine in the SV-40 NLS (K-128 to either threonine or asparagine) abolishes its nuclear targeting capability, whereas substitution of one of the adjacent basic residues reduces but does not completely abolish nuclear import (*124*).

NLS are recognized by carrier proteins of the karyopherin/importin family. Importin-α binds directly to the NLS of cargo proteins destined for the nucleus, and the importin-α is further recognized by importin-β to form a heterotrimer complex that interacts with the hydrophobic repeat domains of nucleoporins that constitute the NPCs. Translocation of the importin-cargo complex across the nuclear pore is regulated by a small GTPase, Ran, which binds to importin-β and induces a conformational shift that results in the release of the cargo-protein into the nucleoplasm. Importin-RanGTP complexes are then exported back to the cytoplasm where they are dissociated (*124*).

1.7.1 Nuclear targeting of Auger electron-emitting radiopharmaceuticals

NLS can be synthetically introduced into biomolecules such as mAbs, peptides, small molecules and oligonucleotides to route Auger electron-emitting radionuclides to the nucleus of cancer cells. For example, Chen et al. (*125*) employed this approach to the treatment of acute myelogenous leukemia (AML) using the anti-CD33 mAb HuM195. Modification of ^{111}In-HuM195 mAb with as many as 12 SV-40 NLS-peptides (CGYG*PKKKRKV*GG) harboring the NLS of the SV-40 large T-antigen (*italicized*), did not substantially diminish its immunoreactivity, but promoted nuclear translocation in HL-60 leukemic cells. Moreover, the increased nuclear uptake of ^{111}In-HuM195 greatly enhanced its toxicity against leukemic cells, as well as against patient AML specimens (*125*).

Ginj et al. (*126*) recently described a somatostatin analog Tyr_3-octreotide (TOC) conjugated to the SV-40 large-T antigen consensus NLS (PKKKRKV) through an aminohexyl (ahx) linker. The NLS-TOC compound was labeled with ^{111}In, using the bifunctional chelator DOTA. Compared to its parent compound, ^{111}In-NLS-DOTA-TOC exhibited an enhanced cellular uptake and a 6-fold increase in the cellular retention in SSTR-positive rat AR4-2J pancreatic tumor cells, as well as in human embryonic kidney cells transfected with $SSTR_{2A}$ (HEK-$SSTR_{2A}$). It has been suggested that the cellular internalization of cationic peptides, such as the SV-40 NLS and other peptides rich in lysine or arginine residues including the HIV-1 TAT (HIV type 1 transactivator of transcription, ^{48}GRKKRRQRRRPPQ^{60}) protein and the Antennapedia homeodomain (amino acids 43-48), may actually be facilitated by their interaction with negatively-charged cell-surface moieties such as heparin sulfate proteoglycans (*127*). Cell membrane penetration is believed to be mediated by cationic peptide destabilization of the lipid bilayer with the formation of inverted micelles that allow the intracellular release of the cationic peptide and their attached cargoes (*127*). More recent models however, have focused on endocytosis. Antennapedia and TAT peptide, for example, have been shown to internalize through lipid-raft dependent endocytosis (*128*). Nevertheless, the nuclear uptake of ^{111}In-DOTA-TOC was increased 45-fold when conjugated to the NLS, whereas an unconjugated ^{111}In-labeled NLS-peptide (^{111}In-DOTA-ahx-PKKKRKV) had no uptake and no binding in both rat (AR4-2J) and human (HEK-$SSTR_{2A}$) cell lines, thereby indicating the prerequisite of specific binding to the SSTR for nuclear importation (*126*). It is possible, however, that the non-

specific cell-membrane penetrating potential of cationic NLS-peptides could increase non-specific toxicity despite the use of NLS to enhance cytotoxicity by promoting nuclear uptake. Further evaluation is required to determine the extent to which this approach will improve the clinical efficacy of Auger-electron radiotherapy using somatostatin analogs. Nevertheless, NLS conjugation represents a novel strategy to enhance peptide-directed receptor radiotherapy, since this approach could be extended to other peptide growth factor receptor ligands, such as bombesin, cholescystokinin, glucagon-like peptide, and vasoactive intestinal peptide, that have high affinity for their receptors, which are frequently overexpressed on a variety of tumors (*129*).

A 12-mer peptide (PKKKRKVEDPYC), harboring the NLS of SV-40 large-T antigen, was also conjugated to a ^{125}I-labeled TFO specific for the *mdr*-1 gene to promote its translocation to the nucleus of KB-V1 cells (*130*). NLS conjugation markedly enhanced nuclear uptake and gene-specific strand breaks within intranuclear DNA. Moreover, none of the cells treated with 10 nM of ^{125}I-TFO-NLS survived; a TFO concentration that was 100-fold lower than that used in antigene therapy experiments using nonradiolabeled oligonucleotides (*130*).

A trifunctional compound comprising an SV-40 NLS-peptide (PKKKRVGG), a pendant DNA-intercalating pyrene moiety, and a triamine tridentate ligand used for labeling with $[^{99m}Tc(OH_2)_3(CO)_3]^-$ was recently described by Haefliger et al. (*131*). By exploiting the strong fluorescence of pyrene, microscopy revealed that the trifunctional compound was taken up in the nucleus of B161F mouse melanoma cells. In contrast, a control conjugate consisting of the pyrene moiety and the ^{99m}Tc tricarbonyl core, but lacking the NLS-peptide, was detected only in the cytoplasm. The concentration required to kill 50% of B161F mouse melanoma cells was nearly 10 times lower for the trifunctional ^{99m}Tc-NLS-bioconjugate, compared to free $[^{99m}TcO_4]^-$ (1.8 nmol/L vs. 12 nmol/L, respectively) (*131*). Moreover, a control NLS-containing analog complexed with nonradioactive rhenium demonstrated no such cytotoxicity, ruling out any toxic effect induced by the pyrene moiety or tricarbonyl complex (*131*).

NLS-conjugation, therefore, represents a novel strategy that can i) overcome the challenge of delivering radiolabeled biomolecules to the nucleus of cancer cells, and ii)

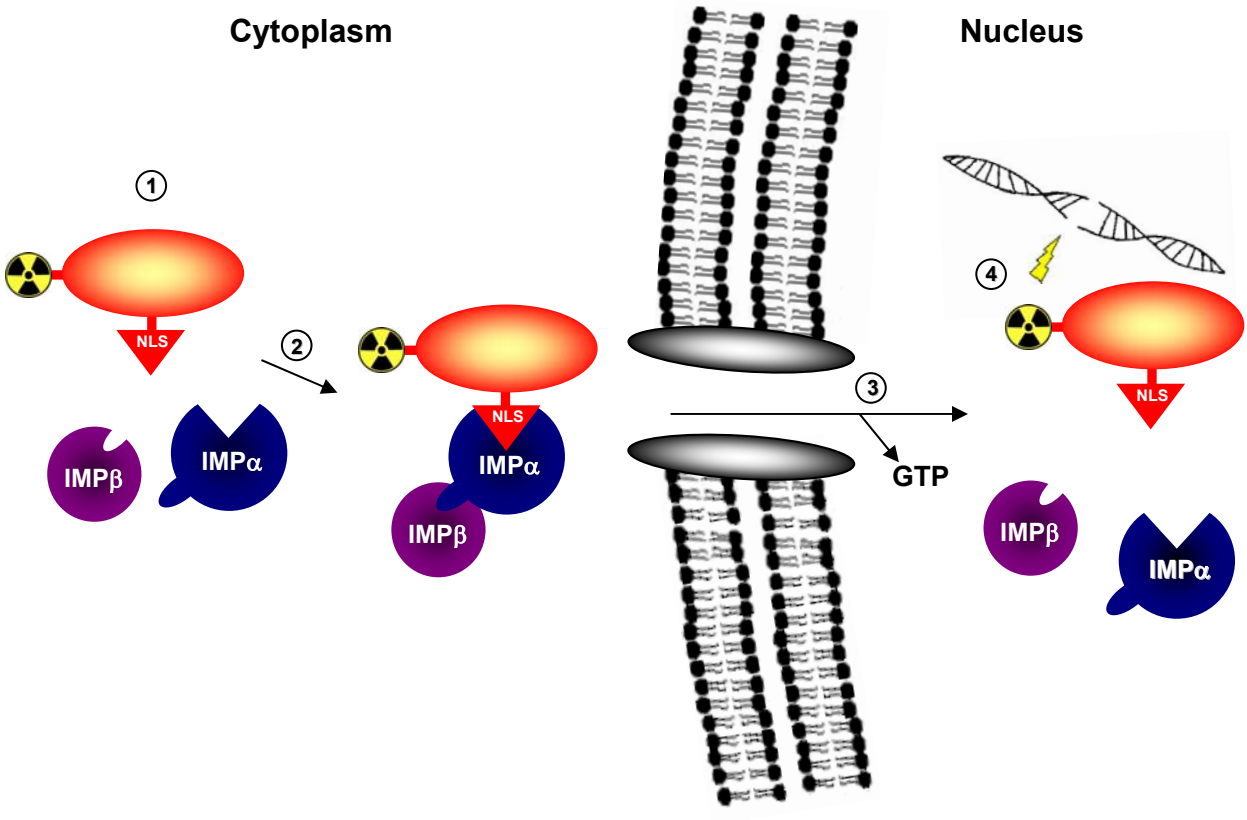

Figure 1.1: Nuclear localizing signal (NLS) mediated transport of Auger-electron emitting biomolecule through the nuclear pore complex. **(1)** Importin-α (IMPα; blue) recognizes and binds to the biomolecule containing an NLS and conjugated to an Auger electron-emitting radionuclide (red). **(2)** Importin-β (IMPβ; purple) interacts with the importin-α bound to the NLS and acts as a carrier of the NLS/importin-α/β trimer. **(3)** The importin/NLS-protein complex is then actively transported into the nucleus through nuclear pores involving the Ran GTPase. **(4)** The nanometer-to-micrometer range Auger electrons are emitted in close proximity to the nuclear DNA and induce highly cytotoxic DNA double strand breaks **(reproduced with permission from Costantini et al. (*124*))** .

dramatically enhance the effectiveness of targeted Auger electron-emitting radiotherapeutics for malignancies (*124*).

1.8 Radiosensitizers

Considerable attention has been given to combining RIT with chemotherapeutic agents. In such an approach, drugs that are known to be radiosensitizers, and that can amplify the lethal effects of ionizing radiation on cancer cells, are combined with RIT regimens (*132*). The chemotherapeutic agent is usually given at a reduced dose or modified schedule primarily to enhance the therapeutic response of RIT. De Nardo et al. (*140*), was the first to report the enhancement of a subtherapeutic dose of paclitaxel when used in combination with the ^{90}Y-labeled chimeric anti-L6 antibody (^{90}Y-ChL6) in mice bearing HBT-3477 human breast cancer xenografts. In mice receiving ^{90}Y-ChL6 alone (9.6 MBq; 315 μg, i.v.), 79% (15 of 19) of tumors responded, although none were cured (*140*). However, when paclitaxel (300 μg or 600 μg, i.p.) was administered 6-24 hours after ^{90}Y-ChL6, 100% (46 of 46) of tumors responded and 48% were cured, whereas no tumor responses were observed in mice receiving paclitaxel alone. The combination of radiosensitizing paclitaxel chemotherapy with RIT did not substantially increase toxicity (*140*). Other chemotherapeutic agents such as platinum-based compounds, topoisomerase-1 inhibitors and pyrimidine analogues, have also been shown to enhance the efficacy of RIT when used at submaximal doses (*132*).

Antimetabolites have also been shown to have radiosensitizing properties *in vitro*, which have been successfully translated into the clinic for drugs such as fluorouracil (FU), 5-fluoro-2'-deoxyuridine (FdUrd) and hydroxyurea (HU) in combination with external beam radiation therapy (*133*). Although antimetabolites target DNA replication, they differ with respect to the mechanism by which they cause radiosensitization. Antimetabolite radiosensitizers may inhibit the biosynthesis of deoxyribonucleotides which are necessary for DNA replication (e.g. dihydrofolate reductase or thymidylate synthase inhibitors, such as methotrexate (MTX) and FU, and ribonucleotides reductase inhibitors, such as HU) (*141,142*). Alternatively, the antimetabolite may be a nucleoside/nucleobase analog (e.g. gemcitabine) that can become incorporated into DNA and interfere with DNA polymerase activity. Radiosensitization of

cancer cells can result, therefore, from antimetabolite-induced increase in DNA double-stand breaks or inhibition of their repair following exposure of these cells to ionizing radiation (*133*).

1.9 Hypothesis of the thesis

The median survival for women with disseminated breast cancer is only 2-4 years (*134*) indicating that current systemic treatments for metastatic breast cancers remain limited and inadequate. New therapies that are more potent towards tumors but less harmful to normal tissues are needed to improve the long-term survival of women with advanced breast cancer.

A better understanding of the phenotypic properties of tumors at the cellular and molecular levels has provided opportunities to selectively target radionuclides to tumors for *in situ* radiation treatment. Indeed, the overexpression of HER2 receptor tyrosine kinases on breast cancer cells can be exploited to create radiopharmaceuticals that will kill these cells with radiation. The overall aim of this thesis, therefore, was to develop a novel radiotherapeutic agent directed against HER2 receptors on breast cancer cells that relies on subcellular range Auger electron-emitters such as ^{111}In to kill these cells, and to evaluate its potential for treatment of breast cancer metastases. Specifically the hypothesis of this thesis research was:

The novel Auger electron-emitting radiotherapeutic agent, ^{111}In-labeled trastuzumab modified with NLS-peptides (^{111}In-NLS-trastuzumab), will be capable of delivering DNA-damaging doses of short-range radiation specifically to the nucleus of HER2-overexpressing breast cancer cells, and will be highly lethal towards these cells while minimizing toxicity towards normal tissues.

1.10 Specific Aims

To test this hypothesis, the following specific aims were examined:

I. To generate ^{111}In-labeled radioimmunoconstructs of trastuzumab containing NLS-peptides that promote its nuclear uptake following HER2-mediated internalization, and to evaluate its purity, its receptor-binding affinity and its nuclear targeting properties in human breast cancer cells that overexpress HER2.

II. To investigate the cytotoxicity of ^{111}In-labeled NLS-trastuzumab by clonogenic survival assays in trastuzumab-sensitive and trastuzumab-resistant human breast cancer cells expressing increasing levels of HER2, and to study the potential for enhancing its cytotoxicity using methotrexate, a know radiosensitizing agent.

III. To study the pharmacokinetics of ^{111}In-labeled NLS-trastuzumab following intravenous or intraperitoneal injection, and to evaluate the normal tissue toxicity of the radiopharmaceutical in normal non-tumor bearing BALB/c mice.

IV. To evaluate the tumor and normal tissue uptake of ^{111}In-labeled NLS-trastuzumab, and its anti-tumor properties in athymic mice implanted s.c. with human breast cancer xenografts expressing intermediate or very low HER2 expression.

1.11 Overview of chapters 2, 3, 4, and 5

The studies addressing the above specific aims are described in Chapters 2 - 4 of the thesis. Chapter 2 describes the synthesis and *in vitro* characterization of ^{111}In-NLS-trastuzumab. This chapter also describes the studies examining the nuclear uptake and the *in vitro* cytotoxicity of ^{111}In-NLS-trastuzumab in human breast cancer cells expressing increasing levels of HER2, as well as its normal tissue distribution and *in vivo* nuclear targeting capability in athymic mice bearing HER2-positive breast cancer xenografts. Chapter 3 also describes the *in vitro* cytotoxicity of ^{111}In-NLS-trastuzumab, but in this case compares this property in trastuzumab-sensitive and resistant breast cancer cells expressing different levels of HER2. Chapter 3 also provides the results of radiosensitizing experiments employing the chemotherapeutic agent methotrexate to enhance the cytotoxicity of ^{111}In-NLS-trastuzumab. Chapter 4 describes the pharmacokinetics and normal tissue toxicity of ^{111}In-NLS-trastuzumab administered in escalating doses to normal non-tumor bearing BALB/c mice, and its anti-tumor properties in athymic mice bearing HER2-positive breast cancer xenografts. In Chapter 5, the overall findings of the thesis are summarized, conclusions are presented, and future research is proposed.

CHAPTER 2:

^{111}IN-LABELED TRASTUZUMAB (HERCEPTIN) MODIFIED WITH NUCLEAR LOCALIZATION SEQUENCES (NLS): AN AUGER ELECTRON-EMITTING RADIOTHERAPEUTIC AGENT FOR HER2-AMPLIFIED BREAST CANCER

This chapter represents a reprint of: "Danny L. Costantini, Conrad Chan, Zhongli Cai, Katherine A. Vallis, and Raymond M. Reilly. ^{111}In-labeled trastuzumab (Herceptin) modified with nuclear localization sequences (NLS): an Auger electron-emitting radiotherapeutic agent for HER2/neu-amplified breast cancer. *J Nucl Med*. 2007 48(8):1357-1368." **Reprinted by permission of the Society of Nuclear Medicine on October 10, 2008.**

All experiments and analyses of data were carried out by Costantini DL, except for the γH2AX-assay studies (Cai Z).

Abstract

Introduction: The cytotoxicity and tumor targeting properties of the anti-HER2/neu monoclonal antibody trastuzumab (Herceptin) modified with peptides (CGYG*PKKKRKV*GG) harboring the nuclear localization sequence (NLS; *italicized*) of simian virus 40 large T-antigen and radiolabeled with ^{111}In were evaluated. **Methods:** Trastuzumab was derivatized with sulfosuccinimidyl-4-(N-maleimidomethyl)-cyclohexane-1-carboxylate (sulfo-SMCC) for reaction with NLS-peptides and labeled with ^{111}In using diethylenetriaminepentaacetic-acid (DTPA). The immunoreactivity of ^{111}In-NLS-trastuzumab was determined by its ability to displace the binding of trastuzumab to SK-BR-3 human breast cancer cells. Cellular uptake and nuclear localization were evaluated in SK-BR-3, MDA-MB-361 and MDA-MB-231 breast cancer cells, expressing high, intermediate or very low levels of HER2, respectively, by cell fractionation and confocal microscopy. Biodistribution and nuclear uptake were compared in athymic mice bearing MDA-MB-361 xenografts. The cytotoxicity of ^{111}In-trastuzumab and ^{111}In-NLS-trastuzumab was studied by clonogenic assays and DNA damage was assessed by probing for γH2AX foci. **Results:** The dissociation constant for binding of ^{111}In-NLS-trastuzumab to SK-BR-3 cells was reduced <3-fold compared to ^{111}In-trastuzumab, demonstrating relatively preserved receptor-binding affinity. The receptor-mediated internalization of ^{111}In-trastuzumab in SK-BR-3, MDA-MB-361 and MDA-MB-231 cells increased significantly from 7.2 ± 0.9%, 1.3 ± 0.1% and 0.2 ± 0.05% to 14.4 ± 1.8%, 6.3 ± 0.2% and 0.9±0.2% for ^{111}In-NLS-trastuzumab harboring 6 NLS-peptides, respectively. NLS-trastuzumab localized in the nuclei of breast cancer cells, whereas unmodified trastuzumab remained surface-bound. Conjugation of ^{111}In-trastuzumab to NLS-peptides did not affect its tissue biodistribution, but promoted specific nuclear uptake in MDA-MB-361 xenografts (2.4-2.9% ID/g for ^{111}In-NLS-trastuzumab and 1.1% ID/g for ^{111}In-trastuzumab). ^{111}In-NLS-trastuzumab was 5- and 2-fold more potent at killing SK-BR-3 and MDA-MB-361 cells than ^{111}In-trastuzumab, respectively, whereas toxicity towards MDA-MB-231 cells was minimal. ^{111}In-NLS-trastuzumab was 6-fold more effective at killing SK-BR-3 cells than unlabeled trastuzumab. Formation of γH2AX-foci occurred in a greater proportion of breast cancer cells after incubation with ^{111}In-NLS-trastuzumab compared to ^{111}In-trastuzumab or unlabeled trastuzumab. **Conclusion:** NLS-peptides routed ^{111}In-trastuzumab to the nucleus of HER2-

positive human breast cancer cells rendering the radiopharmaceutical lethal to the cells through the emission of nanometer-micrometer range Auger electrons. The greater cytotoxic potency of ^{111}In-NLS-trastuzumab compared to unlabeled trastuzumab *in vitro* and its favorable tumor targeting properties *in vivo* suggests that it could be an effective targeted radiotherapeutic agent for HER2-amplified breast cancer in humans.

2.1 Introduction

The development of recombinant antibodies for cancer therapy has emerged as one of the most promising areas in oncology (*29*). Trastuzumab (Herceptin®), in particular, is a humanized monoclonal antibody (mAb) directed against the human epidermal growth factor receptor-2 (HER2/neu), a transmembrane receptor tyrosine kinase that is overexpressed in 25-30% of breast cancers and distant metastases (*36*). Trastuzumab shows clinical activity in women with HER2-overexpressing metastatic breast cancer and exhibits synergistic anti-tumor effects when combined with paclitaxel or anthracyclines, achieving overall response rates of 40-60% (*36*). Despite its effectiveness in combination regimens, the response rate to single-agent trastuzumab is only 7-35%, depending on the level of HER2 expression, and the median duration of response is less than 9 months (*33,34*).

Radioimmunotherapy (RIT) may offer the opportunity to enhance the intrinsic cytostatic activity of trastuzumab by incorporating localized radiation directly into the treatment regimen using the same molecule. Indeed, trastuzumab or its murine mAb analogue 4D5, labeled with β-emitters (e.g. ^{131}I, ^{90}Y or ^{188}Re) (*75,76,133*) or α-emitters (e.g. ^{212}Pb, ^{213}Bi, ^{211}At and ^{225}Ac) (*81,77,76,78*), have been shown to inhibit the growth of HER2-positive human breast, ovarian, nasopharyngeal, prostate, colon and pancreatic cancer cells *in vitro* or provide anti-tumor effects *in vivo* in xenograft mouse models. For RIT of micrometastatic tumors, however, long-range (2-12 mm or 200-1,200 cell diameters) β-particle emitters are generally considered sub-optimal because a significant portion of the radiation-dose is deposited outside the target volume (i.e. in normal tissues surrounding targeted tumor cells) (*85*). Furthermore, hematologic toxicities are common adverse effects associated with β-particle RIT, primarily due to the prolonged retention time of radiolabeled mAbs in the circulation ($t_{1/2}$ ~ 6 days) combined with the long range of the β-particles (2-10 mm) which exposes the bone marrow to excessive levels of radiation (*29,33*). Short-range (40-100 μm) α-particle emitters are theoretically better suited for RIT of micrometastatic disease since a greater fraction of the emitted energy is absorbed by the tumor cells. Their short half-lives (<12 hours), however, place constraints on production, antibody labeling and use, whereas longer lived α-emitters, such as ^{225}Ac ($t_{1/2}$ = 10 days), are limited by

the redistribution of daughter radioisotopes following their decay and consequent irradiation of normal organs (*29,89*).

Low-energy Auger electron-emitters are an appealing alternative to α- or β-particle emitters for RIT. Most Auger electrons travel nanometer-to-micrometer distances in tissue, and have high linear energy transfer (LET) values approaching those of α-emitters (4-26 keV/μm) (*85*). These properties render Auger electron-emitters highly cytotoxic and damaging to DNA when they decay intracellularly, and especially when they decay in close proximity to the cell nucleus (*90*). We recently reported, for example, that the anti-CD33 mAb HuM195, conjugated to the Auger electron-emitter ^{111}In ($t_{1/2}$ = 2.83 days), was toxic to myeloid leukemia cells. Fusion proteins containing a nuclear localization sequence (NLS) have been widely used to exploit intracellular transport mechanisms and promote the translocation of macromolecules into the cell nucleus. NLS-containing macromolecules specifically interact with importin (karyopherin) α-β transport factors which function as carrier molecules and facilitate the passage of cargo-proteins through the nuclear pore complex (*123*). A single cluster of cationic residues (-PKKKRKV-) is required for nuclear localization of simian virus 40 (SV-40) large T-antigen. This NLS-motif has been conjugated to a variety of macromolecules that are excluded from the nucleus such as bovine serum albumin, ferritin, IgG and IgM proteins (*123*). These proteins undergo efficient nuclear translocation following conjugation to NLS. Therefore, we further modified ^{111}In-HuM195 with 13-mer peptides (CGYG*PKKKRKV*GG) harboring the NLS of SV-40 large-T antigen (*italicized*). Conjugation of ^{111}In-HuM195 to NLS-peptides dramatically increased its nuclear uptake in leukemia cells, and enhanced its cytotoxicity towards these cells (*125*). We have now extended this promising approach to the treatment of breast cancer and show that the nuclear uptake and toxicity of ^{111}In-labeled trastuzumab towards HER2-overexpressing breast cancer cells was enhanced by its conjugation to NLS-peptides. More importantly, these peptides did not substantially interfere with the receptor-binding ability of trastuzumab, but enhanced its ability to target the nucleus of breast cancer cells *in vivo* in mice bearing solid tumor xenografts.

2.2 Materials and methods

2.2.1 Cell culture

SK-BR-3, MDA-MB-361 and MDA-MB-231 human breast cancer cells were obtained from the American Type Culture Collection (Manassas, VA). SK-BR-3 cells express 2×10^6 HER2/neu receptors/cell and were cultured in RPMI-1640 with 10% fetal bovine serum (FBS) and 1% penicillin-streptomycin (P/S) (*135*). In comparison, MDA-MB-361 and MDA-MB-231 cells express a 2- and 150-fold lower level of HER2, respectively, and were maintained in Dulbecco's Modified Eagle Medium with 10% FBS and 1% P/S (*136*).

2.2.2 Construction and radiolabeling of ^{111}In-trastuzumab modified with NLS-peptides

Trastuzumab (Herceptin®, Hoffmann-La Roche, Mississauga, ON) was derivatized with diethylenetriaminepentaacetic-acid (DTPA) dianhydride (Sigma-Aldrich) for labeling with ^{111}In (*135*). Briefly, trastuzumab (500 μg, 10 mg/mL) was reacted with a 10-fold molar excess of DTPA for 1 hour at room temperature, and then purified on a Sephadex-G50 mini-column (Sigma-Aldrich) eluted with phosphate-buffered saline (PBS), pH 7.5. Synthetic 13-mer NLS-peptides (CGYGPKKKRKVGG) synthesized by the Advanced Protein Technology Centre (Hospital for Sick Children, Toronto, ON) were then conjugated to DTPA-modified trastuzumab using the heterobifunctional cross-linking agent sulfosuccinimidyl-4-(N-maleimidomethyl)cyclohexane-1-carboxylate (sulfo-SMCC, Pierce) (*125*). Briefly, DTPA-trastuzumab (0.5-2.0 mg, 8 mg/mL in PBS, pH 7.5) were reacted with a 5-to-50 fold molar excess of sulfo-SMCC (2-5 mmol/L) at room temperature for 1 hour, and purified on a Sephadex-G50 mini-column eluted 20-25 times with 100 μL of PBS, pH 7.0. Fractions 9-14 containing maleimide-derivatized DTPA-trastuzumab were pooled and transferred to a Microcon YM-50 ultrafiltration device (Amicon), concentrated to 2-5 mg/mL, and reacted with a 60-fold molar excess of NLS-peptides (5-10 mmol/L in PBS, pH 7.0) overnight at 4^{o}C. DTPA-trastuzumab, modified with NLS-peptides (NLS-DTPA-trastuzumab) was purified on a Sephadex-G50 mini-column eluted with PBS, pH 7.5.

DTPA-trastuzumab or NLS-DTPA-trastuzumab (50-100 μg) was labeled by incubation with 37-111 MBq ^{111}In-acetate for 1 hour at room temperature. ^{111}In-acetate was prepared by mixing ^{111}In-chloride (MDS-Nordion, Inc.) with 1.0 mol/L sodium acetate, pH 6.0 (1:1, v/v).

After purification on a Sephadex-G50 mini-column, radiochemical purity was routinely > 97% as determined by instant thin-layer silica-gel chromatography (ITLC-SG, Pall Corporation) developed in 100 mmol/L sodium citrate, pH 5.0 (R_f ^{111}In-NLS-trastuzumab/^{111}In-trastuzumab: 0.0; free ^{111}In-DTPA: 1.0). Radioactivity measurements were made using an automatic γ-counter (Wallac Wizard-1480, Perkin Elmer).

2.2.3 Characterization of DTPA-trastuzumab modified with NLS-peptides

The purity and homogeneity of NLS-DTPA-trastuzumab immunoconjugates were evaluated by sodium dodecylsulfonate polyacrylamide-gel electrophoresis (SDS-PAGE) on a 5% Tris-HCl minigel (Bio-Rad) electrophoresed under non-reducing conditions and by Western blot. The gel was stained with Coomassie-G250 stain (Bio-Rad). For Western blot, electrophoresed proteins were transferred onto polyvinyldifluoride membranes (Roche) and incubated in 5% skim milk in PBS/0.1% Tween-20 (PBS-T) for 1 hour at room temperature, followed by an overnight incubation at 4^{o}C with horseradish peroxidase-conjugated goat-antihuman Fc antibodies (1:1500, Sigma-Aldrich). After three washes with PBS-T, reactive bands were detected using the chromogenic substrate 3,3′-diaminobenzidine tetrahydrochloride (Sigma-Aldrich) and 0.03% H_2O_2. The migration distance of the reactive bands relative to the front (R_f) were measured and the logarithm of molecular weight (M_r) versus $1/R_f$ were plotted by comparison to standard M_r-reference markers (10-250 kDa; Amersham Biosciences) electrophoresed under identical conditions. To determine the number of NLS-peptides conjugated to DTPA-trastuzumab, the difference between the M_r-values for DTPA-trastuzumab and NLS-DTPA-trastuzumab was divided by the M_r for the NLS-peptide (~1418 Da). Alternatively, the number of NLS-peptides incorporated into trastuzumab were quantified by including a tracer amount of ^{123}I-labeled NLS-peptides in the reaction, measuring the proportion of bound radioactivity following purification, and multiplying by the peptides-to-trastuzumab molar ratio used in the reaction (*125*). NLS-peptides were radiolabeled to a specific activity of 2-5 MBq/mg with ^{123}I-sodium iodide (MDS-Nordion, Inc.) using the Iodogen® method (*125*). Radiochemical purity of ^{123}I-NLS-peptides was > 95% as determined by paper chromatography developed in 85% methanol (R_f ^{123}I-NLS-peptides: 0.0; ^{123}I iodide: 1.0).

2.2.4 Competition Receptor-Binding Assays

Approximately 5×10^4 SK-BR-3 cells were incubated in 96-well plates for 24 hours in culture medium. After a gentle rinse with PBS, pH 7.5, the cells were incubated with ^{111}In-NLS-trastuzumab or ^{111}In-trastumuzab (10 nmol/L), in the presence of unlabeled trastuzumab (0-300 nmol/L) in 100 μL PBS, pH 7.5 containing 0.1% bovine serum albumin (BSA) (Sigma-Aldrich) for 3.5 hours at 4°C. The cells were rinsed with PBS (pH 7.5) and solubilized in 100 mmol/L NaOH. Cell suspensions were collected and the radioactivity measured in a γ-counter. The proportion of ^{111}In-trastuzumab/^{111}In-NLS-trastuzumab displaced from SK-BR-3 cells by increasing concentrations of trastuzumab was plotted, and Origin® v.6.0 (Microcal Software, Inc., Northampton, MA) was used to fit the curves and determine the dissociation constants (K_d).

2.2.5 Radioligand Internalization Studies

Approximately 1×10^6 cells were incubated at 37°C with agitation in microtubes containing ^{111}In-trasuzumab or ^{111}In-NLS-trastuzumab (10 nmol/L) in 500 μL PBS (pH 7.5) with 0.1% BSA. At selected time points up to 24 hours, the cells were centrifuged and the medium was removed. Cells were washed twice with PBS, pH 7.5, to remove unbound radioactivity and resuspended in a 0.5 mL mixture of 200 mmol/L sodium acetate and 500 mmol/L sodium chloride (pH 2.5) for 5 minutes on ice (*87*). Cells were then centrifuged again to separate internalized-radioactivity (pellet) from surface-bound radioactivity present in the acid wash (supernatant). After two more washes with PBS (pH 7.5), the pellets and supernatants were measured in a γ-counter.

2.2.6 Confocal Immunofluorescence Microscopy

Cells were cultured on chamber-slides (Nunc, Life Technologies) overnight at 37°C in medium. To assess the subcellular distribution of trastuzumab, cells were incubated with DTPA-trastuzumab or NLS-DTPA-trastuzumab (1.5 μg/mL) in 1 mL of medium for 24 hours at 37°C. Cells were then fixed with 3.7% paraformaldehyde and permeabilized for 10 minutes with PBS, pH 7.5 containing 0.1% Triton X-100, 1% BSA and 2% goat serum. After three 10 minute washes with PBS, pH 7.5, the slides were blocked for 2 hours with 10% goat serum and incubated with AlexaFluor-594 anti-human IgG (Molecular Probes).

An early step in the response of cells to DNA-double strand breaks (DSBs) after exposure to ionizing radiation is the phosphorylation of histone-H2AX at serine-139 (γH2AX) which can be detected as discrete nuclear foci using γH2AX-specific antibodies (*137*). The ability of ^{111}In-trastuzumab and ^{111}In-NLS-trastuzumab to cause DNA-DSBs in breast cancer cells was evaluated using this γH2AX-assay. Briefly, cells were cultured overnight in 1 mL of medium containing PBS, pH 7.5, trastuzumab, ^{111}In-trastuzumab or ^{111}In-NLS-trastuzumab (67.5 μg/ml: 19.8 MBq), and then fixed with 2% paraformaldehyde containing 0.5% Triton X-100 in PBS, pH 8.2 for 15 minutes. After three 10 minute washes with PBS, pH 7.5 containing 0.5% BSA and 0.2% Tween-20, the cells were permeabilized for 15 minutes with PBS, pH 8.2 containing 0.5% Nonidet P-40, and blocked for 1 hour in 2% BSA and 1% donkey serum. The slides were then incubated with anti-phospho-γH2AX (1:800, Upstate Biotechnology) in 3% BSA overnight at 4^{o}C, then AlexaFluor-488 anti-mouse IgG (Molecular Probes) for 45 minutes at room temperature.

All slides were mounted with Vectashield® mounting media containing 4,6-diamidino-2-phenylindole (DAPI) (Vector Laboratories) and kept at 4^{o}C overnight. Images were taken with an inverted LSM510 confocal microscope (Carl Zeiss) at the Advanced Optical Microscopy Facility (Princess Margaret Hospital, Toronto, ON). Excitation was at 364 nm, 488 nm or 543 nm for visualization of DAPI, AlexaFluor-488 or AlexaFluor-594, using 385-470 nm, 505-550 nm or 560 nm emission filters, respectively. For imaging of γH2AX, 10-15 *Z*-stack images at 1.2 μm intervals were acquired throughout the entire cell nucleus, merged using LSM-Viewer software (v.3.5.0.376, Zeiss) and stored as tiff files. The number of γH2AX-foci present in each cell was counted manually using ImageJ software (v.1.36b, National Institutes of Health, USA) and cells with more than 10 foci per nucleus were classified as positive for radiation-induced γH2AX (*137*).

2.2.7 Clonogenic Assays

Approximately 2×10^6 cells were incubated with ^{111}In-trastuzumab (244 ± 22 MBq/mg) or ^{111}In-NLS-trastuzumab (239 ± 8.9 MBq/mg) in 1 mL of medium in microtubes for 24 hours at 37^{o}C. Controls included cells cultured with medium alone, medium containing unlabeled trastuzumab or an irrelevant NLS-conjugated human IgG (NLS-hIgG; Sigma-Aldrich) labeled

with ^{111}In (228 ± 13 MBq/mg) as described above. Cells were then centrifuged at 1000×g for 5 minutes and washed twice with medium. Sufficient cells were then plated in triplicate in 12-well plates and cultured in medium at 37^{o}C. After 14-21 days, colonies of ≥ 50 cells (or ≥ 0.2 mm for MDA-MB-361 cells) were stained with methylene blue and counted. The surviving fraction (SF) was calculated by the dividing the number of colonies formed for treated cells by the number for untreated cells. Survival curves were derived by plotting the SF values versus the concentration (μg/mL) of antibody used.

2.2.8 Tumor and Normal Tissue Biodistribution Studies

The tissue biodistribution of ^{111}In-trastuzumab, ^{111}In-NLS-trastuzumab and ^{111}In-NLS-hIgG were evaluated in athymic mice implanted subcutaneously (s.c.) with MDA-MB-361 breast cancer xenografts. Mice were implanted intradermally with a 17-β-estradiol pellet (Innovative Research of America, Sarasota, FL) 24 hours prior to inoculation in the flank with 1×10^{7} MDA-MB-361 cells in 100 μL of Matrigel (Becton–Dickinson Labware, Bedford, MA) and culture medium mixture (1:1, v/v). When the tumors reached a diameter of 2-5 mm (6-8 weeks), the mice received an intravenous (i.v.) injection of ^{111}In-trastuzumab, ^{111}In-NLS-trastuzumab or ^{111}In-NLS-hIgG (10 μg; 1-2 MBq). At 72 hours post-injection (p.i.), the mice were sacrificed and a blood sample was taken by intracardiac puncture. The tumor and samples of selected normal tissues were removed, blotted dry and weighed. Uptake of radioactivity by these tissues was measured in a γ-counter and expressed as percent of injected dose per gram (% ID/g) and as tumor-to-normal tissue (T/NT) ratios. The principles of Laboratory Animal Care (NIH Publication No.86-23, revised 1985) were followed, and animal studies were approved by the Animal Care Committee at the University Health Network (Protocol No.TG:282.2) following Canadian Council on Animal Care guidelines.

2.2.9 Nuclear uptake *in vivo* in tumors and normal tissues

The accumulation of radioactivity in the nuclei of breast cancer cells, as well as in cells of selected normal tissues (liver, kidney, spleen and heart) was determined by subcellular fractionation following i.v. injection (10 μg; 1-2 MBq) of ^{111}In-trastuzumab, ^{111}In-NLS-trastuzumab or ^{111}In-NLS-hIgG in athymic mice bearing s.c. MDA-MB-361 tumor xenografts.

At 72 h p.i., groups of three mice were sacrificed and tissue samples were taken in order to measure the tissue radioactivity concentration (% ID/g). The nuclei were separated from the cytoplasm/membrane using the Nuclei PURE Prep Nuclei Isolation Kit (Sigma-Aldrich) following the manufacturer's directions. We previously demonstrated (*138*) by Western blot for calpain, an abundant cytoplasmic protein and p84, a nuclear matrix protein (unpublished results), that this method provides a highly pure nuclear and cytoplasm/membrane fraction. Nuclear uptake was quantified by multiplying the % ID/g values by the percentage of radioactivity present in the nuclear fraction.

2.2.10 Statistical Methods

Data were presented as mean ± standard error of the mean (SEM). Statistical comparisons were made using the Student's *t*-test. For the γH2AX study, a chi-square analysis was used to evaluate differences between treatment groups. $P < 0.05$ was considered significant.

2.3 Results

2.3.1 Characterization of NLS-trastuzumab immunoconjugates

As determined by SDS-PAGE and Western blot, the M_r for trastuzumab IgG increased from 159 ± 2.0 kDa to 178 ± 3.6 kDa as the SMCC-to-trastuzumab molar ratio increased, indicating incremental NLS-peptide substitution (Fig. 2.1A-B). According to these M_r values, approximately 1.6 ± 0.3, 3.4 ± 0.2, 6.3 ± 0.2 and 10.4 ± 0.8 NLS-peptides were conjugated to trastuzumab at an SMCC-to-IgG molar ratio of 5:1, 15:1, 25:1 and 50:1, respectively. Higher molecular-weight dimer and polymer IgG complexes were also observed, likely due to the bicyclic nature of DTPA-dianhydride (*139*). The proportion of polymeric forms was not significantly different for DTPA-trastuzumab modified with 3 or 6 NLS-peptides (14.2 ± 5.9% and 14.9 ± 3.9%) than for unmodified DTPA-trastuzumab (14.9 ± 5.4%; $p>0.05$). There was an excellent correlation ($r^2 = 0.99$) between the number of NLS-peptides introduced into trastuzumab determined by M_r-analysis or by measuring the proportion of tracer ^{123}I-NLS-

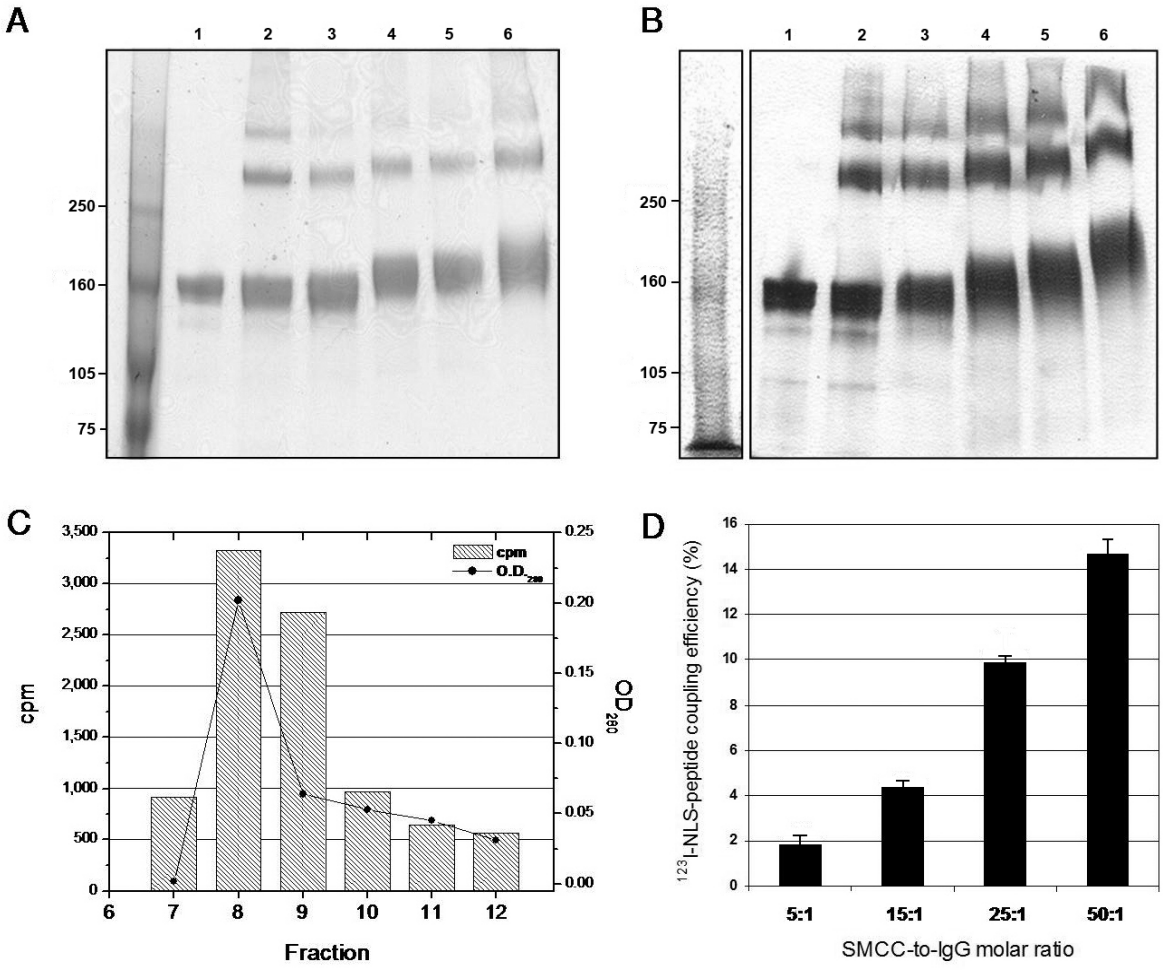

Fig. 2.1: (A) SDS-PAGE and **(B)** Western blot of unmodified trastuzumab (lane 1) or DTPA-trastuzumab (lane 2) reacted with a 5, 15, 25 or 50-fold molar excess of sulfo-SMCC followed by conjugation to a 60-fold molar excess of NLS-peptides (lanes 3-6, respectively). **(C)** Representative size-exclusion chromatograms of purification of ^{123}I-NLS-peptides bound to trastuzumab from free peptides. Elution curves were obtained by measuring UV absorbance (OD_{280nm}) (solid line) and radioactivity (hatched bars) in each fraction. The peak in fractions 7-10 represents trastuzumab-bound ^{123}I-NLS-peptides. **(D)** ^{123}I-NLS-peptide coupling efficiency to trastuzumab increases as the SMCC-to-IgG molar ratio increases. Values shown are the mean ± SEM of triplicate determinations.

peptides incorporated. Indeed, the ^{123}I-NLS-peptide coupling efficiency increased from 4.4 ± 0.3% to 9.8 ± 0.4% for an SMCC-to-IgG ratio of 15:1 to 25:1, respectively, to 14.8 ± 0.7% at a ratio of 50:1 (Fig. 2.1C-D). Thus, a 60-fold molar excess of ^{123}I-NLS-peptides used in the reaction represents 2.5 ± 0.3, 5.6 ± 0.5 and 8.4 ± 0.9 incorporated peptides at a 15:1, 25:1 and 50:1 molar ratio, respectively.

2.3.2 Immunoreactivity of ^{111}In-trastuzumab and ^{111}In-NLS-trastuzumab

In competition receptor-binding assays, ^{111}In-trastuzumab and ^{111}In-NLS-trastuzumab were displaced by increasing amounts of unlabeled trastuzumab (Fig. 2.2). Although specific binding to HER2-overexpressing SK-BR-3 cells was found, there was a 1.4-fold and 2.6-fold significant decrease in the receptor-binding affinity for ^{111}In-NLS-trastuzumab bearing 3 (^{111}In-NLS_3-trastuzumab) and 6 (^{111}In-NLS_6-trastuzumab) NLS-peptides (K_d = 5.9 ± 0.4 nmol/L and 3.1 ± 0.4 nmol/L, respectively), compared to ^{111}In-trastuzumab (K_d = 8.2 ± 0.5 nmol/L).

2.3.3 Internalization and nuclear translocation of ^{111}In-NLS-trastuzumab

The internalization of ^{111}In-trastuzumab and ^{111}In-NLS-trastuzumab were compared in SK-BR-3, MDA-MB-361 and MDA-MB-231 cells expressing high, intermediate or very low levels of HER2, respectively. The fraction of radioactivity that internalized in SK-BR-3 cells, with respect to the total amount of ^{111}In-NLS_3-trastuzumab or ^{111}In-NLS_6-trastuzumab that was added to the incubation media, increased from 7.3 ± 2.3% and 5.7 ± 1.5% after 2 hours of incubation, to 11.6 ± 1.9% and 14.4 ± 1.8% after 24 hours, respectively (Fig. 2.3A). Conversely, the fraction of radioactivity that internalized in SK-BR-3 cells for ^{111}In-trastuzumab reached a plateau at 12 hours, and decreased after 24 hours to 7.2 ± 0.9%. The uptake of radioactivity was almost completely blocked by the addition of unlabeled trastuzumab to the incubation media, thus demonstrating specificity for HER2. The uptake of radioactivity in MDA-MB-361 and MDA-MB-231 cells, with respect to the total amount of ^{111}In-NLS-trastuzumab or ^{111}In-trastuzumab added to the incubation media, was significantly lower at 24 hours compared to SK-BR-3 cells (Fig. 2.3B and C); however, conjugation to NLS-peptides markedly enhanced the fraction of radioactivity that accumulated in these cells following

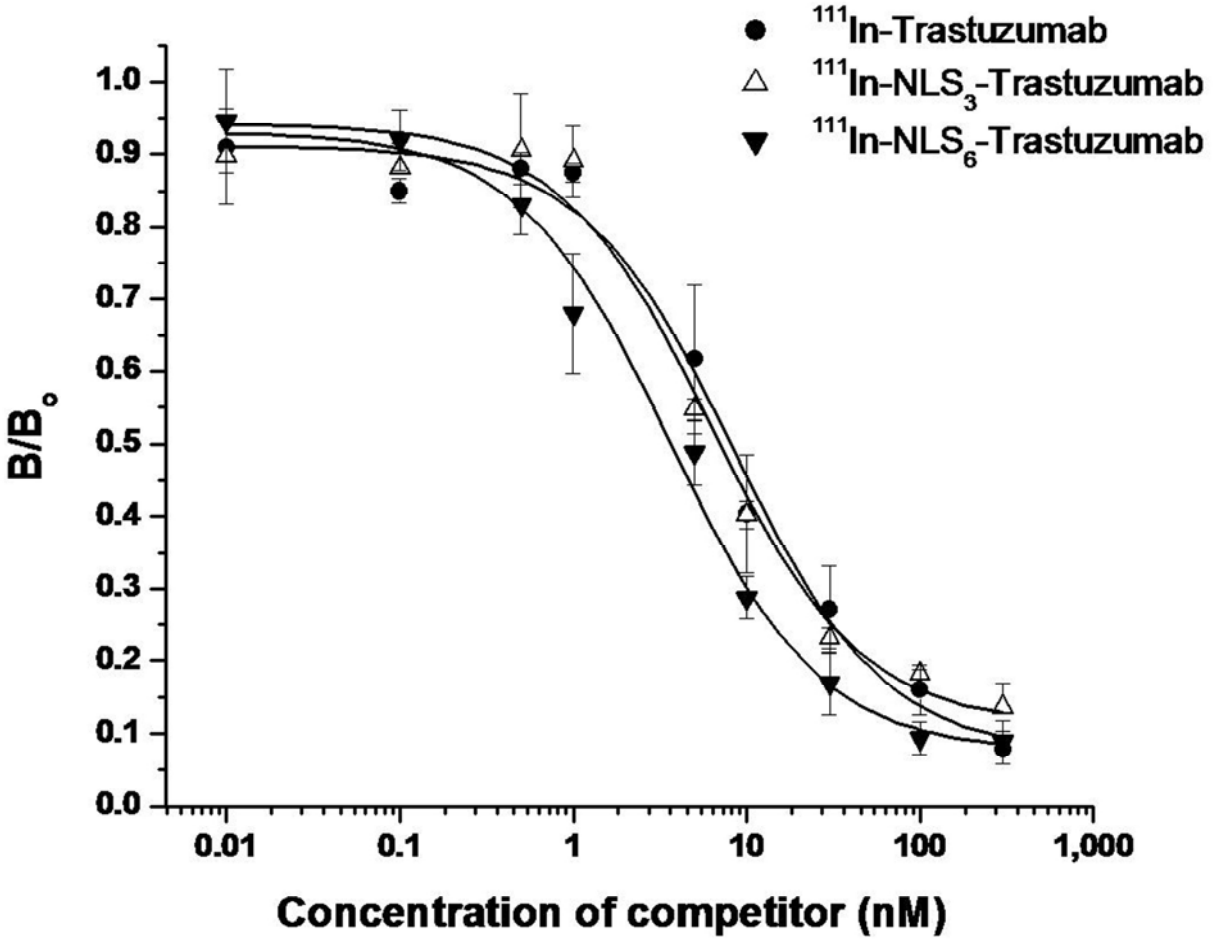

Fig. 2.2: Competition binding-curve showing effect of increasing concentrations of unlabeled trastuzumab on the displacement of the binding of ^{111}In-trastuzumab or ^{111}In-NLS-trastuzumab to SK-BR-3 cells. B = radioligand bound in the presence of competitors; Bo = radioligand bound without competitor. Each point represents the mean ± SEM of 3 assays performed in triplicate.

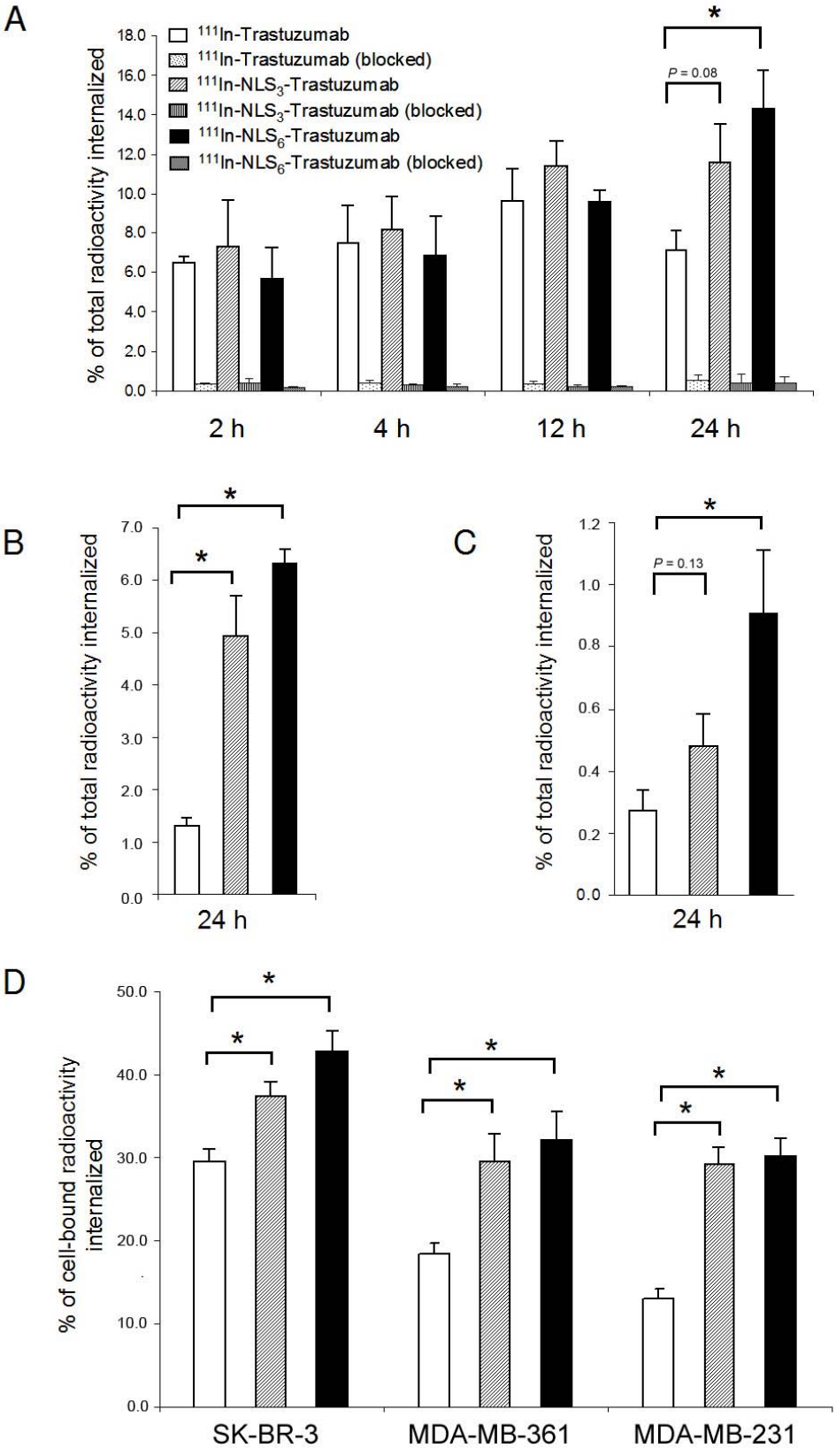
A
111In-Trastuzumab
111In-Trastuzumab (blocked)
111In-NLS3-Trastuzumab
111In-NLS3-Trastuzumab (blocked)
111In-NLS6-Trastuzumab
111In-NLS6-Trastuzumab (blocked)
% of total radioactivity internalized
18.0
16.0
14.0
12.0
10.0
8.0
6.0
4.0
2.0
0.0
*
P = 0.08
2 h
4 h
12 h
24 h
B
% of total radioactivity internalized
7.0
6.0
5.0
4.0
3.0
2.0
1.0
0.0
*
*
24 h
C
% of total radioactivity internalized
1.2
1.0
0.8
0.6
0.4
0.2
0.0
*
P = 0.13
24 h
D
% of cell-bound radioactivity internalized
50.0
40.0
30.0
20.0
10.0
0.0
*
*
*
*
*
*
SK-BR-3
MDA-MB-361
MDA-MB-231

Fig. 2.3: Internalization of ^{111}In-NLS-trastuzumab and ^{111}In-trastuzumab by **(A)** SK-BR-3, **(B)** MDA-MB-361 and **(C)** MDA-MB-231 breast cancer cells (solid bars) with respect to the total amount of radioactivity added to the incubation media. Internalization was measured in the presence or absence of an excess of unlabeled trastuzumab (100 nmol/L) in the incubation medium to block the HER2 receptors. **(D)** Internalized fraction of cell-bound radioactivity. Values shown are the mean ± SEM of triplicate determinations. *, $P < 0.05$.

incubation with ^{111}In-trastuzumab. Figure 2.3D shows the internalized fraction expressed as a percentage of the total cell-bound radioactivity associated with each cell line. These were all significantly greater after incubation with ^{111}In-NLS$_3$-trastuzumab and ^{111}In-NLS$_6$-trastuzumab, compared to ^{111}In-trastuzumab. The remaining fraction of radioactivity that was removed in the acid wash was considered to be membrane bound.

After incubation with DTPA-trastuzumab or DTPA-NLS-trastuzumab, SK-BR-3, MDA-MB-361 and MDA-MB-231 cells were fixed and permeabilized before incubation with fluorophore-conjugated secondary antibodies specific for human IgG. As shown in Figure 2.4A-B, the nucleus and plasma membrane of MDA-MB-361 and SK-BR-3 cells demonstrated moderate to strong immunofluorescence after incubation with NLS-DTPA-trastuzumab, whereas the signal was restricted to the plasma membrane in cells treated with DTPA-trastuzumab. In contrast, the fluorescence signal was not detected in HER2-negative MDA-MB-231 cells after incubation with DTPA-trastuzumab or NLS-DTPA-trastuzumab (Fig. 2.4C), or in SK-BR-3 cells incubated without trastuzumab (data not shown), thus demonstrating the specificity of the interactions.

2.3.4 Cytotoxicity of ^{111}In-NLS-trastuzumab and DNA damage in breast cancer cells

There was a dose-dependent effect on the clonogenic survival of SK-BR-3 cells treated with ^{111}In-NLS$_3$-trastuzumab or ^{111}In-NLS$_6$-trastuzumab and the survival was significantly reduced to 24.0 ± 4.7% and 10.5 ± 2.1%, respectively, at the highest concentration tested, whereas ^{111}In-trastuzumab and unlabeled trastuzumab reduced the survival to 52.7 ± 3.0% and 64.6 ± 3.0%, respectively (Fig. 2.5A). There was no significant toxicity towards SK-BR-3 cells after treatment with irrelevant ^{111}In-NLS-hIgG. MDA-MB-361 cells were less sensitive to the cytotoxic effects of ^{111}In-NLS-trastuzumab, however, their clonogenic survival was similarly reduced in a dose-dependent fashion to 40.3 ± 7.6% and 26.6 ± 6.7% when treated at the highest concentration of ^{111}In-NLS$_3$-trastuzumab or ^{111}In-NLS$_6$-trastuzumab, respectively (Fig. 2.5B). Modest killing of MDA-MB-361 cells was obtained with ^{111}In-trastuzumab without NLS-peptides and unlabeled trastuzumab; at similar concentrations the survival of MDA-MB-361 cells was reduced to 66.0 ± 3.4% and 83.7 ± 1.8% respectively. Conversely, ^{111}In-trastuzumab

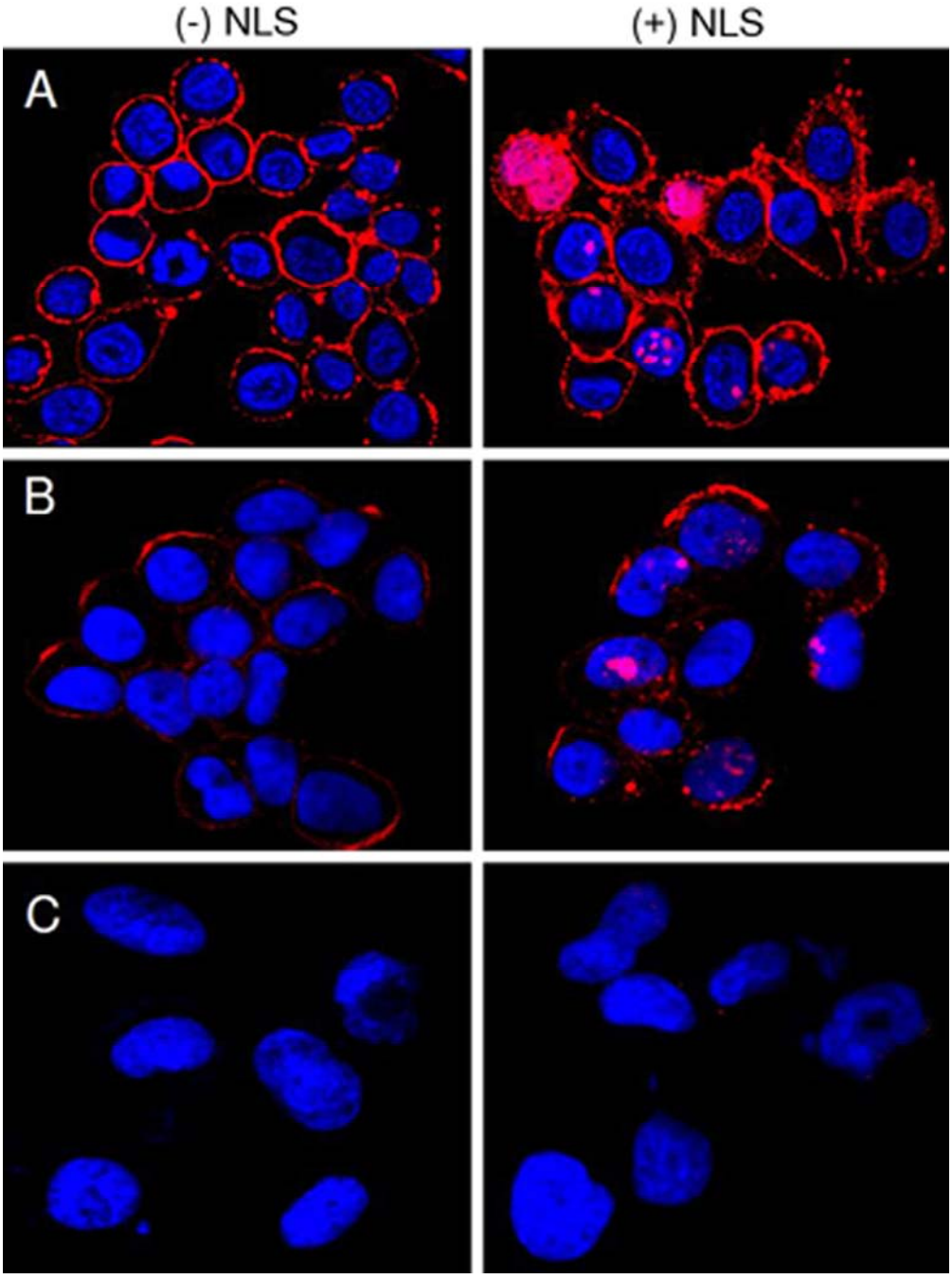
(-) NLS
(+) NLS
A
B
C

Fig. 2.4: Confocal immunofluorescence microscopy of **(A)** SK-BR-3, **(B)** MDA-MB-361 and **(C)** MDA-MB-231 cells incubated with DTPA-trastuzumab with (+) or without (-) NLS-peptides. Trastuzumab was detected using an AlexaFluor-564 anti-human IgG secondary antibody (red), and the nucleus was visualized with DAPI (blue). Merging of the two signals are shown and the images are 1 μm slices through the cells.

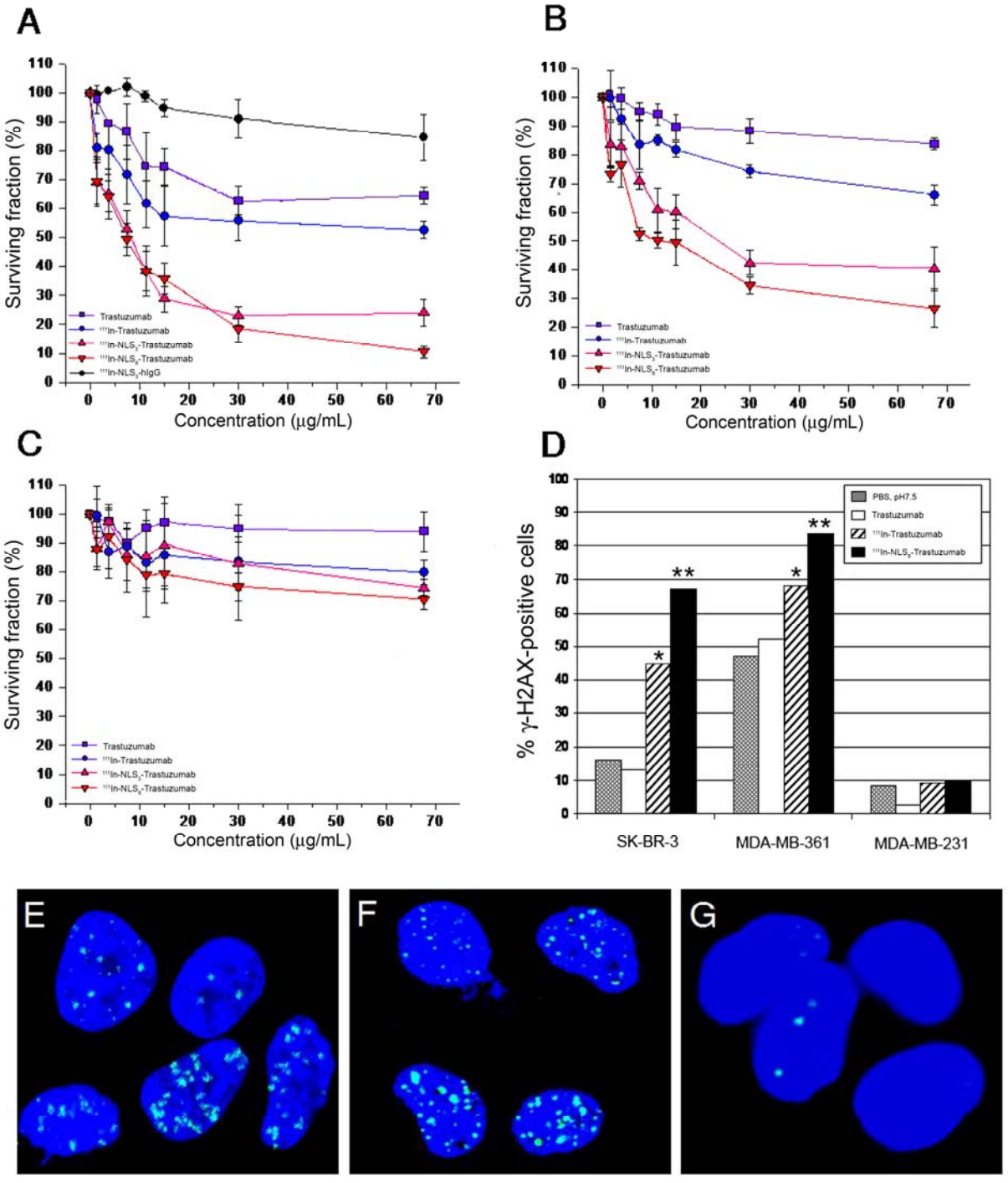
A
Surviving fraction (%)
Concentration (μg/mL)
Trastuzumab
111In-Trastuzumab
111In-NLS1-Trastuzumab
111In-NLS2-Trastuzumab
111In-NLS1-hIgG
B
Surviving fraction (%)
Concentration (μg/mL)
Trastuzumab
111In-Trastuzumab
111In-NLS1-Trastuzumab
111In-NLS2-Trastuzumab
C
Surviving fraction (%)
Concentration (μg/mL)
Trastuzumab
111In-Trastuzumab
111In-NLS1-Trastuzumab
111In-NLS2-Trastuzumab
D
% γ-H2AX-positive cells
PBS, pH7.5
Trastuzumab
111In-Trastuzumab
111In-NLS2-Trastuzumab
SK-BR-3
MDA-MB-361
MDA-MB-231
E
F
G

Fig. 2.5: Cell survival curves measured in clonogenic assays for **(A)** SK-BR-3, **(B)** MDA-MB-361 and **(C)** MDA-MB-231 breast cancer cells treated with increasing concentrations of ^{111}In-trastuzumab, ^{111}In-NLS$_3$-trastuzumab or ^{111}In-NLS$_6$-trastuzumab. Controls consisted of cells treated with unlabeled trastuzumab or irrelevant ^{111}In-NLS$_3$-IgG. Each point represents the mean ± SEM of 3 experiments performed in triplicate. **(D)** Percentage of cells positive for DNA damage (>10 γH2AX-foci/cell) after treatment with PBS-pH7.5, unlabeled trastuzumab, ^{111}In-trastuzumab or ^{111}In-NLS$_6$-trastuzumab. Significant differences are *P<0.05: ^{111}In-trastuzumab compared with unlabeled trastuzumab and **P<0.05: ^{111}In-NLS$_6$-trastuzumab compared with ^{111}In-trastuzumab. Induction of γH2AX-foci (green) in **(E)** SK-BR-3, **(F)** MDA-MB-361 and **(G)** MDA-MB-231 cells after ^{111}In-NLS$_6$-trastuzumab treatment. Nuclear DNA was stained with DAPI (blue).

and ^{111}In-NLS-trastuzumab demonstrated only weak cytotoxicity towards HER2-negative MDA-MB-231 cells (Fig. 2.5C).

As shown in Fig. 2.5 D-G, the percentage of γH2AX-positive SK-BR-3 and MDA-MB-361 cells increased significantly from 45% and 68% after treatment with ^{111}In-trastuzumab, to 67% and 84% after treatment with ^{111}In-NLS-trastuzumab, respectively (chi-square analysis, $P<0.05$). In contrast, the proportion of γH2AX-positive trastuzumab-treated SK-BR-3 or MDA-MB-361 cells were not significantly different than PBS-treated controls. Less than 10% of MDA-MB-231 cells exposed to any of the treatments were γH2AX-positive.

2.3.5 Biodistribution and nuclear importation of ^{111}In-NLS-trastuzumab in breast cancer xenografts and normal tissues

Tumor uptake in athymic mice bearing s.c. HER2-positive MDA-MB-361 breast cancer xenografts at 72 hours p.i. was relatively high and ranged from 13.2 ± 2.2% ID/g for ^{111}In-trastuzumab to 12.4 ± 1.3% and 12.6 ± 0.4% ID/g for ^{111}In-NLS_3-trastuzumab and ^{111}In-NLS_6-trastuzumab, respectively ($p > 0.05$; Table 2.1). Tumor-to-blood ratios were 6.04 ± 0.8 and 5.7 ± 0.7 for ^{111}In-NLS_3-trastuzumab and ^{111}In-NLS_6-trastuzumab, respectively, compared to 6.6 ± 1.1 for ^{111}In-trastuzumab. The highest concentration of radioactivity in normal tissues was found in liver, kidney and spleen. In contrast, tumor uptake of ^{111}In-NLS-hIgG was significantly lower than for ^{111}In-NLS-trastuzumab (4.8 ± 0.8%) and the tumor-to-blood ratio was only 1.7 ± 0.4, indicating that ^{111}In-NLS-trastuzumab specifically targeted HER2-positive tumors in athymic mice.

Radioactivity that accumulated in the nuclei of tumor cells, as well as cells of selected normal tissues (liver, kidneys, spleen and heart) in athymic mice bearing s.c. MDA-MB-361 xenografts at 72 h p.i. of ^{111}In-trastuzumab or ^{111}In-NLS-trastuzumab are shown in Table 2.2. The percentage of radioactivity associated with the nuclei of MDA-MB-361 cells for ^{111}In-NLS_3-trastuzumab and ^{111}In-NLS_6-trastuzumab was significantly higher than that for ^{111}In-trastuzumab or ^{111}In-NLS_3-hIgG. Conversely, the percentage of radioactivity in the nuclei of cells in liver, spleen, kidney or heart was not significantly different for any of the ^{111}In-labeled antibodies. On a %ID/g basis, approximately 20% of the radioactivity that accumulated in MDA-MB-361 tumor xenografts for ^{111}In-NLS-trastuzumab was present in the nuclear fraction,

Table 2.1 - Tumor and normal tissue uptake in MDA-MB-361 tumor bearing mice 72 h post i.v. injection

	^{111}In-trastuzumab	^{111}In-NLS$_3$-trastuzumab	^{111}In-NLS$_6$-trastuzumab	^{111}In-NLS$_3$-hIgG
Blood	2.30 ± 0.37	2.31 ± 0.48	2.20 ± 0.12	3.18 ± 0.51
Bladder	2.81 ± 0.53	2.26 ± 0.37	2.37 ± 0.22	3.83 ± 0.66
Large Intestine	1.59 ± 0.13	1.20 ± 0.21	1.26 ± 0.07	1.36 ± 0.09
Small Intestine	2.44 ± 0.21	1.87 ± 0.21	1.91 ± 0.16	2.05 ± 0.15
Stomach	1.06 ± 0.10	0.89 ± 0.16	0.84 ± 0.12	0.99 ± 0.10
Spleen	7.17 ± 0.47	6.68 ± 0.83	7.05 ± 1.08	7.13 ± 0.61
Liver	11.46 ± 0.51	11.02 ± 0.37	12.27 ± 0.41	12.60 ± 0.91
Kidney	7.95 ± 0.53	7.70 ± 0.80	8.01 ± 0.26	8.23 ± 0.84
Lung	3.20 ± 0.21	2.64 ± 0.33	2.81 ± 0.05	3.63 ± 0.33
Heart	2.35 ± 0.26	2.08 ± 0.37	2.27 ± 0.13	2.54 ± 0.33
Muscle	1.37 ± 0.18	1.03 ± 0.22	0.90 ± 0.07	1.33 ± 0.26
Skin	2.11 ± 0.21	2.10 ± 0.50	2.05 ± 0.20	2.90 ± 0.38
Bone Marrow	2.73 ± 0.71	2.92 ± 0.12	2.68 ± 0.28	3.33 ± 0.54
Tumor	13.17 ± 2.22[a]	12.14 ± 1.34[b]	12.62 ± 0.44[c]	4.78 ± 0.76[d]

The results are expressed as mean % ID/g with the SEM (n=6, except bone marrow where n=3).

[a-d, b-d, c-d] Significantly different. [a-b, a-c, b-c] Not significantly different. Statistical comparisons between groups were made by Student's *t* test (P<0.05).

Table 2.2 - *In vivo* nuclear uptake in MDA-MB-361 tumor bearing mice 72 h post i.v. injection

	^{111}In-trastuzumab	^{111}In-NLS$_3$-trastuzumab	^{111}In-NLS$_6$-trastuzumab	^{111}In-NLS$_3$-hIgG
Liver	0.78 ± 0.17	1.11 ± 0.30	1.14 ± 0.35	1.21 ± 0.30
Kidney	0.80 ± 0.28	1.16 ± 0.13	1.00 ± 0.35	1.14 ± 0.24
Spleen	0.51 ± 0.22	0.85 ± 0.13	1.08 ± 0.05	0.87 ± 0.22
Heart	0.15 ± 0.02	0.12 ± 0.04	0.15 ± 0.07	0.11 ± 0.02
Tumor	1.13 ± 0.32[a]	2.42 ± 0.24[b]	2.89 ± 0.35[c]	0.48 ± 0.08[d]

The results are expressed as mean % ID/g with the SEM (n=3).

[a-b, a-c, b-d, c-d] Significantly different. [a-d, b-c] Not significantly different. Statistical comparisons between groups were made by Student's *t* test ($P<0.05$).

whereas only 10% was detected in the nuclear fraction for ^{111}In-trastuzumab or ^{111}In-NLS$_3$-hIgG (Tables 2.1 and 2.2).

2.4 Discussion

The results of this study demonstrated that synthetic 13-mer peptides (CGYGPKKKRKVGG) harboring the NLS of SV-40 large-T antigen facilitated the translocation of ^{111}In-trastuzumab into the nucleus of HER2-overexpressing breast cancer cells, where the cytotoxicity of the emitted Auger electrons was enhanced. Furthermore, the dose-dependent cytotoxicity of ^{111}In-NLS-trastuzumab against breast cancer cells was shown to be specific and directly correlated with the cell surface expression level of HER2. In the clinical setting, metastatic breast cancer patients are selected for treatment with trastuzumab only if the primary tumor demonstrates significantly amplified HER2 expression (i.e. Herceptest® or other immunohistochemical (IHC) score of 3^+ and/or moderate-high levels of gene amplification by fluorescence *in situ* hybridization [FISH]); these patients exhibit a better response than those with lower gene copy number by FISH-and/or intermediate staining tumors (i.e. Herceptest® score $\leq 2^+$) (*34,140*). Nevertheless, those patients who show an initial response to trastuzumab often acquire resistance to the drug in less than a year (*140*). The dramatically enhanced cytotoxic effects of ^{111}In-NLS-trastuzumab compared to unlabeled trastuzumab found in this study if translated into *in vivo* anti-tumor effects suggest that this radiotherapeutic agent could potentially offer a more effective treatment for HER2-positive metastatic breast cancer.

^{111}In-labeled 4D5 and 21.1 murine mAbs specific for HER2 have previously been found effective for killing SK-BR-3 breast and SK-OV-3.ip1 ovarian carcinoma cells, either alone or in combination (*103*). It was anticipated that the cytotoxic effects of ^{111}In-trastuzumab (humanized version of 4D5) would be equally as effective as its ^{111}In-labeled 4D5 murine counterpart. At the specific activities used in this study (~240 MBq/mg), ^{111}In-trastuzumab only demonstrated a 1.2-fold increase in toxicity compared to unlabeled trastuzumab (Fig. 2.5). Nearly 99% of the low-energy Auger electrons emitted by ^{111}In have a range of less than 1 μm in tissues (*141*), and the radiation absorbed dose to the nucleus is 2-fold and 35-fold greater when ^{111}In decays in the nucleus compared to when the decay occurs in the cytoplasm or on the

cell surface, respectively (*87*). Therefore, we further modified ^{111}In-trastuzumab with NLS-peptides in order to enhance its radiotoxicity through promoting its nuclear uptake following receptor-mediated endocytosis. Indeed, ^{111}In-NLS-trastuzumab substituted with 6 NLS-peptides was approximately 2-fold and 5-fold more potent at killing MDA-MB-361 and SK-BR-3 cells compared to ^{111}In-trastuzumab, and nearly 3-fold and 6-fold more effective than unlabeled trastuzumab, respectively (Fig. 2.5). Moreover, the increased sensitivity to cell killing correlated with an increase in γH2AX-foci in MDA-MB-361 and SK-BR-3 cells after exposure to ^{111}In-trastuzumab (1.3 and 3.5-fold increase, respectively) and ^{111}In-NLS-trastuzumab (1.6 and 5.2-fold increase, respectively), illustrating the effects of subcellular distribution in determining the biological impact of Auger electron emitters (*90,87*). Unexpectedly, MDA-MB-361 cells demonstrated substantial basal levels of γH2AX-foci; these findings may be explained by a mutation in p53 in these cells that could result in an inability to respond appropriately to DNA strand breaks (*142*). Less than 10% of MDA-MB-231 cells were killed after exposure to ^{111}In-NLS-trastuzumab, suggesting that the toxicity of the radiopharmaceutical was HER2-selective.

After incubation with ^{111}In-trastuzumab or ^{111}In-NLS-trastuzumab, 55-80% of the radioactivity associated with HER2-positive breast cancer cells remained surface bound (Fig. 2.3D), which was consistent with the robust membrane immunofluorescence that was visualized on these cells after incubation with the antibodies (Fig. 2.4). These findings are in agreement with previous observations that HER2-bound trastuzumab is predominantly surface-localized, and is slowly taken up into SK-BR-3 cells with an internalization half-life of approximately 19 h (*143*). However, the NLS of SV-40 large-T antigen (*123*) was nevertheless able to mediate the translocation of covalently linked ^{111}In-trastuzumab molecules into the nuclei of HER2-expressing breast cancer cells following their receptor mediated-internalization (Fig. 2.4 and Table 2.2). Other NLS-containing bioconjugates labeled with Auger electron-emitting radionuclides have been described. For example, we recently reported that NLS-peptide modification of ^{111}In-HuM195 mAb, specific for CD33-epitopes, promoted its nuclear translocation in HL-60 leukemic cells, and was 12-fold more radiotoxic than unmodified ^{111}In-HuM195 (*125*). Similarly, NLS-peptides promoted the translocation of radioactivity into the nucleus of human embryonic kidney (HEK-293) cells (transfected with the somatostatin receptor-2A [SSR2A]) when incubated with an ^{111}In-labeled somatostatin-based analogue (*126*).

NLS-peptides have also been shown to promote the translocation of a $[^{99m}Tc(OH_2)_3(CO)_3]^+$-labeled DNA-intercalating pyrene moeity into the nuclei of B16F1 mouse melanoma cells, where the Auger electrons from ^{99m}Tc were lethal (*131*). Taken together, these studies demonstrate that bioconjugates internalized into tumor cells through receptor-mediated processes can be efficiently routed to the nucleus through their modification with NLS-containing peptides.

The NLS-peptides mediated nuclear translocation of ^{111}In-trastuzumab but it was critical to preserve HER2 receptor-binding to permit internalization into breast cancer cells *in vitro* as well as to target these radiopharmaceuticals to HER2-positive tumors *in vivo*. Despite the minor (< 3-fold) decrease in HER2 receptor-binding affinity (Fig. 2.2), the magnitude of internalization of ^{111}In-NLS-trastuzumab into SK-BR-3, MDA-MB-361 and MDA-MB-231 cells was correlated with their relative expression of HER2 (Fig. 2.3). It should be noted, however, that the internalization values are possibly underestimates since it has been shown that exposure of cells to low pH buffers to remove surface-bound radioligands may also remove some internalized radioactivity (*144*). Nevertheless, the internalization of ^{111}In-NLS-trastuzumab was significantly higher than the uptake of ^{111}In-trastuzumab without NLS-peptides. As discussed previously, NLS-peptides mediate nuclear importation, but the mechanism of this NLS-enhanced but HER2 receptor-mediated cellular penetration of ^{111}In-trastuzumab is not known. However, Ginj et al. similarly reported a 3.6-fold higher uptake of an ^{111}In-labeled somatostatin-based conjugate in AR4-2J rat pancreatic acinar tumor cells when modified with the NLS of SV-40 large-T antigen (*126*). It has been suggested that cationic macromolecules rapidly undergo endocytosis via an absorptive-mediated process through binding to negatively charged cell-surface proteins (*145*). Although the SV-40 NLS-peptides employed in our study possess several cationic lysine residues, the uptake of radioactivity by SK-BR-3 cells exposed to ^{111}In-NLS-trastuzumab was blocked by unlabeled trastuzumab, demonstrating that internalization was HER2-mediated. Ginj et al. (*126*) further showed that unconjugated ^{111}In-labeled NLS peptides (PKKKRKV) harboring the same SV-40 large-T antigen NLS as that in the NLS-peptides employed in our study were not significantly bound or internalized into tumor cells.

There were no significant differences in tumor uptake and T/B ratios for ^{111}In-NLS-trastuzumab and ^{111}In-trastuzumab in MDA-MB-361 xenograft bearing mice, but these were significantly higher than for irrelevant ^{111}In-NLS_3-hIgG, thus demonstrating that tumor uptake was HER2-specific (Table 2.1). Normal tissue uptake was comparable to that reported for ^{111}In-trastuzumab in mice bearing SK-OV-3 human ovarian cancer xenografts (*146*). Thus, the NLS-peptides did not affect the biodistribution properties of ^{111}In-trastuzumab, but did promote HER2-specific nuclear uptake *in vivo* in MDA-MB-361 breast cancer xenografts (Table 2). In contrast, no differences in nuclear uptake between ^{111}In-trastuzumab and ^{111}In-NLS-trastuzumab were found in cells isolated from the liver, spleen, kidneys and heart, which may be attributable to the fact that trastuzumab only recognizes human HER2 (*146*); the inability to cross-recognize mouse c-erbB-2 would preclude receptor-mediated internalization of ^{111}In-NLS-trastuzumab into these cells, although there remains the possibility of Fc-mediated internalization by hepatocytes or splenocytes.

Microdosimetry estimates to the nucleus of a single MDA-MB-361 cell (1×10^6 HER2 receptors/cell) from exposure to ^{111}In-NLS-trastuzumab (specific activity 240 MBq/mg; 3.6×10^{10} MBq/mole) at receptor-saturation conditions were calculated using the method of Goddu et al. (*147*) (Table 2.3) based on the following assumptions: i) the compartmental distribution in the cells was 70% bound to the membrane, 10% in the cytoplasm and 20% in the nucleus based on the results of the internalization and nuclear fractionation experiments (Fig. 2.3 and Table 2.2), ii) the diameter of the cell and nucleus were 10 μm and 6 μm, respectively, and iii) there was elimination from these subcellular compartments only by radioactive decay. The microdosimetry estimates revealed that ^{111}In-NLS-trastuzumab could potentially deliver as much as 27.9 Gy to the nucleus of a MDA-MB-361 cell. These radiation absorbed doses are 1.4-fold higher than those previously reported by us for MDA-MB-468 cells (19.3 Gy) for ^{111}In-DTPA-hEGF, an Auger electron-emitting radiotherapeutic agent for metastatic breast cancer overexpressing EGFR (*87*). Furthermore, they reveal that the 20% of radioactivity imported into the nucleus of a MDA-MB-361 cell accounts for approximately 90% of the total radiation absorbed dose in the cell nucleus. Higher doses would obviously be delivered to SK-BR-3 cells (2×10^6 HER2 receptors/cell), and lower doses to MDA-MB-231 cells that express 150-fold lower level of HER2 (*136*).

Table 2.3 - Radiation absorbed dose estimates to cell nucleus by ^{111}In-NLS-trastuzumab localized in compartments of MDA-MB-361 human breast cancer cell*

Cell Compartment	$\tilde{A}^{\dagger}$ (Bq × s)	S ([Gy/Bq × s] × 10^{-4})	Radiation dose to cell nucleus $D^{\ddagger}$ (Gy)
Membrane	14,500	1.78	2.58
Cytoplasm	2,100	3.18	0.67
Nucleus	4,100	60.30	24.72
		Total	27.97

*Cellular radiation dosimetry model of Goddu et al. (*147*) was used to estimate radiation absorbed dose (D) to cell nucleus: $D = \tilde{A} \times S$, where S is radiation absorbed dose in nucleus (Gy) per unit of cumulated radioactivity in source compartment, $\tilde{A}$ (Bq × s).

†Assumes rapid localization of ^{111}In-NLS-trastuzumab in compartment and rate of elimination corresponding to radioactive decay of radionuclide, ^{111}In. $\tilde{A} = A_0/\lambda$, where A_0 is amount of radioactivity localized in compartment at time 0 and λ is radioactive decay constant for ^{111}In (2.83×10^{-6}/s).

‡Based on targeting a single MDA-MB-361 human breast cancer cell with diameter of 10 μm and nucleus with diameter of 6 μm to receptor saturation with ^{111}In-NLS-trastuzumab. At concentrations of radioligand leading to receptor saturation, ~60 mBq ^{111}In-NLS-trastuzumab would be bound to each MDA-MB-361 cell at specific activity of 3.6×10^{10} MBq/mol.

2.5 Conclusion

We conclude that NLS-peptides efficiently routed ^{111}In-trastuzumab to the nucleus of HER2-positive human breast cancer cells, where the nanometer-to-micrometer Auger electrons rendered the radiotherapeutic agent damaging to DNA and lethal to the cells. The efficacy of ^{111}In-NLS-trasutuzumab for eradicating cultured HER2-overexpressing breast cancer cells *in vitro* and its favorable tumor-targeting properties *in vivo* warrants future radioimmunotherapeutic studies in mice to evaluate its anti-tumor properties and normal tissue toxicities. These studies are currently being planned by our group.

CHAPTER 3:

TRASTUZUMAB RESISTANT BREAST CANCER CELLS REMAIN SENSITIVE TO THE AUGER ELECTRON-EMITTING RADIOTHERAPEUTIC AGENT ^{111}IN-NLS-TRASTUZUMAB AND ARE RADIOSENSITIZED BY METHOTREXATE

This chapter represents a reprint of: “Danny L. Costantini, Katherine Bateman, Kristin McLarty, Katherine A. Vallis, and Raymond M. Reilly. Trastuzumab resistant breast cancer cells remain sensitive to the Auger electron-emitting radiotherapeutic agent ^{111}In-NLS-trastuzumab and are radiosensitized by methotrexate. *J Nucl Med*. 2008 49(9):1498-505.” **Reprinted by permission of the Society of Nuclear Medicine on October 10, 2008.**

All experiments and analyses of data were carried out by Costantini DL, except for the clonogenic assay studies (Bateman K).

3.0 Abstract

Introduction: Our goals were to determine if ^{111}In-trastuzumab coupled to peptides harboring nuclear localizing sequences (NLS) could kill trastuzumab-resistant breast cancer cell lines through the emission of Auger electrons, and whether the combination of radiosensitization with methotrexate (MTX) would augment the cytotoxicity of this radiopharmaceutical. **Methods:** Trastuzumab was derivatized with sulfosuccinimidyl-4-(N-maleimidomethyl)cyclohexane-1-carboxylate for reaction with NLS-peptides and then conjugated with diethylenetriaminepentaacetic acid for labeling with ^{111}In. HER2 expression was determined by Western blot and by radioligand binding assay using ^{111}In-trastuzumab in a panel of breast cancer cell lines, including SK-BR-3, MDA-MB-231, its HER2-transfected subclone (231-H2N), and two trastuzumab-resistant variants (TrR1 and TrR2). Nuclear importation of ^{111}In-NLS-trastuzumab and of ^{111}In-trastuzumab in breast cancer cells was measured by subcellular fractionation, whereas the clonogenic survival of these cells was determined after incubation with ^{111}In-NLS-trastuzumab, ^{111}In-trastuzumab or trastuzumab, combined with or without MTX. Survival curves were analyzed according to the dose-response model and the radiation enhancement ratio (RER) was calculated from the survival curve parameters. **Results:** The expression of HER2 was highest in SK-BR-3 cells (12.6×10^5 receptors/cells) compared to 231-H2N and TrR1 cells (6.1×10^5 and 5.1×10^5 receptors/cell, respectively), and lowest in MDA-MB-231 and TrR2 cells (0.4×10^5 and 0.6×10^5 receptors/cell, respectively). NLS-peptides increased the nuclear uptake of ^{111}In-trastuzumab in MDA-MB-231, 231-H2N, TrR1 and TrR2 cells from 0.1±0.01%, 2.5±0.2%, 2.8±0.7% and 0.5±0.1%, to 0.5±0.1%, 4.6±0.1%, 5.2±0.6% and 1.5±0.2%, respectively. The cytotoxicity of ^{111}In-NLS-trastuzumab on breast cancer cells was directly correlated with their HER2 expression densities. On a molar concentration basis, the effective concentration required to kill 50% (EC_{50}) of 231-H2N and TrR1 cells for ^{111}In-NLS-trastuzumab was 9 to 12-fold lower than ^{111}In-trastuzumab, and 16 to 77-fold lower than trastuzumab. MDA-MB-231 and TrR2 cells were less sensitive to ^{111}In-NLS-trastuzumab or ^{111}In-trastuzumab, and both cell lines were completely insensitive to trastuzumab. The RER induced by MTX for 231-H2N and TrR1 cells after exposure to ^{111}In-NLS-trastuzumab was 1.42 and 1.68, respectively. **Conclusion:** We conclude that targeted Auger electron

radioimmunotherapy with ^{111}In-NLS-trastuzumab can overcome resistance to trastuzumab, and that MTX can potently enhance the sensitivity of HER2-overexpressing breast cancer cells to the lethal Auger electrons emitted by this radiopharmaceutical.

3.1 Introduction

Amplification of the HER2/c-erbB-2 proto-oncogene is estimated to occur in 25-30% of human breast cancers (*36*), and has been correlated with resistance to hormonal (*136,148,149*) and chemotherapy (*150*), and is directly associated with poor long-term survival (*36*). Trastuzumab (Herceptin®) is a humanized IgG_1 anti-HER2 monoclonal antibody (mAb) approved for immunotherapy of *HER2*-amplified breast cancer (*36*). Patients are eligible for treatment with trastuzumab based on immunohistochemical (IHC) staining of a tumor biopsy for HER2 protein overexpression (IHC scores of 2+ or 3+) or probing for *HER2* gene amplification by fluorescence *in situ* hybridization (FISH) (*151*). Even in this highly pre-selected population, however, only 12-35% respond to the drug as a single agent, and only half benefit when it is combined with chemotherapy (*36,34*). Especially disappointing is that almost all patients who respond to trastuzumab become refractory within a year, due to the emergence of resistance (*34,33*). Clearly, there is a need to substantially improve the effectiveness of trastuzumab, as well as devise alternative treatments for patients whose tumors are resistant to the drug despite HER2 overexpression, or that acquire resistance with treatment.

Our group is developing a new class of targeted radioimmunotherapeutics that rely on high linear energy transfer (LET) nanometer-to-micrometer range Auger electron-emitters such as ^{111}In to kill cancer cells (*101,125,152*). These densely ionizing radionuclides are highly cytotoxic and damaging to DNA when they decay in close vicinity to the cell nucleus, making them highly selective for killing targeted single cancer cells (*153*). To fully exploit Auger electrons for cancer therapy, however, the radionuclide must be delivered to tumor cells, internalized and transported to the nucleus, where these extremely short-range electrons are especially damaging and lethal (*90*). We recently reported a novel strategy to insert ^{111}In-labeled trastuzumab mAbs directly into the nucleus of HER2-amplified breast cancer cells by conjugating them to 13-mer synthetic peptides [CGYG*PKKKRKV*GG] harboring the localizing sequence (NLS) of the simian virus (SV)-40 large T-antigen (*italicized*) (*152*). ^{111}In-NLS-trastuzumab was internalized and imported into the nucleus of HER2-overexpressing breast cancer cells where it induced frequent DNA double strand breaks (DSBs), and strongly decreased their clonogenic survival. The SV-40 NLS-motif has similarly been used by others as

a means to route radiolabeled biomolecules into the nucleus of cancer cells for targeted Auger electron radiotherapy of malignancies (*124*).

Another possible approach to improving the tumoricidal effect of Auger electron radiotherapy is to amplify the potency of the targeted radiation dose through the use of radiosensitizers (*85,155*). The antimetabolite methotrexate (MTX), for example, is a known potent radiosensitizer that can amplify the lethal effects of ionizing radiation on tumor cells (*154*). MTX enters cells through the reduced folate carrier, and competes with intracellular folate to bind and inhibit the enzyme dihydrofolate reductase (DHFR) which results in the depletion of folate substrates such as tetrahydrofolate and 5,10-methylenetetrahydrofolate. The lack of reduced folates subsequently causes a critical shortage of thymidylate (deoxythymidine-5′-monophosphate [dTMP]) and purine nucleotides, resulting in arrest of both DNA synthesis and repair (*155*). The lethal effects of ionizing radiation are therefore exacerbated in thymidylate-depleted cells that have diminished DNA repair capacity (*155,133*). Our goal in the current study was to capitalize on the potential synergy between targeted Auger electron radiotherapeutics and the radiosensitizing agent MTX, in order to devise an alternative and potentially much more effective strategy for killing HER2-positive breast cancer cells with acquired trastuzumab resistance. We hypothesized that trastuzumab-resistant breast cancer cells that overexpress HER2 receptors would be sensitive to the cytotoxic effects of ^{111}In-trastuzumab modified with NLS-peptides, and that MTX would dramatically radiosensitize these cells to the DNA-damaging and lethal effects of the Auger electrons emitted from this radiotherapeutic agent.

3.2 Methods

3.2.1. Cell Culture

MDA-MB-231, SK-BR-3 and MCF-7 human breast cancer cells were obtained from the American Type Culture Collection (Manassas, VA), whereas the 231-H2N and trastuzumab resistant-1 and -2 (TrR1 and TrR2) cell lines were kindly provided by Dr. Robert S. Kerbel (Sunnybrook and Woman's College Health Sciences Centre, Toronto, ON). The 231-H2N cell

line was derived from MDA-MB-231 cells that were transfected to stably overexpress c-erbB-2 (HER2), whereas TrR1 and TrR2 cells were isolated from 231-H2N tumors in athymic mice with acquired trastuzumab resistance (*156*). All cell lines were cultured in Dulbecco's minimal essential medium (Ontario Cancer Institute, Toronto, ON) supplemented with 10% fetal bovine serum (FBS, Sigma-Aldrich, St. Louis, MO) containing 100 U/mL penicillin and 100 μg/mL streptomycin (P/S) at 37°C in an atmosphere of 5% CO_2, except for SK-BR-3 cells which were cultured in RPMI-1640 with 10% FBS and P/S.

3.2.2 ^{111}In-Trastuzumab and ^{111}In-human IgG modified with NLS-peptides

Trastuzumab (Herceptin) or non-specific, irrelevant human IgG (hIgG, product no. I4506; Sigma-Aldrich) were derivatized with diethylenetriaminepentaacetic acid dianhydride (DTPA) (Sigma-Aldrich) and sulfosuccinimidyl-4-(N-maleimidomethyl)cyclohexane-1-carboxylate (sulfo-SMCC; Pierce) for reaction with synthetic 13-mer NLS-peptides (CGYGPKKKRKVGG) and labeling with ^{111}In as described previously (*152*). Briefly, trastuzumab or hIgG (500 μg, 10 mg/mL) was reacted with a 10-fold molar excess of DTPA for 1 h at room temperature and then purified on a Sephadex-G50 mini-column prior to reaction with a 15-fold molar excess of sulfo-SMCC (2-5 mmol/L) at room temperature for 1 h. Maleimide-derivatized DTPA-trastuzumab or hIgG was purified on a Sephadex-G50 mini-column, transferred to a Microcon YM-50 ultrafiltration device (Amicon), concentrated to 2-5 mg/mL, and reacted overnight at 4^{o}C with a 60-fold molar excess of NLS-peptides (5-10 mmol/L diluted in PBS, pH 7.0). DTPA-trastuzumab or hIgG, modified with NLS-peptides (NLS-DTPA-trastuzumab or NLS-DTPA-hIgG), was purified on a Sephadex-G50 mini-column eluted with phosphate buffered saline (PBS), pH 7.5. We previously determined that 3-4 NLS-peptides are conjugated to trastuzumab at an SMCC:IgG:NLS-peptide molar ratio of 15:1:60 (*152*).

NLS-conjugated or unmodified DTPA-trastuzumab, or DTPA-NLS-hIgG, were radiolabeled by incubation of 37-111 MBq of mAbs with $^{111}InCl_3$ (MDS-Nordion, Kanata, ON) for 60 mins at room temperature. ^{111}In-labeled mAbs were purified on a Sephadex-G50 minicolumn and buffer exchanged to PBS, pH 7.5 using a Microcon YM-50 ultrafiltration device (Amicon). The radiochemical purity was routinely >97% as determined by instant thin-layer silica-gel chromatography (ITLC-SG; Pall Corp.) developed in 100 mmol/L sodium

citrate, pH 5.0. All radioactivity measurements were made using an automatic γ-counter (Wallac Wizard-1480; Perkin Elmer).3.1.3 Protein isolation and Western blot

Cells were grown in T-175 tissue culture flasks (Sarstedt Inc.) to 75-80% confluency in normal culture conditions. Plates were placed on ice, rinsed with ice-cold PBS, and lysed with cold buffer containing 20 mmol/L Tris (pH 7.5), 137 mmol/L NaCl, 100 mmol/L NaF, 10% glycerol, and protease inhibitors (Roche). Cells were scraped from plates, incubated on ice for 40 minutes, and centrifuged at 10,000 x g for 15 min. Protein concentration of the supernatant was determined using the bicinchoninic acid (BCA) protein assay kit (Pierce) with bovine serum albumin (BSA) as a standard.

For Western blot analysis, 50 μg of protein was aliquoted in 2 x SDS sample buffer containing β-mercaptoethanol and heated for 5 min. Proteins were fractionated on 4-20% SDS-polyacrylamide mini-gels and transferred to polyvinyldifluoride (PVDF) membranes (Roche). The PVDF membranes were blocked with 5% skim milk in PBS with 0.1% Tween 20 (PBS-T), and probed with primary antibody overnight at 4^{o}C. Extracellular erbB2 Ab-20 (L87 + 2ERB19, Medicorp, Montreal, Quebec) or β-actin (Sigma-Aldrich) were diluted 1:1000 in 5% milk in PBS-T, and detected with horse-radish peroxidase-conjugated anti-mouse IgG (Promega, Madison, WI) diluted 1:5000. Chemiluminescence detection was performed using the Western Lightning Reagent Plus (Perkin Elmer).

3.2.3 Radioligand binding assay

The number of HER2 receptors on breast cancer cells was determined by saturation radioligand binding assay at a single excess concentration of ^{111}In-trastuzumab. Approximately 1 x 10^{6} cells were incubated in microtubes for 4 h at 4^{o}C in 250 μL of medium containing 100 nmol/L of ^{111}In-trastuzumab. This concentration is 1000-fold greater than the K_d value of 0.1 nmol/L reported by Carter et al. (*31*) for trastuzumab IgG on HER2-overxpressing SK-BR-3 cells (1.0-2.0 x 10^{6} receptors per cell), and therefore was considered high enough to saturate the HER2 receptors on MDA-MB-231, 231-H2N, TrR1 and TrR2 breast cancer cells. After incubation, the cells were pelleted by centrifugation at 1000 x g for 5 min, rinsed twice with ice-cold media to remove unbound radioactivity (supernatant) from total cellular bound radioactivity (pellets), and measured in a γ-counter. The assay was performed in the absence

(total binding) or presence (non-specific binding) of a 100 μmol/L excess of unlabeled trastuzumab. Subtraction of non-specific binding from total binding yielded specific binding (nmol/L), which represented the maximum number of HER2 receptors on breast cancer cells assuming i) a 1:1 molar ratio of trastuzumab to receptor, and ii) all receptors were saturated (i.e. bound to antibody).

3.2.4 *In vitro* nuclear importation of ^{111}In-NLS-trastuzumab and ^{111}In-trastuzumab

Breast cancer cells were plated into T-75 tissue culture flasks (Sarstedt Inc.) at a density of 1 x 10^7 cells per flask and cultured overnight. After aspirating the media, cells were rinsed twice with PBS, pH 7.5 and incubated in medium containing 100 nmol/L of ^{111}In-NLS-trastuzumab or ^{111}In-trastuzumab for 24 h at 37^{o}C. The 24 h time point was chosen as we have shown previously that nuclear accumulation of ^{111}In-NLS-trastuzumab increases for up to 24 h in HER2-overexpressing breast cancer cells (*152*). After the incubation period, the medium was decanted and the cells were rinsed twice with ice-cold PBS, pH 7.5, to remove unbound radioactivity that was measured in a γ-counter. The cells were then harvested by scraping them into 1 mL of Nuclei EZ Lysis buffer (Sigma-Aldrich) and lysed according to the manufacturer's instructions. Nuclei (pellets) were separated from the cytoplasmic/membrane fraction (supernatant) by centrifugation for 5 min at 1000 x g, and the radioactivity in each fraction was measured in a γ-counter. We previously determined that this cell fractionation procedure yields a very pure nuclear fraction (*138*).

3.2.5 Clonogenic Assays

Approximately 2 x 10^6 breast cancer cells were incubated with ^{111}In-NLS-trastuzumab (1 - 450 nmol/L; 190 ± 8.9 MBq/mg) alone, or concurrently with a single, non-toxic concentration of MTX (i.e., concentration of drug resulting in >90% cell survival) in 1 mL of culture medium in microtubes for 24 h at 37^{o}C. Controls consisted of cells treated with normal saline, MTX (0.001 - 100 μmol/L), ^{111}In-trastuzumab (182 ± 10.5 MBq/mg), unlabeled trastuzumab or ^{111}In-labeled non-specific hIgG modified with NLS (171.0 ± 12.2 MBq/mg). For treatments including MTX, cells were 'serum-starved' by lowering the serum concentration from 10% to 1% in order to reduce the concentrations of thymidine, 5-methyl tetrahydrofolate, and purine ribonucleosides that counteract the effects of MTX (*157*). After treatment, the cells were then centrifuged at

1000 x g for 5 min and washed twice with 'normal' culture medium containing 10% serum. Sufficient cells were then plated in triplicate in 12-well plates and cultured in normal medium at 37^{o}C. After 10-14 d, colonies of ≥ 50 cells were stained with methylene blue and counted. The surviving fraction (SF) was calculated by dividing the number of colonies formed for treated cells by the number for untreated cells. Survival curves were derived by plotting the SF values versus the log molar concentration of antibody used, and the effective concentration 50 (EC_{50}) values were estimated using Origin 6.0 using the dose-response equation: $y = A1 + [(A2 - A1) / (1 + 10^{(\log EC50 - x)*p}]$, where p is the slope (set to equal -1), and A1 and A2 are the amplitudes of the baseline and maximum response, respectively. The mean inactivation dose (MID, area under the survival curve) and the radiation enhancement ratio for MTX (RER = MID [^{111}In-NLS-trastuzumab / (^{111}In-NLS-trastuzumab + MTX)] were also determined, and a RER value > 1 indicated radiosensitization by MTX (*158*).

3.2.6 Statistical Methods

Data are presented as mean ± SEM. Statistical comparisons were made using the Student *t* test. $P < 0.05$ was considered significant.

3.3 Results

3.3.1 Expression levels of HER2 extracellular domain

Trastuzumab binds HER2 on the C-terminal portion of the extracellular domain (ECD) near the juxtamembrane region in domain IV of the receptor (*30*). We therefore evaluated the expression of the HER2-ECD by Western blot in a panel of human breast cancer cell lines, including trastuzumab-sensitive SK-BR-3 cells, trastuzumab-insensitive MDA-MB-231 cells, its HER2-transfected subclone (231-H2N cells), and two trastuzumab-resistant subclones of 231-H2N cells (TrR1 and TrR2) (*152,156*). As shown in Fig. 3.1A, the HER2-ECD was abundantly expressed at a high level in whole cell lysates from SK-BR-3 cells, and at an intermediate level in 231-H2N and TrR1 cells. In contrast, the HER2-ECD was not detected in the lysates from MDA-MB-231 or TrR2 cells (Fig. 3.1A), in agreement with previously reported data (*168*).

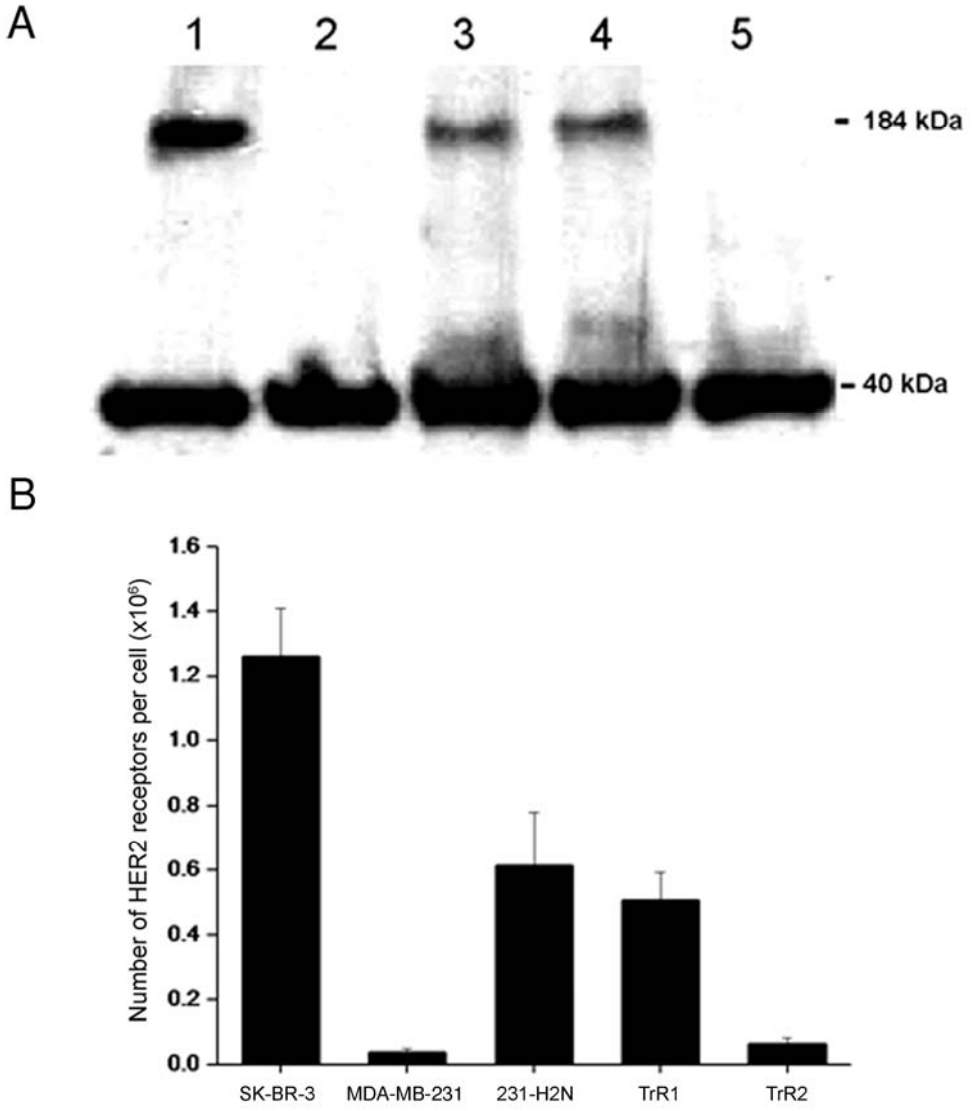

Figure 3.1: (A) Western blot for expression of HER2 extracellular domain (ECD; 184 kDa) in SK-BR-3 (lane 1), MDA-MB-231 (lane 2), 231-H2N (lane 3), TrR1 (lane 4) and TrR2 (lane 5) human breast cancer cells. β-actin (40 kDa) was used as a loading control. **(B)** Number of HER2 receptors on these cells determined by radioligand binding assay using a saturating concentration of ^{111}In-trastuzumab, with or without excess unlabeled trastuzumab (10 μmol/L).

The number of HER2 receptors in these cells was also quantified by radioligand binding assay using a single saturating concentration of ^{111}In-trastuzumab, with or without excess unlabeled trastuzumab (10 μmol/L). The number of HER2 receptors for SK-BR-3 cells was approximately 2-fold greater compared to 231-H2N and TrR1 cells (12.6×10^5 receptors per cell, versus 6.1×10^5 and 5.1×10^5 receptors per cell, respectively), and approximately 10-fold higher compared to MDA-MB-231 and TrR2 cells (0.4×10^5 and 0.6×10^5 receptors per cell, respectively) (Fig. 3.1B).

3.3.2 Nuclear importation of ^{111}In-NLS-trastuzumab and ^{111}In-trastuzumab in breast cancer cells

There was increasing nuclear importation of ^{111}In in breast cancer cells in accordance with their HER2 density when exposed to ^{111}In-NLS-trastuzumab or ^{111}In-trastuzumab (Fig. 3.2). After 24 h, the nuclear uptake of ^{111}In-NLS-trastuzumab in MDA-MB-231, 231-H2N, TrR1 and TrR2 breast cancer cells, with respect to the total amount of radioactivity added to incubation media, was 0.5% ± 0.1%, 4.6% ± 0.1%, 5.2% ± 0.6% and 1.5% ± 0.2%, respectively, compared to 0.1% ± 0.01%, 2.5% ± 0.2%, 2.8% ± 0.7% and 0.6% ± 0.1% for ^{111}In-trastuzumab.

3.3.3 Effect of ^{111}In-NLS-trastuzumab and ^{111}In-trastuzumab on the survival of breast cancer cells

The cytotoxicity of ^{111}In-NLS-trastuzumab against trastuzumab-sensitive and trastuzumab-resistant breast cancer cells was evaluated by clonogenic assay. There was a strong dose-dependent decrease in colony formation of H2N-231 and TrR1 cells treated with increasing amounts of ^{111}In-NLS-trastuzumab (Fig. 3.3B and 3.3C). The effective concentration required to kill 50% (EC_{50}) of 231-H2N cells for ^{111}In-NLS-trastuzumab was 9- and 16-fold lower compared to the EC_{50} for ^{111}In-trastuzumab or unlabeled trastuzumab (Table 3.1). Similar results were observed for TrR1 cells where the EC_{50} for ^{111}In-NLS-trastuzumab was significantly lower compared to that for ^{111}In-trastuzumab or unlabeled trastuzumab. In contrast, TrR2 and MDA-MB-231 cells were less sensitive to ^{111}In-NLS-trastuzumab or ^{111}In-trastuzumab, and both cell lines were completely refractory to unlabeled trastuzumab (Fig. 3.3A

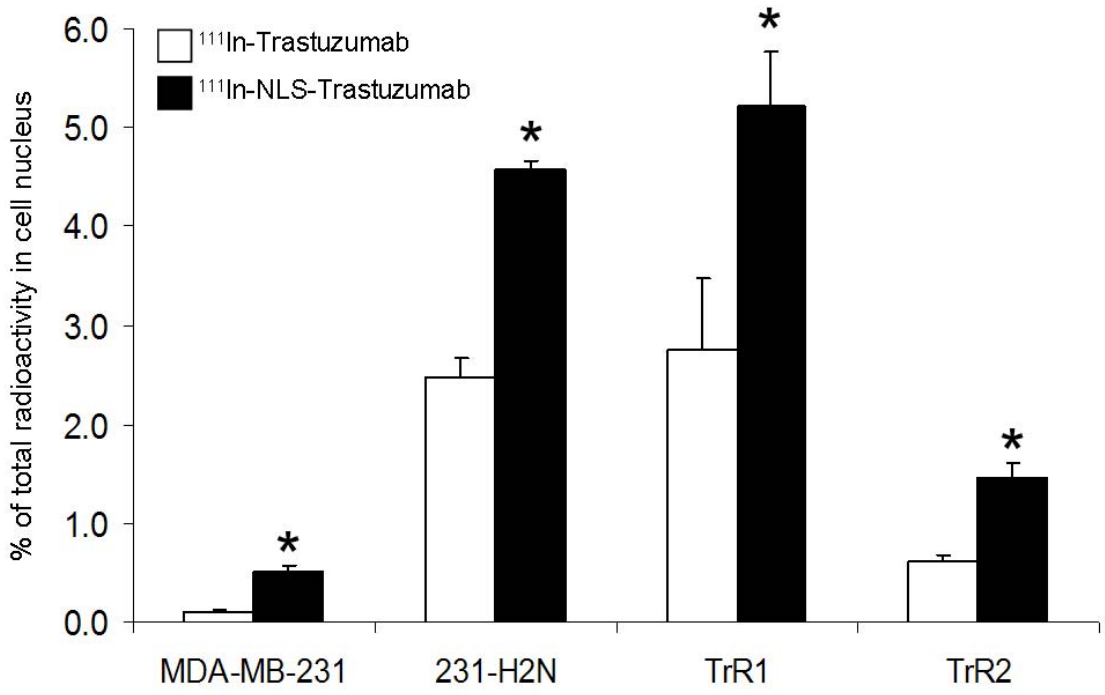

Figure 3.2: Nuclear importation of ^{111}In-trastuzumab and ^{111}In-NLS-trastuzumab by MDA-MB-231, H2N-231, TrR1 and TrR2 human breast cancer cells with respect to the total amount of radioactivity added to the incubation media. Values shown are mean ± SEM of four independent determinations (*, $P < 0.05$).

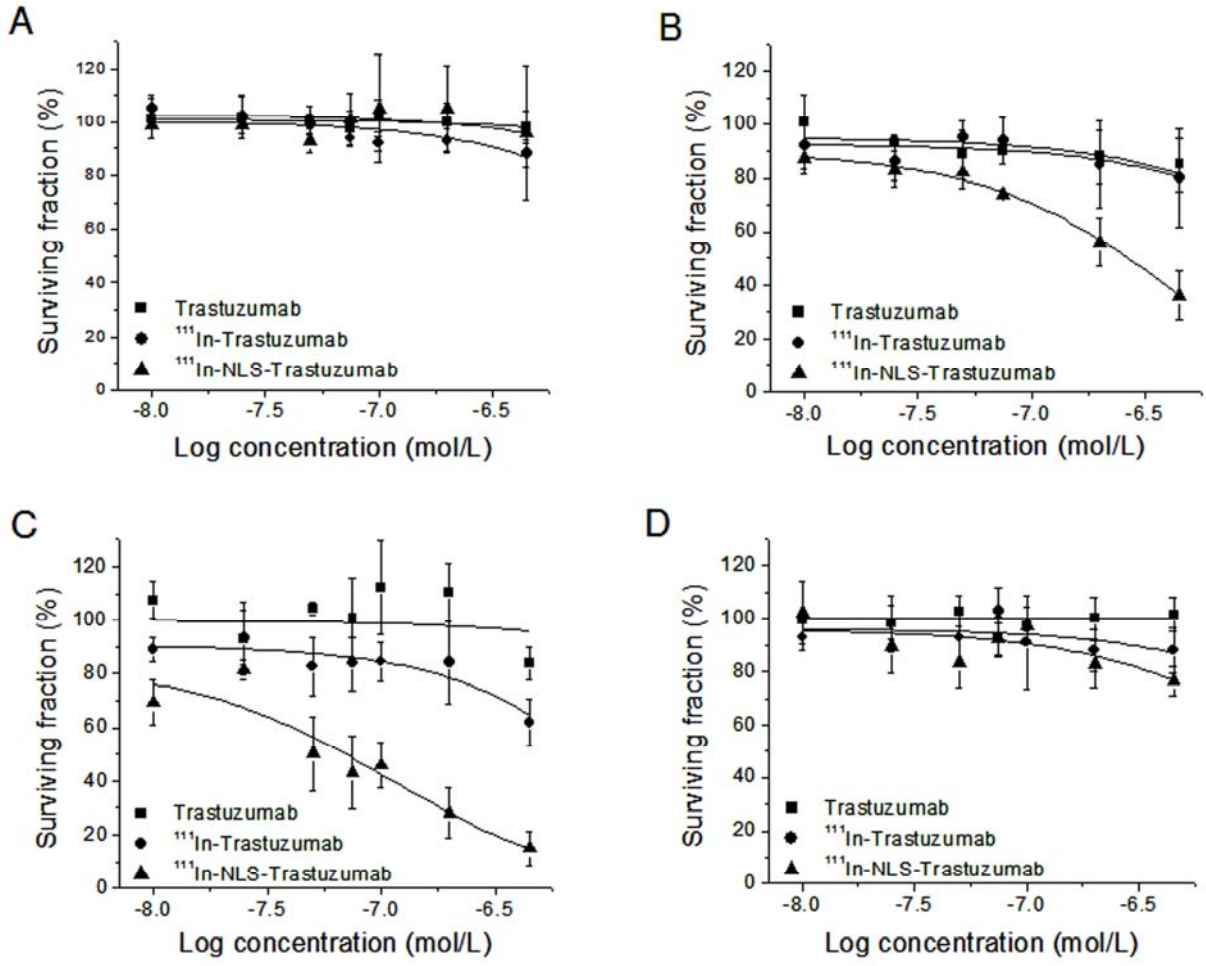

Figure 3.3: Clonogenic survival of trastuzumab-insensitive MDA-MB-231 **(A)** trastuzumab-sensitive 231-H2N **(B)** and trastuzumab-resistant TrR1 **(C)** and TrR2 **(D)** human breast cancer cells after exposure to increasing concentrations of trastuzumab, ^{111}In-trastuzumab or ^{111}In-NLS-trastuzumab. Each point represents the mean ± SEM of 3 to 5 experiments performed in triplicate.

Table 3.1 - EC_{50} for Trastuzumab, ^{111}In-Trastuzumab and ^{111}In-NLS-Trastuzumab on breast cancer cells with different HER2 expression and trastuzumab-resistance status*

	Trastuzumab	**^{111}In-Trastuzumab**	**^{111}In-NLS-Trastuzumab**
MDA-MB-231	8.3 ± 1.3	4.5 ± 0.6	5.4 ± 1.0
231-H2N	$3.2 \pm 0.8^{a,b,c}$	1.8 ± 0.5^{a}	$0.2 \pm 0.02^{a,c,d,e}$
TrR1	7.7 ± 1.3	$1.2 \pm 0.4^{a,c,d}$	$0.1 \pm 0.03^{a,c,d,e}$
TrR2	7.4 ± 1.2	3.4 ± 0.6^{d}	3.2 ± 0.7^{d}

* EC_{50} values are in μmol/L.

$P < 0.05$, compared to [a] MDA-MB-231, [b] TrR1, [c] TrR2, [d] Trastuzumab or [e] ^{111}In-Trastuzumab. Statistical comparisons between groups were made by Student *t* test. Results are expressed means ± SEM (n = 3-5).

and 3D, and Table 3.1). There was no significant toxicity toward 231-H2N cells after treatment with non-specific, irrelevant ^{111}In-NLS-hIgG control immunoconjugates (data not shown).

3.3.4 Effect of MTX treatment on the survival of breast cancer cells

The toxicity of exposure to MTX for 24 h for the different breast cancer cell lines was assessed by clonogenic assay, prior to evaluating its ability to sensitize these cells to Auger electron radiation. As illustrated in Fig. 3.4, MTX exerted a dose-dependent reduction in the clonogenic survival of serum-starved breast cancer cells. MCF-7 human breast cancer cells have previously been shown to be MTX-sensitive (*159*), and were therefore used as positive controls; this cell line exhibited a 50-fold greater sensitivity to MTX compared to MDA-MB-231, 231-H2N and TrR2 cells (EC_{50} 2.3 ± 0.6 μmol/L, versus 103.3 ± 13.4 μmol/L, 91.7 ± 13.9 μmol/L, 102.4 ± 10.7 μmol/L, respectively). In contrast, TrR1 cells gave an EC_{50} of 0.14 ± 0.03 μmol/L, which was 10-times lower compared to MCF-7 cells. The reason for this high sensitivity of TrR1 cells to MTX is not known.

3.3.5 Effect of combined treatment with ^{111}In-NLS-trastuzumab or unlabeled trastuzumab and low-dose MTX

The cytotoxicity of ^{111}In-NLS-trastuzumab was most evident against 231-H2N and TrR1 cells. Therefore, a fixed and non-cytotoxic concentration of MTX resulting in >90% survival of 231-H2N and TrR1 cells was chosen to evaluate the effect of combined treatment with ^{111}In-NLS-trastuzumab or unlabeled trastuzumab. For 231-H2N and TrR1 cells, the lowest non-cytotoxic dose of MTX was determined to be 10 μmol/L and 0.01 μmol/L, respectively. Fig. 3.5 compares the survival curves of serum-starved cells after combined treatment with low-dose MTX and increasing concentrations of ^{111}In-NLS-trastuzumab or unlabeled trastuzumab, and of serum-starved cells treated with ^{111}In-NLS-trastuzumab alone. The EC_{50} for ^{111}In-NLS-trastuzumab against 231-H2N and TrR1 cells treated concurrently with low-dose MTX was approximately 5-fold lower compared to cells treated with only ^{111}In-NLS-trastuzumab (Table 3.2). The RER induced by MTX for 231-H2N and TrR1 cells after exposure to ^{111}In-NLS-trastuzumab was estimated to be 1.42 and 1.68, respectively. Low-dose MTX had no effect on

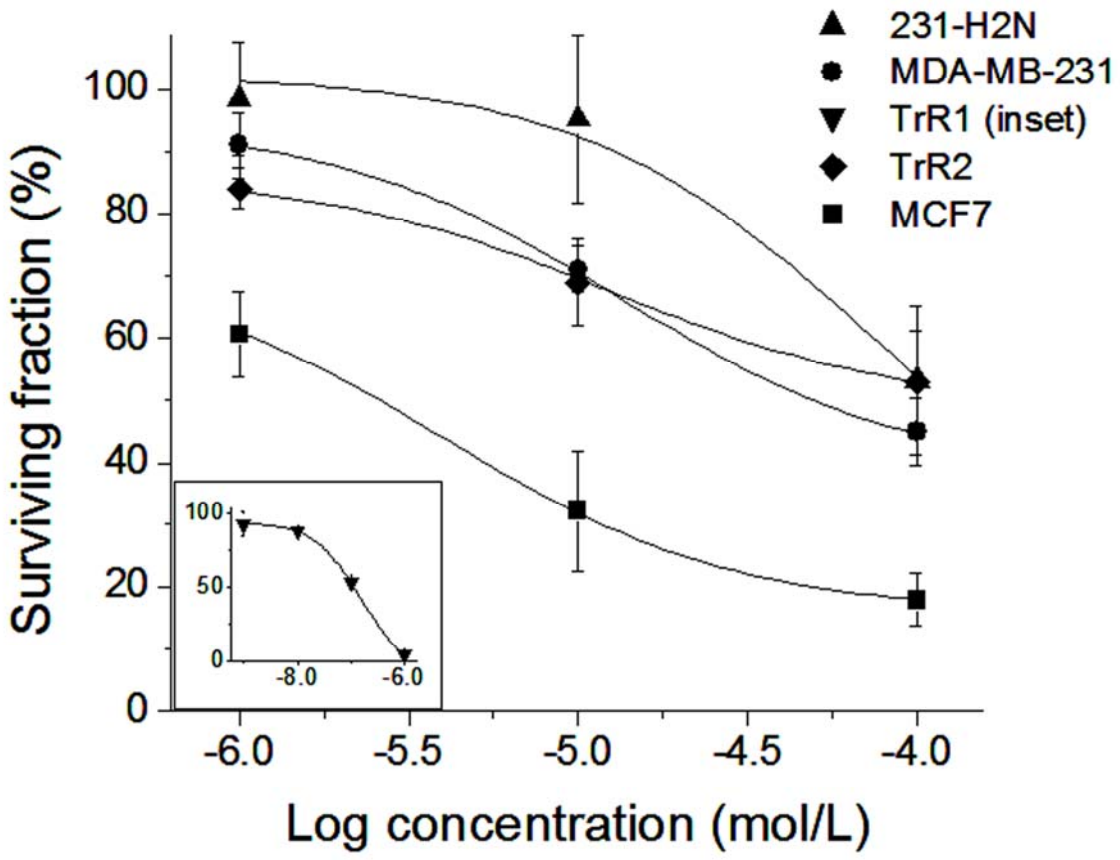

Figure 3.4: Clonogenic survival of serum-starved MCF7, MDA-MB-231, H2N-231, TrR1 (inset) and TrR2 human breast cancer cells after exposure to increasing concentrations of MTX. Each point represents the mean ± SEM of 3 experiments performed in triplicate.

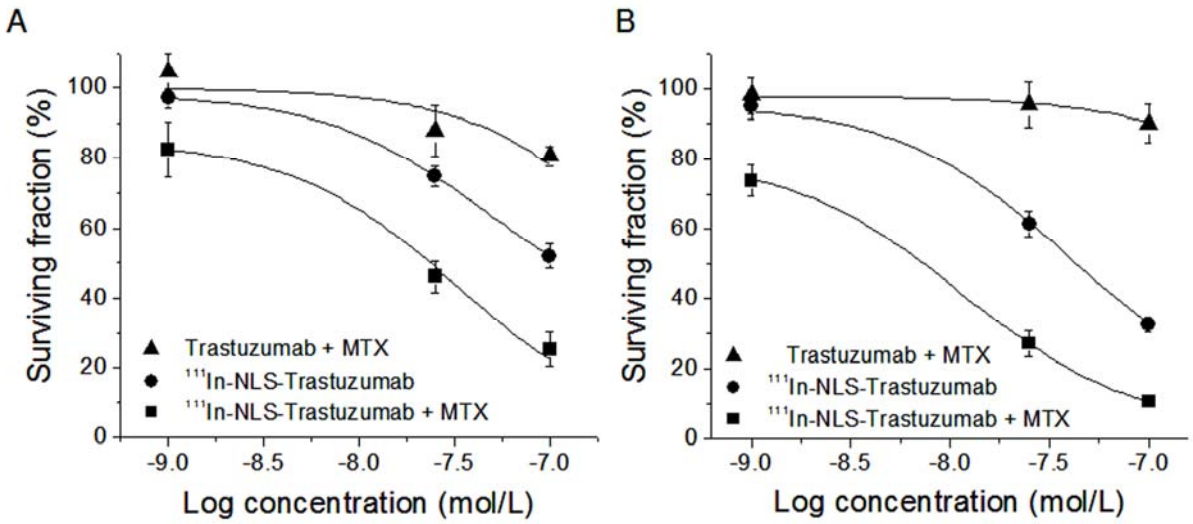

Figure 3.5: Clonogenic survival of serum-starved **(A)** 231-H2N and **(B)** TrR1 breast cancer cells after exposure to MTX plus trastuzumab, MTX plus ^{111}In-NLS-trastuzumab, or ^{111}In-NLS-trastuzumab alone. Each point represents the mean ± SEM of 3 experiments performed in triplicate.

Table 3.2 - EC_{50} for Trastuzumab and ^{111}In-NLS-Trastuzumab combined with MTX, or ^{111}In-NLS-Trastuzumab alone, on serum-starved 231-H2N and TrR1 breast cancer cells *

	231-H2N	**TrR1**
^{111}In-NLS-Trastuzumab [a]	139.7 ± 4.9	69.6 ± 13.1
^{111}In-NLS-Trastuzumab + MTX [b]	28.0 ± 5.6	13.5 ± 1.7
Trastuzumab + MTX [c]	2700 ± 0.2	5400 ± 1.4

* EC_{50} values are in nmol/L.

[a-b, a-c, b-c] Significantly different. Statistical comparisons between groups were made by Student *t* test ($P < 0.05$). Results are expressed means ± SEM (n = 3).

the EC_{50} value elicited by trastuzumab in TrR1 and 231-H2N cells compared to treatment with trastuzumab alone (Tables 3.1 and 3.2).

3.4 Discussion

Our results demonstrated that ^{111}In-labeled trastuzumab, modified with 13-mer peptides (CGYG*PKKKRKV*GG) harboring the NLS of SV-40 large T-antigen (*italicized*), can kill HER2-positive breast cancer cells resistant to trastuzumab. Furthermore, non-cytotoxic concentrations of MTX potently radiosensitized these cells to the high-LET and lethal Auger electron radiation emitted by ^{111}In-NLS-trastuzumab. Resistance to trastuzumab is a major challenge in the treatment of metastatic breast cancer (*49*). Even in responding patients, the effectiveness of trastuzumab is limited, and the duration of response short (*34,33*). If the results of this study are promising following *in vivo* testing, then the combination of radiosensitizing chemotherapy and targeted Auger electron radiotherapy using ^{111}In-NLS-trastuzumab represents a viable strategy to address this resistance issue.

The 231-H2N cell line is a HER2-transfected variant of MDA-MB-231 human breast cancer cells; these cells are growth inhibited by trastuzumab when grown as orthotopic tumors in severe combined immunodeficient mice (*168*). In our study, however, only a 20% reduction in the clonogenic survival of 231-H2N cells was observed after incubation with trastuzumab (Fig. 3.3). Many mechanisms are linked to the therapeutic effect of trastuzumab, some of which, like angiogenesis suppression, are only observed in an *in vivo* tumor xenograft model (*49*). 231-H2N cells were nevertheless efficiently killed by exposure to increasing concentrations of ^{111}In-NLS-trastuzumab. TrR1 cells were similarly killed by ^{111}In-NLS-trastuzumab, which is particularly intriguing because this variant cell line was derived from a mouse bearing a 231-H2N tumor xenograft with acquired resistance to trastuzumab (*156*). TrR2 cells were also isolated from trastuzumab-resistant 231-H2N tumor xenografts (*158*), however, this variant cell line was less sensitive to ^{111}In-NLS-trastuzumab or ^{111}In-trastuzumab, and was completely refractory to trastuzumab, likely due to a 10-fold lower HER2 density (Fig. 3.1 and Fig. 3.3).

The mechanism of resistance of TrR1 and TrR2 cells to trastuzumab is not known, but there are multiple mechanisms by which HER2-positive breast cancer cells are able to evade the

antiproliferative effects of the drug, including the loss of PTEN function (*162*), down-regulation of the cyclin-dependent kinase (CDK) inhibitor $p27^{kip1}$ (*160*), or up-regulation of epidermal growth factor (EGF) or insulin-like growth factor-I (IGF-I) receptors that compensate for the loss of HER2 signaling (*61,67*). Despite the emergence of these resistant pathways that block the growth-inhibiting effects of trastuzumab, the HER2-mediated internalization and nuclear-importation and of ^{111}In-NLS-trastuzumab in 231-H2N and TrR1 cells was preserved, irrespective of their trastuzumab resistance status (Fig. 3.2). Thus, these findings suggest for the first time that ^{111}In-NLS-trastuzumab could potentially be used to treat tumors in patients that are resistant to trastuzumab. Moreover, it is possible that targeted Auger electron radiotherapy may be able to overcome other forms of treatment resistance in breast cancer and other malignancies. For example, we previously demonstrated that ^{111}In-NLS-trastuzumab can kill MDA-MB-361 and SK-BR-3 breast cancer cells (*152*), that are known to have high levels of the multi-drug resistant (MDR) transporter, p-glycoprotein 170, and are resistant to paclitaxel (*161*). In addition, we have shown that ^{111}In-labeled anti-CD33 mAbs conjugated to NLS-peptides can kill HL-60/MX-1 myeloid leukemia cells that are resistant to mitoxantrone, as well as patient AML specimens that display high levels of MDR transporters, including pgp-170 (*162*).

The cytotoxicity of ^{111}In-NLS-trastuzumab on breast cancer cells was also directly correlated with their HER2 expression densities, with the greatest toxicity observed for 231-H2N and TrR1 cells, and the least toxicity found for MDA-MB-231 and TrR2 cells. These results confirm those previously reported for ^{111}In-NLS-trastuzumab against trastuzumab-sensitive SK-BR-3 (1-2 x 10^6 receptors/cell) and MDA-MB-361 (0.5 x 10^6 receptors/cell) breast cancer cells, where the radiopharmaceutical was significantly more potent at killing these cells than unlabeled trastuzumab (*152*). Nuclear localization is critically important for exploiting the lethality of Auger electron emitting radiopharmaceuticals towards cancer cells because more than 99% of the low-energy Auger electrons emitted by ^{111}In travel less than 1 μm in tissue. Consequently, the radiation absorbed dose deposited in the nucleus is amplified 17-times when ^{111}In is deposited in the nucleus compared to when it is localized in the cytoplasm, and >34-times compared to when it is localized on the cell membrane (*124*). Indeed, microdosimetry analysis of MDA-MB-361 breast cancer cells exposed to ^{111}In-NLS-trastuzumab revealed that the 80% of radioactivity bound to the cell surface and imported into the cytoplasm accounts for

approximately 10% of the radiation-absorbed dose to the nucleus, whereas the 20% of radioactivity imported into the nucleus accounts for nearly 90% of the radiation dose to the nucleus (*152*).

Trastuzumab is commonly combined with taxane- or platinum-based chemotherapy regimes (*49*), but it was recently demonstrated that significant clinical benefit could be achieved in patients refractory to trastuzumab by combining the drug with oral low-doses of cyclophosphamide and MTX (*163*). The goal of low-dose chemotherapy is to lessen the side-effects of treatment and inhibit tumor growth, possibly through an antiangiogenic effect (*156,163*). In these studies, however, we exploited a new opportunity to employ similarly low, clinically achievable levels of MTX (<10 μmol/L) to enhance the radiosensitivity of breast cancer cells to ^{111}In-NLS-trastuzumab. The differential sensitivity of breast cancer cells to MTX was not further assessed, but antimetabolites are among the most potent radiosensitizers, and are often active at concentrations below those necessary to induce cytotoxicity (*164*). Indeed, other studies have demonstrated that the efficacy of Auger electron radiotherapy can be significantly enhanced by MTX. For example, the administration of MTX prior to the injection of 5-[^{125}I]iodo-2'-deoxyuridine (^{125}IUdR) in rats with intrathecal TE-671 human rhabdomyosarcoma enhanced ^{125}IUdR uptake by tumor cells, and augmented the therapeutic efficacy of this Auger-electron-emitting radiopharmaceutical (*93*). Paclitaxel, taxotere, gemcitabine, topotecan, 5-fluorouracil, doxorubicin, tirapazamine or halogenated pyrimidines have also been combined with targeted α- or β-radioimmunotherapy, and have been shown to inhibit the growth of various malignant cell lines *in vitro*, or provide anti-tumor effects in mouse xenograft models and in human clinical trials more effectively than either treatment alone (*83,165*).

MTX exerts its toxicity by inhibiting purine *de novo* synthesis, which is thought to impede DNA synthesis and repair, and augment cell killing with ionizing radiation (*155*). Alternatively, the redistribution of cells to a more radiosensitive phase of the cell-cycle (i.e. at the G_1/S boundary or early S-phase), or elimination of radioresistant S-phase cells, have also been suggested as mechanisms for MTX radiosensitization (*154*). The latter mechanism seems unlikely, however, because non-toxic concentrations of MTX were used to radiosensitize breast cancer cells to the DNA-damaging and lethal effects of the Auger electron emissions from ^{111}In-NLS-trastuzumab. Regardless of the mechanism, there is the potential that this combination may

also increase the radiotoxicity on normal cells that accumulate the agent *in vivo* (e.g. liver and kidney). However, toxicity assessments in mice currently in progress show the regimen to be well tolerated, although it should be appreciated that trastuzumab does not cross-react with mouse c-erbB-2 (homologue of human HER2) and thus, it remains that cardiotoxicity could potentially be a side-effect associated with this treatment (*21*). As in the case with trastuzumab, it may only be possible to evaluate this in clinical trials of the radiopharmaceutical.

3.4 Conclusion

We conclude that 13-mer synthetic peptides harboring the NLS of SV-40 large T-antigen efficiently routed ^{111}In-trastuzumab to the nucleus of trastuzumab-sensitive and trastuzumab-resistant human breast cancer cell lines overexpressing HER2, where the nanometer-to-micrometer Auger electrons rendered the radiotherapeutic agent lethal to these cells. We further demonstrated that ^{111}In-NLS-trastuzumab, combined with low-doses of MTX, is more cytotoxic to these cells compared to either of these agents alone. Overcoming trastuzumab resistance represents an important challenge to improving outcomes for patients with HER2-amplified metastatic breast cancer. Achieving a synergistic interaction by combining MTX and targeted Auger electron radioimmunotherapy could dramatically improve the response compared to either of these therapies alone.

CHAPTER 4:

THE PHARMACOKINETICS, NORMAL TISSUE TOXICITY AND ANTI-TUMOR EFFECTS OF ^{111}IN-NLS-TRASTUZUMAB IN MICE BEARING HER2-OVEREXPRESSING BREAST CANCER XENOGRAFTS

This chapter represents a manuscript in preparation of: “Danny L. Costantini, Kristin McLarty, Helen Lee, Susan J. Done, Katherine A. Vallis, and Raymond M. Reilly. The pharmacokinetics, normal tissue toxicity and anti-tumor effects of ^{111}In-NLS-trastuzumab in mice bearing HER2-overexpressing breast cancer xenografts”.

All experiments and analyses of data were carried out by Costantini DL, except for the pharmacokinetic modeling analyses (Lee H) and histopathologic examination of normal tissues (Done S).

4.0 Abstract

Purpose: Monoclonal antibodies conjugated to nuclear localization sequences (NLS) and labeled with Auger electron-emitters such as ^{111}In have great potential for targeted radiotherapy of cancer. Indeed, potent killing of breast cancer cells was achieved *in vitro* with ^{111}In-trastuzumab modified with peptides (CGYG*PKKKRKV*GG) harboring the NLS of simian virus 40 large T-antigen (*italicized*). The objective of this study, therefore, was to examine the pharmacokinetics and normal tissue toxicity of ^{111}In-NLS-trastuzumab, and to assess its efficacy in mice implanted with breast cancer xenografts expressing increasing levels of HER2. **Experimental Design:** Blood pharmacokinetics of ^{111}In-NLS-trastuzumab was measured in non-tumor bearing mice. Toxicity was assessed by histopathologic examination of tissues and by determination of hematology and clinical biochemistry parameters. For radioimmunotherapy, MDA-MB-361 or MDA-MB-231 tumor-bearing mice were injected with a single dose of ^{111}In-NLS-trastuzumab. Control groups were administered saline, trastuzumab, ^{111}In-trastuzumab, or an ^{111}In-labeled isotype-matched non-specific antibody. **Results:** The blood $t_{1/2}$ of ^{111}In-NLS-trastuzumab was 23-34 h, and the maximum tolerable dose (MTD) was 9.2-18.5 MBq; doses >18.5 MBq caused decreased leukocyte and platelet counts. There was no biochemical or morphological evidence of damage to the liver, kidneys or heart. ^{111}In-NLS-trastuzumab exhibited strong anti-tumor effects against MDA-MB-361 xenografts, decreasing their growth rate 4-fold compared with that in saline-treated mice. ^{111}In-NLS-trastuzumab had no effect on the growth of HER2-negative MDA-MB-231 xenografts. **Conclusion:** ^{111}In-NLS-trastuzumab was well tolerated at the MTD, and exhibited strong anti-tumor effects against HER2-overexpressing MDA-MB-361 xenografts. These studies warrant further exploration of the radiopharmaceutical in the treatment of breast cancer metastases with HER2 overexpression.

4.1 Introduction

The HER2 proto-oncogene encodes a 185 kDa transmembrane tyrosine kinase growth factor receptor ($p185^{HER2}$) that belongs to the erbB protein family and plays an important role in cell growth, differentiation and survival (*49*). HER2 represents an ideal therapeutic target because it is accessible as a cell surface receptor and is expressed at high levels in approximately 30% of invasive breast cancers (*49*). Moreover, HER2 overexpression in breast cancer has been found to promote tumorigenesis and metastasis, and is associated with high histologic grade, high proliferation rate, and shorter survival rates (*25*). Given the importance of HER2 in breast cancer, extensive research has focused on HER2 inhibitors as potential anticancer agents. Indeed, the humanized anti-HER2 monoclonal antibody trastuzumab (Herceptin) is among the first target-specific drugs to be developed for immunotherapy of HER2-amplified breast cancer (*49*). In the clinical setting, trastuzumab has been shown to prolong survival in women with HER2-overexpressing metastatic breast cancer when used alone or with chemotherapy (*36*). However, only 30-50% of patients with metastatic disease respond to trastuzumab combined with chemotherapy despite having tumors with amplified HER2 (*34*). Moreover, the majority of patients who initially respond to trastuzumab demonstrate disease progression within a year of treatment initiation due to the emergence of resistance (*33*).

Our group has been exploring the possibility of enhancing the efficacy of HER2-targeted immunotherapy of breast cancer by combining trastuzumab with an Auger electron-emitting radionuclide such as ^{111}In for targeted radiotherapy of the disease (*177,164*). Auger electrons are very low energy (<30 keV) electrons that deposit all their energy over nanometer to at most micrometer distances in tissues. The decay of an Auger electron-emitter inside a cell can cause severe DNA double strand breaks (DSBs) and cell death (*90*). However, to fully exploit this phenomenon for cancer therapy, the radionuclide must be delivered to the tumor cell nucleus where these extremely short-range electrons are especially damaging and lethal (*124*). Nuclear localizing sequences (NLS) have previously been shown to have the capability of inserting mAbs and peptide growth factors, conjugated to nanometer-micrometer range Auger electron-emitting radionuclides, to the nucleus of cancer cells following their receptor-mediated internalization (reviewed in (*124*)). Therefore, we further modified ^{111}In-labeled trastuzumab with 13-mer peptides (CGYG*PKKKRKV*GG) harboring the NLS of the simian virus (SV)-40

large T-antigen (*italicized*). NLS-conjugation to ^{111}In-trastuzumab enhanced its nuclear uptake and cytotoxicity towards HER2-overexpressing human breast cancer cells *in vitro* (*152*). Moreover, the NLS-peptides did not substantially interfere with the receptor-binding ability or the biodistribution properties of ^{111}In-trastuzumab, but did promote HER2-specifc nuclear uptake *in vivo* in mice bearing MDA-MB-361 xenografts. We subsequently reported that ^{111}In-NLS-trastuzumab could kill breast cancer cells with acquired trastuzumab resistance, thereby illustrating that the radiopharmaceutical may have the potential to target both trastuzumab-sensitive and -resistant breast cancer metastases with HER2 overexpression (*166*).

In the current study, our goal was to evaluate the pharmacokinetics, normal tissue toxicity and the anti-tumor effects of ^{111}In-NLS-trastuzumab administered to mice implanted subcutaneously with human breast cancer xenografts expressing increasing levels of HER2. Bone marrow toxicity is generally dose-limiting for most radiotherapeutic applications (*167*). However, the use of radiopharmaceuticals labeled with ^{111}In that emit nanometer-micrometer range Auger electrons should restrict killing to targeted breast cancer cells and minimize toxicity towards non-targeted cells, such as bone marrow stem cells which do not express HER2 (*168*). We hypothesized, therefore, that ^{111}In-NLS-trastuzumab would exhibit potent and selective tumor-growth inhibitory effects against HER2-overexpressing breast cancer xenografts *in vivo*, while causing low or at least acceptable normal tissue toxicity, particularly towards the bone marrow.

4.2 Methods

4.2.1 Cell culture

MDA-MB-361 and MDA-MB-231 human breast cancer cells lines were obtained from the American Type Culture Collection (Manassas, VA). MDA-MB-361 human breast cancer cells were cultured in Leibovitz (L-15) cell culture medium (Invitrogen) supplemented with 20% fetal bovine serum (FBS, Sigma-Aldrich, St. Louis, MO), whereas MDA-MB-231 human breast cancer cells were cultured in Dulbecco's minimal essential medium (Ontario Cancer Institute, Toronto, ON) supplemented with 10% fetal bovine serum (FBS, Sigma-Aldrich, St. Louis, MO) containing 100 U/mL penicillin and 100 μg/mL streptomycin.

4.2.2 Radiolabeling and conjugation of NLS-peptides to trastuzumab and human IgG

Trastuzumab (Herceptin, Roche Pharmaceuticals) or non-specific, irrelevant human IgG (hIgG, product no. I4506; Sigma-Aldrich) were conjugated to diethylenetriaminepentaacetic acid dianhydride (DTPA) (Sigma-Aldrich) and sulfosuccinimidyl-4-(N-maleimidomethyl)cyclohexane-1-carboxylate (sulfo-SMCC; Pierce) for reaction with synthetic 13-mer NLS-peptides (CGYGPKKKRKVGG) and labeling with ^{111}In as described previously (*152*). Briefly, trastuzumab or hIgG (500 μg, 10 mg/mL) was reacted with a 10-fold molar excess of DTPA for 1 h at room temperature and then purified on a Sephadex-G50 mini-column prior to reaction with a 15-fold molar excess of sulfo-SMCC (2-5 mmol/L) at room temperature for 1 h. Maleimide-derivatized DTPA-trastuzumab or hIgG was purified on a Sephadex-G50 mini-column, concentrated to 2-5 mg/mL using a Microcon YM-50 ultrafiltration device (Amicon), and reacted overnight at 4^{o}C with a 60-fold molar excess of NLS-peptides (5-10 mmol/L diluted in PBS, pH 7.0). DTPA-trastuzumab or hIgG, modified with NLS-peptides (NLS-DTPA-trastuzumab or NLS-DTPA-hIgG), was purified on a Sephadex-G50 mini-column eluted with phosphate buffered saline (PBS), pH 7.5. We previously determined that 3-4 NLS-peptides are conjugated to trastuzumab at an SMCC:IgG:NLS-peptide molar ratio of 15:1:60 (*152*).

NLS-conjugated or unmodified DTPA-trastuzumab, or DTPA-NLS-hIgG, were radiolabeled by incubation of 37-111 MBq of mAbs with $^{111}InCl_3$ (MDS-Nordion, Kanata, ON) for 1 h at room temperature. ^{111}In-labeled mAbs were purified using a Sephadex-G50 minicolumn and a Microcon YM-50 ultrafiltration device (Amicon) using PBS, pH 7.5. The radiochemical purity was routinely >97% as determined by instant thin-layer silica-gel chromatography (ITLC-SG; Pall Corp.) developed in 100 mmol/L sodium citrate, pH 5.0. All radioactivity measurements were made using an automatic γ-counter (Wallac Wizard-1480; Perkin Elmer).

4.2.3 Pharmacokinetics of ^{111}In-NLS-trastuzumab

The pharmacokinetics of ^{111}In-NLS-trastuzumab (9.25 MBq; 4 mg/kg) administered by intraperitoneal (i.p.) or intravenous (i.v.) (tail vein) injection were compared in non–tumor-bearing BALB/c mice. Blood samples (5-10 μL) were collected in heparinized microcapillary

tubes (Fisher Scientific Co.) at various time points between 5-30 min, and 1-72 h after radiopharmaceutical injection by nicking the saphenous vein with a sterile scalpel blade. Radioactivity in the blood samples was measured with a γ-counter and the concentration of ^{111}In was expressed as counts per minute per microliter of blood (cpm/μL). The elimination phase for the blood radioactivity–versus–time curve for the i.v. administration was fitted to a 2-compartment pharmacokinetic model, whereas the curve for the i.p. administration was fitted to a 1-compartment pharmacokinetic model with an absorption phase, using Prism software (GraphPad Software Inc.). Standard pharmacokinetic parameters were calculated including, distribution half-life ($t_{1/2[\alpha]}$), elimination half-life ($t_{1/2[\beta]}$), absorption half-life ($t_{1/2[absorption]}$; determined for i.p. administration only), volume of distribution of the central compartment (V_1), volume of distribution at steady state (V_{ss}), systemic clearance (CLs) and the area under the curve (AUC). The AUC from the i.p. curve was divided by the AUC from the i.v. curve in order to calculate the bioavailability (F) which was defined as the fraction of radiopharmaceutical that reaches the systemic circulation following an i.p. administration. The principles of Laboratory Animal Care (NIH Publication No.86-23, revised 1985) were followed, and all animal studies were approved by the Animal Care Committee at the University Health Network following Canadian Council on Animal Care guidelines.

4.2.4 Normal tissue toxicity and clinical biochemistry

Groups of normal female BALB/c mice were injected i.p. with a single-dose or two-biweekly doses of ^{111}In-NLS-trastuzumab (3.7 - 27.8 MBq; 4 mg/kg) in 150 μL 150 mmol/L sodium chloride. Control mice received an i.p. injection of ^{111}In-NLS-hIgG (single-dose only, 18.5 MBq; 4 mg/kg) or the equivalent volume of 150 mmol/L sodium chloride. Hematological toxicity was monitored by obtaining peripheral blood cell counts at the end of a 2, 3, 5 or 7 week observation period after the final dose of radiopharmaceutical was administered. Blood was removed via cardiac puncture, and approximately 250-500 μL of the sample was collected into EDTA-coated tubes (Becton-Dickinson Co.). Hematology analysis included leukocyte / white blood cell (WBC) counts, erythrocyte / red blood cell (RBC) counts, platelet counts and measurement of hemoglobin, all of which were measured at the Clinical Biochemistry Laboratory at the Hospital for Sick Children (Toronto, Ontario, Canada). Normal tissues were

also removed, sectioned and stained with hematoxylin and eosin (H&E) for histopathologic examination by light microscopy for any evidence of acute toxicity manifested by morphological changes. Kidney sections were also stained with periodic-acid Schiff (PAS) and periodic acid silver methenamine (PASM) stains in order to assess the extracellular matrix.

The potential for acute hepatotoxicity and renal toxicity from ^{111}In-NLS-trastuzumab was also assessed by measuring serum alanine transaminase (ALT) and creatinine (CR) levels at 72 h post i.p. injection of ^{111}In-NLS-trastuzumab. Blood was collected in microtubes and allowed to clot at room temperature for 15 min to form serum, followed by centrifugation at 1000 x g for 10 min at 4°C. No hemolysis was visible in any samples from control and treated animals. Serum CR was measured using a picric-acid based colorimetric assay kit (Infinity Creatinine, Thermo Electron Corp., Lousiville, CO), whereas serum ALT activities were measured with Infinity ALT reagent (Thermo Electron Corp., Lousiville, CO), using the rates of change in absorbance at 340 nm and the absorption coefficient for NADH (6.22 cm^{-1} mM^{-1}) to calculate activities.

4.2.5 Radioimmunotherapy of athymic mice with breast cancer xenografts

The anti-tumor properties of trastuzumab, ^{111}In-trastuzumab, ^{111}In-NLS-trastuzumab and ^{111}In-NLS-hIgG were evaluated in female athymic CD-1 mice implanted subcutaneously (s.c.) with MDA-MB-361 (5.0 x 10^5 HER2 receptors per cell (*169*)) or MDA-MB-231 (0.5 x 10^5 HER2 receptors per cell (*169*)) xenografts. Mice were implanted intradermally with a 17-β-estradiol pellet (Innovative Research of America, Sarasota, FL) 24 hours prior to inoculation in the flank with 1×10^7 MDA-MB-361 cells or 1×10^6 MDA-MB-231 cells in 100 μL of Matrigel (Becton-Dickinson Labware, Bedford, MA) and culture medium mixture (1:1, v/v). For the single-dose RIT study, the mice received an intraperitoneal (i.p.) injection of 9.25 MBq of ^{111}In-trastuzumab, ^{111}In-NLS-trastuzumab or ^{111}In-NLS-hIgG when the tumors reached a diameter of 2-5 mm (6-8 weeks). The administered IgG dose was 4 mg/kg, or approximately 80 μg for a mouse weighing 20 g. This is comparable to the clinical setting where trastuzumab (Herceptin) is administered as a loading dose of 4 mg/kg followed by 2 mg/kg weekly doses (*33*). The tumor length (L) and width (W) were measured using calipers every 3-5 days, and body weights were monitored every 7-14 days for 8 weeks. Treatment experiments were terminated at a pre-determined end point when tumor size exceeded a mean tumor diameter of 12 mm or at the

planned end of the study (8 weeks). The tumor volume was calculated as $V = [(L \times W^2) \times 0.5]$, and the tumor growth index (TGI) was calculated by dividing the tumor volume at each time point by the initial tumor volume. Similarly, body weight indices (BWI) were calculated by dividing the body weight at each time point by the pretreatment body weight. The mean TGI and BWI were plotted against the time from the start of treatment in order to obtain tumor growth and body weight curves.

4.2.6 Statistical methods

Data were presented as mean ± standard error of the mean (SEM). Significance was evaluated by one-way ANOVA followed by Tukey's post-hoc test using GraphPad Prism Ver 4.0 software. The rate of tumor growth in animals treated with ^{111}In-NLS-trastuzumab or in control animals was determined from the slope of the tumor growth index–versus–time curve fitted by linear regression. Statistical comparisons of slopes were made by use of the F test. $P < 0.05$ was considered significant.

4.3 Results

4.3.1 Pharmacokinetics of ^{111}In-NLS-trastuzumab after i.v. and i.p. injection

In preclinical studies, athymic mice bearing HER2-overexpressing BT-474 human breast cancer xenografts demonstrated a marked regression in tumor growth when treated with multiple i.p. doses of trastuzumab (0.1-30 mg/kg) (*181*). We therefore examined the bioavailability (F) and characterized the pharmacokinetics of ^{111}In-NLS-trasuzumab (single-dose, 9.25 MBq; 4 mg/kg) after i.p. and i.v. injection in non-tumor bearing BALB/c mice. The mean concentrations of radioactivity (cpm/μL) in the blood were determined at different time points after injection of ^{111}In-NLS-trastuzumab (Fig. 4.1). The elimination phase of the radiopharmaceutical following i.v. injection was described by a 2-compartment pharmacokinetic model. The α-phase (distribution) half-life was 0.14 h, and the β-phase (elimination) half-life was 33.7 h (Table 4.1). The volume of distribution of the central compartment (V_1) and the volume of distribution at steady state (V_{ss}) for ^{111}In-NLS-trastuzumab was 1.1 mL (57 mL/kg) and 1.7 mL (85 mL/kg), respectively. The V_{ss} was equivalent to the expected blood volume of a

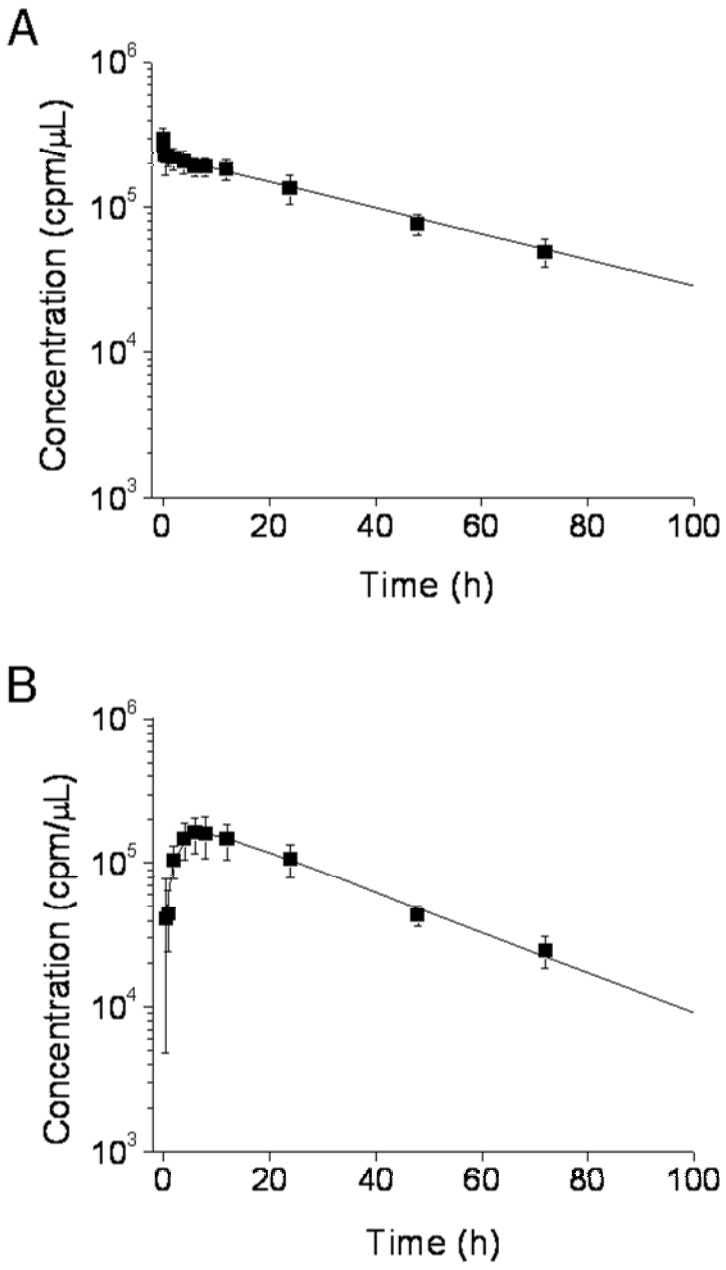

Figure 4.1: The mean concentration of radioactivity (cpm/μL) in the blood of non-tumor bearing BALB/c mice after intravenous **(A)** or intraperitoneal **(B)** injection of ^{111}In-NLS-trastuzumab (9.25 MBq; 4 mg/kg).

Table 4.1 - Pharmacokinetic parameters for ^{111}In-NLS-trastuzumab administered intravenously to non-tumor bearing BALB/c mice

Pharmacokinetic Parameter	**Estimate**
Distribution half-life ($t_{1/2[\alpha]}$) (h)	0.14
Elimination half-life ($t_{1/2[\beta]}$) (h)	33.7
V_1 (mL)	1.13
V_{ss} (mL)	1.69
CL_s ($\mu L \cdot h^{-1}$)	34.7
AUC_{iv} ($cpm \cdot h \cdot \mu L^{-1}$)	10.9×10^9

Mice were administered ^{111}In-NLS-tratuzumab via i.v. injection (10 MBq; 4 mg/kg) (n = 5). Blood samples were withdrawn at selected time points up to 120 h p.i., and then analyzed to evaluate the pharmacokinetics. Data were fit to a 2-compartment pharmacokinetic model. Pharmacokinetic parameters calculated include: distribution half-life ($t_{1/2[\alpha]}$), elimination half-life ($t_{1/2[\beta]}$), volume of distribution of the central compartment (V_1), volume of distribution at steady state (V_{ss}), systemic clearance (CL_s) and the area under the i.v. curve (AUC_{iv}).

Table 4.2 - Pharmacokinetic parameters for ^{111}In-NLS-trastuzumab administered intraperitoneally to non-tumor bearing BALB/c mice

Pharmacokinetic Parameter	**Estimate**
Absorption half-life ($t_{1/2(absorption)}$) (h)	1.93
Elimination half-life ($t_{1/2[\beta]}$) (h)	23.1
t_{max} (h)	6.87
V_d (mL)	1.19
CL_s ($\mu L \cdot h^{-1}$)	37.9
AUC_{ip} ($cpm \cdot h \cdot \mu L^{-1}$)	7.0×10^9
F	0.70

Mice were administered ^{111}In-NLS-tratuzumab via i.p. injection (10 MBq; 4 mg/kg) (n = 5). Blood samples were withdrawn at selected time points up to 120 h p.i., and then analyzed to evaluate the pharmacokinetics. Data were fit to a 1-compartment pharmacokinetic model with an absorption phase. Pharmacokinetic parameters calculated include: absorption half-life ($t_{1/2[absorption]}$), elimination half-life ($t_{1/2[\beta]}$), time at which the maximum blood concentration occurs (t_{max}), volume of distribution (V_d), and the area under the i.p. curve (AUC_{ip}). The bioavailability (F) = AUC_{ip} / AUC_{iv} (the i.v. pharmacokinetic data are shown in Table 4.1).

mouse (70-80 mL/kg). The pharmacokinetics of ^{111}In-NLS-trastuzumab following an i.p. injection was described by a one-compartment model with an absorption and elimination phase (Table 4.2). The bioavailability (F) of ^{111}In-NLS-trastuzumab after i.p. administration was approximately 70%, and the time to maximum concentration (t_{max}) was reached by 6.9 h after injection. The volume of distribution (V_d) of ^{111}In-NLS-trastuzumab after i.p. injection was 1.2 mL; this was slightly lower compared to when the radiopharmaceutical was administered by i.v. injection.

4.3.2 Determination of MTD and examination of hematological toxicity

Non-tumor bearing BALB/c mice were injected (i.p.) with increasing doses of ^{111}In-NLS-trastuzumab ranging from 3.7 MBq to 27.8 MBq (4 mg/kg). Analysis of peripheral blood counts obtained at 2 weeks post-injection revealed that the maximum tolerated dose (MTD) of ^{111}In-NLS-trastuzumab was 9.25 - 18.5 MBq. The MTD was defined as the dose which did not cause any significant change in the blood counts compared to normal values or those for control mice. As shown in Fig. 4.2A-B, doses $\geq$ 18.5 MBq of ^{111}In-NLS-trastuzumab caused a significant decrease in leukocyte and platelet counts compared to normal saline treated mice, and these parameters were well below the normal lower limit for mice (*174*). The erythrocyte count also fell slightly below the normal lower limit at the highest administered dose, whereas hemoglobin levels were unaffected by the radiopharmaceutical (Fig. 4.2C-D). The platelet count recovered by the 5th week after injection, however, the leukocyte count did not return to normal levels, even at 7 weeks after injection. (Fig. 4.2E-F). Leukocyte and platelet counts were similarly reduced after injection of 18.5 MBq of isotype-matched non-specific control antibody ^{111}In-NLS-hIgG (3.23 ± 0.21 x 10^9 /L and 567.7 ± 63.5 x 10^9 /L, respectively).

Peripheral blood counts were also assessed in normal BALB/c mice that received 2-biweekly injections (i.p.) of ^{111}In-NLS-trastuzumab (9.25 MBq). At 2 weeks after the last injection, the hematological parameters from each mouse remained above the normal lower limit, and the mean leukocyte, platelet, erythrocyte and hemoglobin counts were 5.72 ± 0.21 x 10^9 /L, 711.5 ± 38.1 x 10^9 /L, 7.66 ± 0.13 x 10^{12} /L, and 128.5 ± 2.62 g/L, respectively.

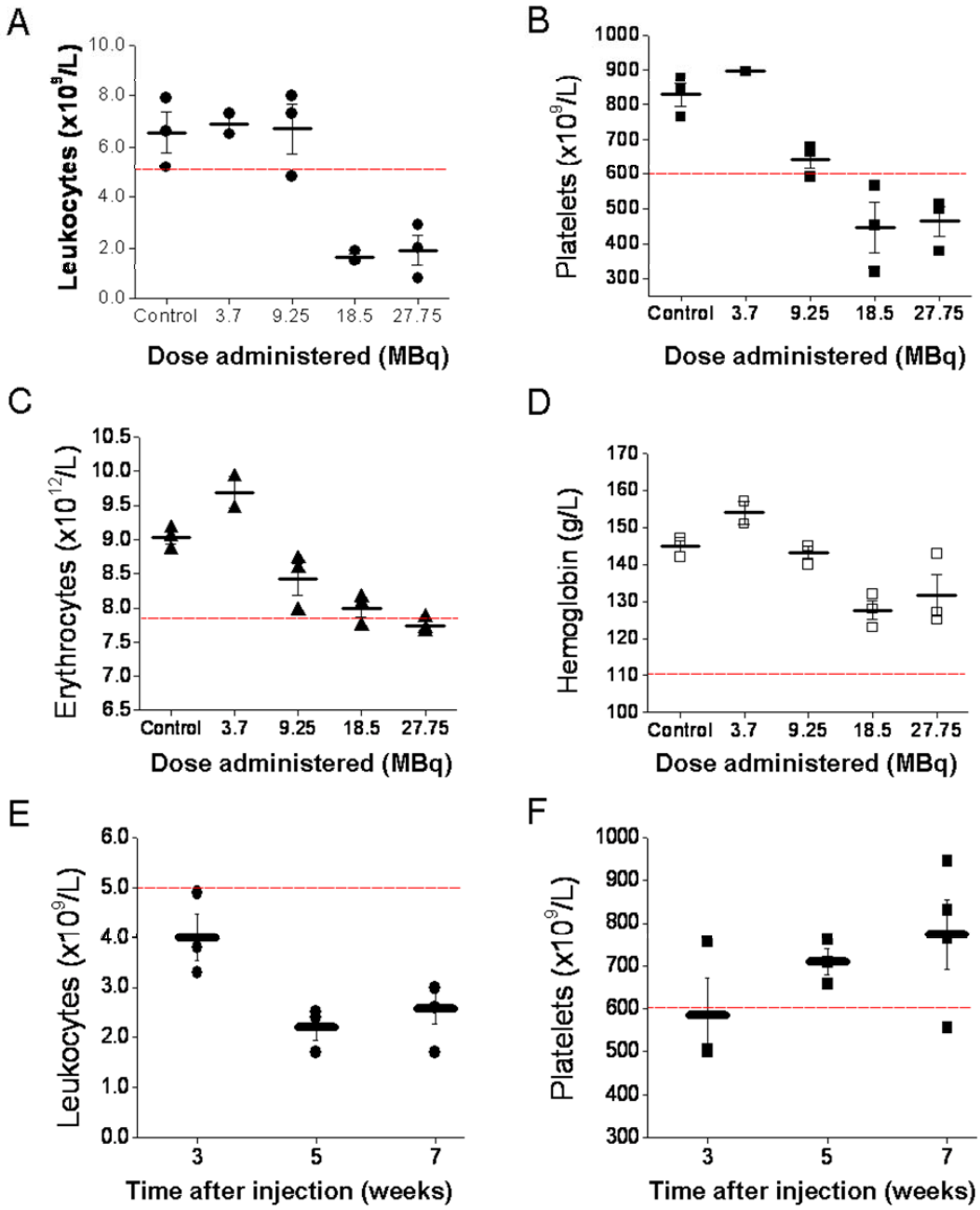

Figure 4.2: Leukocyte counts **(A)**, platelet counts **(B)**, erythrocyte counts **(C)** and measurement of hemoglobin **(D)** in the blood of non-tumor bearing mice 14 days after i.p. injection of increasing doses of ^{111}In-NLS-trastuzumab or normal physiologic saline (control). Leukocyte and platelet counts were also measured at 3, 5 and 7 weeks after i.p. injection of 18.5 MBq of ^{111}In-NLS-trastuzumab **(E-F)**. Red line indicates normal lower limit of indicated parameter.

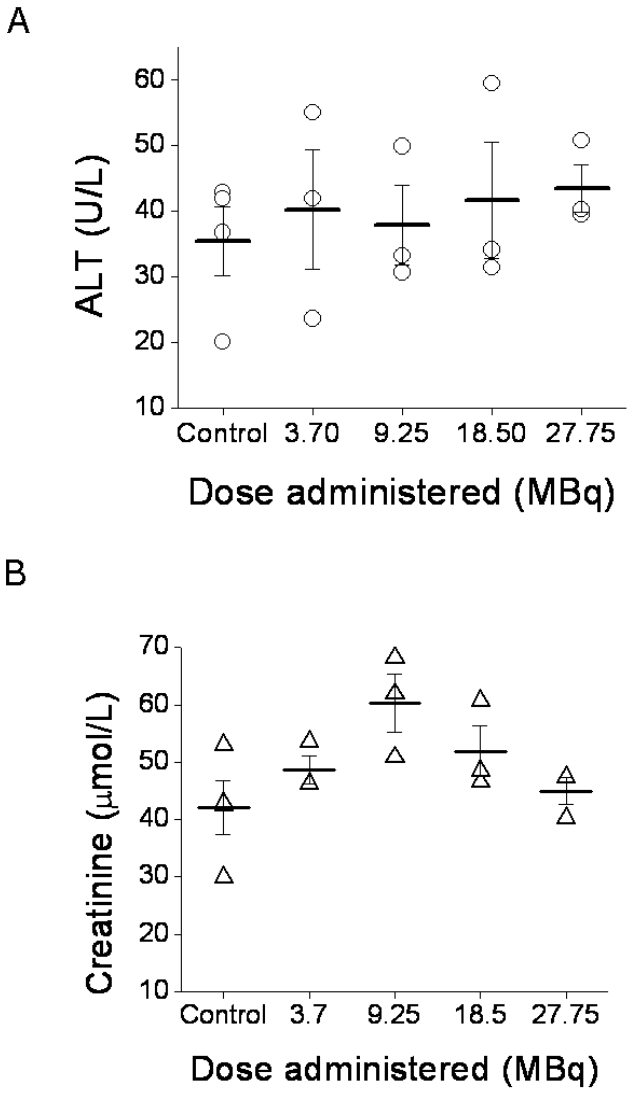

Figure 4.3: Serum alanine transaminase (ALT) **(A)** and creatinine **(B)** concentrations at 72 h post i.p. injection of increasing doses of ^{111}In-NLS-trastuzumab or normal physiologic saline (control) in non-tumor bearing BALB/c mice.

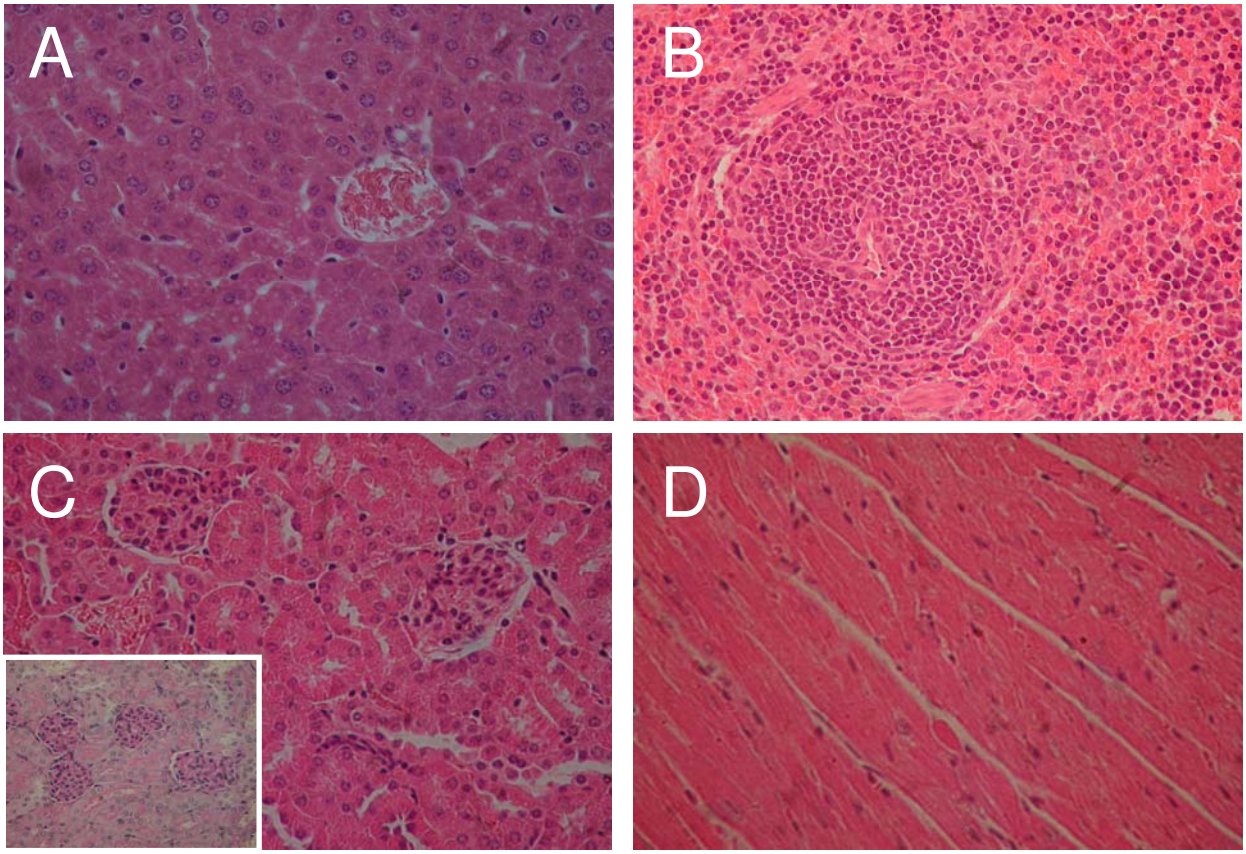

Figure 4.4: Histopathologic examination (hematoxylin and eosin stain or periodic acid-Schiff stain [inset in **(C)**]) by light microscopy of sections of liver **(A)**, spleen **(B)**, kidney **(C)** and heart **(D)** from non-tumor bearing BALB/c mice at 14 d after i.p. injection of ^{111}In-NLS-trastuzumab (9.25 MBq; 4 mg/kg). There were no morphologic changes to the heart or spleen, and no changes characteristic of hepatotoxicity or renal toxicity (changes in renal tubular structure).

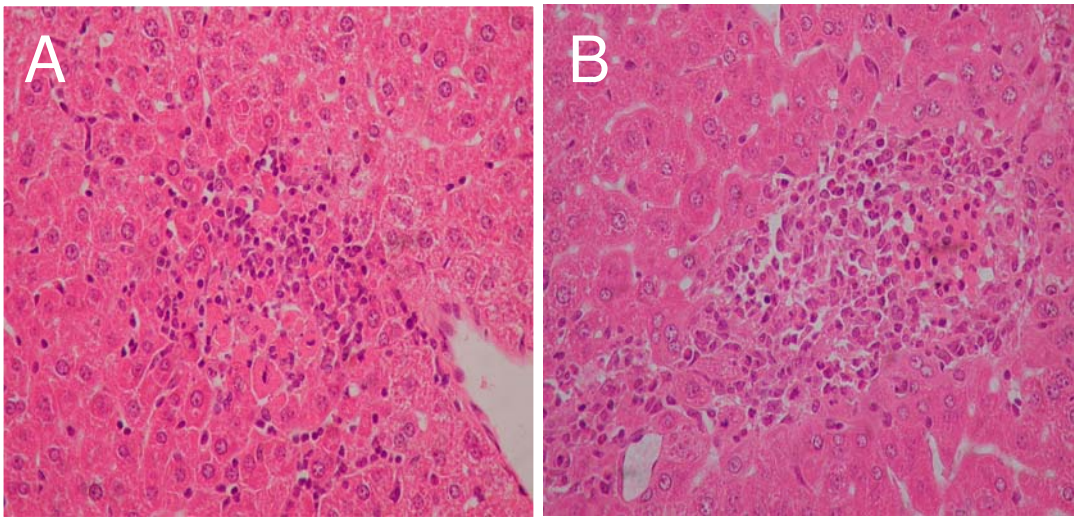

Fig. 4.5: Mild liver cell degeneration with leukocyte infiltration indicative of necrosis in 1 of 4 mice administered ^{111}In-NLS-trastuzumab **(A)** and in 1 of 4 saline-treated control mice **(B)**.

4.3.3 Evaluation of normal tissue toxicity of ^{111}In-NLS-trastuzumab

Figure 4.3 depicts the concentration of ALT and CR present in the serum of normal BALB/c mice as a function of the dose of ^{111}In-NLS-trastuzumab (3.7 - 27.8 MBq; 80 μg). At 72 h post-i.p. injection, serum ALT or CR levels were not significantly increased in mice receiving ^{111}In-NLS-trastuzumab compared to normal saline-treated controls indicating no obvious toxicity to the liver or kidney. Serum ALT ranged in value from 23 to 55 units/L for treated mice and from 20 to 42 units/L for control mice, whereas the serum CR concentration ranged from 40 to 68 μmol/L for treated mice and 30 to 53 μmol/L for control mice. There was a modest increase in serum CR levels at one of the intermediate doses of ^{111}In-NLS-trastuzumab (9.25 MBq), but these nevertheless remained within the normal range for mice (*125*).

The results of the histopathological examination by hematoxylin and eosin staining revealed no morphologic changes to normal tissues (brain, heart, lung, stomach, small intestine, large intestine, liver, kidney, spleen and muscle) and no changes characteristic of hepatoxicity or renal toxicity (Fig. 4.4). PAS staining of the renal glomeruli did not reveal basement membrane thickening, and the mesangial matrix was otherwise unremarkable. There were small foci of centrilobular liver necrosis in 1 of 4 mice administered ^{111}In-NLS-trastuzumab (18.5 MBq) and in 1 of 4 control mice administered saline (Fig. 4.5).

4.3.4 Treatment of mice with MDA-MB-361 or MDA-MB-231 xenografts

The inhibitory effect of ^{111}In-NLS-trastuzumab on tumor growth was evaluated in athymic mice implanted with breast cancer xenografts expressing high or low levels of HER2. Mice bearing HER2-positive MDA-MB-361 and HER2-negative MDA-MB-231 breast cancer xenografts were treated with a single i.p. injection of trastuzumab, ^{111}In-trastuzumab or ^{111}In-NLS-trastuzumab (9.25 MBq; 80 μg) equivalent to the MTD for ^{111}In-NLS-trastuzumab. Control groups received i.p. injections of saline or 9.25 MBq (80 μg) of non-specific ^{111}In-NLS-hIgG. The average initial tumor volume in each treatment and control group ranged between 41.6 ± 4.9 mm^3 to 51.7 ± 7.4 mm^3 ($P > 0.05$, ANOVA). Linear regression analysis of the tumor growth curves revealed that the rate of tumor growth was the slowest in mice treated with a single-dose of ^{111}In-NLS-trastuzumab, and that this was approximately 4-

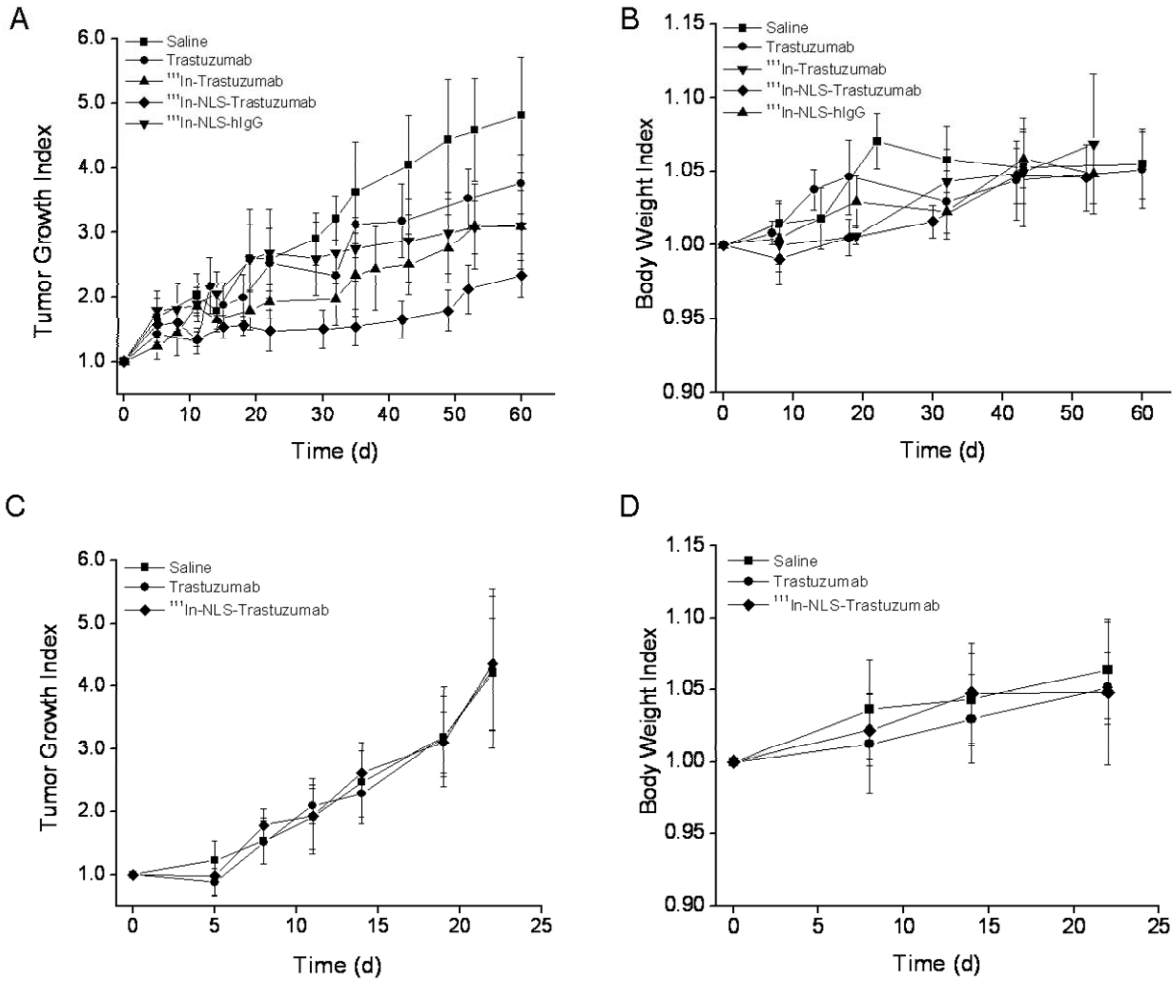

Figure 4.6: Tumor growth index versus time (days) and body weight index versus time (days) for athymic mice implanted with HER2-overexpressing MDA-MB-361 **(A-B, respectively)** or very low HER2-expressing MDA-MB-231 **(C-D, respectively)** human breast cancer xenografts. Data were obtained after treatment with a single i.p. dose of ^{111}In-NLS-trastuzumab at the MTD (9.2 MBq; 4 mg/kg). Control groups were administered equivalent doses of trastuzumab, ^{111}In-trastuzumab, ^{111}In-NLS-trastuzumab, ^{111}In-NLS-hIgG or normal physiologic saline. Treatments were started on day 0. Error bars represent the SEM and 6-7 mice were treated per group.

fold less than the rate of tumor growth in normal saline-treated mice (slopes of tumor growth curves, 0.014 d^{-1} and 0.061 d^{-1}, respectively; F test; $P < 0.05$) (Fig. 4.6A). The tumor growth rate was also significantly lower in mice treated with ^{111}In-NLS-trastuzumab compared to that in mice treated with ^{111}In-trastuzumab, trastuzumab or non-specific ^{111}In-NLS-hIgG (slopes, 0.033 d^{-1}, 0.046 d^{-1} and 0.030 d^{-1}, respectively; F test; $P < 0.05$). In contrast, a single-dose of ^{111}In-NLS-trastuzumab had no effect on the growth of MDA-MB-231 xenografts when compared to the trastuzumab- or saline-treated groups (slopes, 0.150 d^{-1} versus 0.144 d^{-1} and 0.151 d^{-1}, respectively) (Fig. 4.6C). Analysis of the body weight indices over the 60-day observation period also revealed no significant differences between the treated and control groups, suggesting no generalized toxicity from the radiopharmaceuticals in athymic tumor-bearing mice (Fig. 4.6B and D).

4.4 Discussion

Significant progress has been made in improving the prognosis for women with early stage tumors such that the 10-year survival for women with Stage 0 or I disease treated by surgery and local radiation combined with adjuvant chemotherapy is 85-90% (*134*). The median survival for women with disseminated breast cancer, however, is only 2-4 years (*134*). This is partly due to the relative ineffectiveness of chemotherapy for treating metastatic disease because of dose-limiting toxicity to hematopoietic and other normal tissues, and due to the rapid emergence of multidrug resistance (*170*). This dire statistic highlights the need for new treatments that will improve the long-term survival of women with metastatic breast cancer. The results of this study reveal that trastuzumab, a drug commonly used and effective for treating breast cancer, can be re-designed by conjugation with NLS-peptides and the Auger electron-emitter ^{111}In to create an improved therapeutic agent with potent anti-tumor activity against HER2-overexpressing tumor xenografts. Importantly, ^{111}In-NLS-trastuzumab at the MTD was not toxic to hematopoietic or other normal tissues. Currently, patient selection for trastuzumab therapy is based on immunohistochemical staining (IHC) of a tumor biopsy for HER2 protein overexpression, with IHC scores of 2^+ and 3^+ being considered eligible (*171*). However, only about half of patients with HER2-overexpressing metastases respond to this treatment, and in

almost all initially-responding patients, resistance to trastuzumab rapidly develops within a year (*49*). The enhanced tumor growth inhibitory effects of ^{111}In-NLS-trastuzumab compared with unlabeled trastuzumab suggests that this radiotherapeutic agent could offer a more effective treatment option for patients with HER2-amplified metastatic breast cancer.

RIT of solid tumors is limited by the irradiation and killing of normal cells (e.g. bone marrow stem cells) by the moderate energy and long-range (2-10 mm) β-particles emitted by radionuclides such as ^{131}I or ^{90}Y that have been commonly conjugated to radiotherapeutic agents (i.e. "cross-fire" effect) (*67*). This effect can be beneficial for eradicating non-targeted cancer cells in a large solid tumor mass in which there may be heterogeneous distribution of the radiotherapeutic agents. However, it is also responsible for non-specific and dose-limiting myelotoxicity of RIT (*67*). Auger electron-emitting radionuclides, such as ^{125}I and ^{111}In, represent an appealing alternative to β-particle emitters for targeted radiotherapy of small tumor deposits and micrometastatic disease because they are only radiotoxic to cells which are able to internalize the radionuclide, due the extremely short, subcellular range of these electrons (*85*). Indeed, recent studies have suggested the use of low-energy Auger electron-emitters, conjugated to mAbs that internalize selectively into targeted cancer cells, for targeted radiotherapy of malignancies (*116*). CO17-1A, for example, is an internalizing mAb specific for a 41 kDa glycoprotein on gastrointestinal adenocarcinoma cells. Behr et al. (*119*) compared the anti-tumor efficacy of CO17-1A labeled with Auger electron-emitters (^{123}I, ^{111}In), to conventional β-emitters (^{131}I, ^{90}Y), in athymic mice bearing GW-39 human colon cancer xenografts (*119*). At the MTD, ^{125}I- and ^{111}In-labled CO17-1A (85-111 MBq) were more effective at controlling tumor growth compared to ^{131}I- or ^{90}Y-labeled CO17-1A (4-11 MBq), with complete and partial remissions being achieved only with CO17-1A labeled with the Auger electron-emitters (*119*). Likewise, Mattes and Goldenberg (*104*) reported significantly prolonged survival in mice bearing SK-OV-3 ovarian tumor xenografts treated with 59 MBq of ^{111}In-4D5 (murine parent of trastuzumab), compared to mice receiving the same dose of an irrelevant control mAb. Thus, the advantage of using low-energy Auger emitters, versus conventional β-emitters, is the lack of "cross-fire" effect and the more selective irradiation and killing of tumor tissues (*116*).

One approach to improving the effectiveness of Auger electron radiotherapy with internalizing mAbs is to promote their importation into the nucleus of tumor cells through NLS-

mediated processes, where the Auger electrons are most damaging to DNA, and lethal to these cells. Indeed, we previously reported that trastuzumab mAbs labeled with ^{111}In and modified with 13-mer peptides (CGYG*PKKKRKV*GG) harboring the NLS of SV-40 large T-antigen (*italicized*) were internalized and routed to the nucleus of HER2-overexpressing breast cancer cells (*152*). ^{111}In-NLS-trastuzumab induced frequent DNA-DSBs, and strongly decreased the clonogenic survival of HER2-positive MDA-MB-361 and SK-BR-3 breast cancer cells (*152*). ^{111}In-NLS-trastuzumab was also avidly and specifically taken up by MDA-MB-361 tumor xenografts in athymic mice. SK-BR-3 cells, expressing ~1.0 x 10^6 HER2 receptors per cell (*169*), were not used to establish HER2-positive tumor xenografts because they are not tumorigenic in athymic mice (*135*). Nevertheless, ^{111}In-NLS-trastuzumab was preferentially imported *in vivo* into the nucleus of MDA-MB-361 tumor cells expressing intermediate-high levels of HER2 (~0.5 x 10^6 receptors per cell (*169*)) (*152*). Consistent with these previous *in vivo* data, we found in the current study that ^{111}In-NLS-trastuzumab exhibited strong anti-tumor effects against MDA-MB-361 breast cancer xenografts, decreasing their growth rate 2-fold and 3-fold compared with that in mice treated with the equivalent amount of ^{111}In-trastuzumab or unlabeled trastuzumab, respectively (Fig 4.6). In contrast, MDA-MB-231 tumor xenografts, expressing very low levels of HER2 (~0.05 x 10^6 receptors per cell (*169*)), were relatively resistant to ^{111}In-NLS-trastuzumab. Unfortunately, no MDA-MB-361 tumor-bearing mice were cured with a single-dose of ^{111}In-NLS-trastuzumab, suggesting that multiple administrations of the radiopharmaceutical are needed to further improve its therapeutic efficacy. The tumor growth-inhibitory effect of ^{111}In-NLS-trastuzumab administered in multiple-doses is presently being evaluated, however, acute toxicity studies in non-tumor bearing BALB/c mice administered 2-biweekly injections of ^{111}In-NLS-trastuzumab (9.25 MBq x 2, i.p.) revealed no decreases in leukocytes, erythrocytes, platelet counts or hemoglobin levels from this dosing regimen. On the basis of body surface areas of 0.009 m^2 and 1.73 m^2, the total cumulative dose of ^{111}In-NLS-tratuzumab administered to mice in single- or multiple-doses (9.25 - 18.5 MBq) would correspond to 1.8 - 3.6 GBq in humans, respectively (*101*). These doses are very conservative considering that patients have been safely injected with as much as 18.5 GBq of ^{125}I on an Ab (*117*), and 148 GBq of ^{111}In conjugated to octreotide in multiple doses (*99,100*).

In the RIT experiments, tumor-bearing mice were administered ^{111}In-NLS-trastuzumab as a single i.p. injection. This administration route was preferred over the i.v. route because of its ease of administration and favorable pharmacokinetics (Fig. 4.1 and Tables 4.1-4.2). Indeed, high bioavailability (~70%) was achieved after i.p. injection of ^{111}In-NLS-trastuzumab in non-tumor bearing BALB/c mice, and the $t_{1/2[\beta]}$ (elimination from the systemic circulation) was ~23 h; this was moderately shorter compared to when the radiopharmaceutical was administered intravenously (~34 h). Moreover, the maximum volume of distribution of ^{111}In-NLS-trastuzumab after i.v. and i.p. administration were comparable to the expected blood volume for a mouse (~70-80 mL/kg) (*172*), suggesting minimal extravasation of the radiopharmaceutical into the extravascular space. This is consistent with the results of clinical trails of trastuzumab in women with metastatic breast cancer where the volume of distribution was approximately that of the serum volume (44 mL/kg) (*173*). Intraperitoneal RIT is currently being evaluated as a therapeutic modality for the loco-regional management of peritoneal metastases from colorectal or ovarian cancers (*186,87*). However, breast cancer metastasis normally affect the bones, lungs and liver (*3*), suggesting that in this setting, the i.v. route of administration of ^{111}In-NLS-trastuzumab may be more appropriate and preferred over the i.p. route in human patients.

Behr et al. (*116*) demonstrated that the MTD for ^{111}In-labeled mAb CO17-1A, defined as the highest possible dose that did not result in any animal deaths, was 85 MBq in mice bearing GW-39 human colon cancer xenografts. Mattes and Goldenberg (*104*) similarly assessed the toxicity of ^{111}In-labeled 4D5 and determined that doses greater than 60-68 MBq caused > 20% body weight loss and/or death from radiation toxicity in non-tumor bearing athymic mice. Although body weight loss and/or death were the only measures of toxicity in these studies, it was likely that myelosuppression caused by the ^{111}In-mAbs was a major dose-limiting side-effect (*104*). Indeed, in the current study, doses of ≥ 18.5 MBq of ^{111}In-NLS-trastuzumab caused significant leukopenia and thrombocytopenia in non-tumor bearing BALB/c mice (Fig. 4.2). However, there were no deaths in non-tumor BALB/c mice or decreases in the body weights of tumor-bearing mice that were administered ^{111}In-NLS-trastuzumzb suggesting that higher amounts of the radiopharmaceutical could be administered by establishing a different end-point other than blood count changes to define the MTD (i.e. body weight loss and/or death). The decreases in leukocyte and platelet counts were likely due to the non-specific irradiation and

killing of normal peripheral blood mononuclear cells and bone marrow cells by the low LET γ-emissions of ^{111}In (energy of γ-emissions, 172 and 247 keV) because a similar effect was observed with an equitoxic dose of ^{111}In-NLS-hIgG, an isotype-matched non-specific control antibody. Moreover, murine bone marrow cells do not express the human homologue of HER2 which is necessary for trastuzumab binding (*168,17*), and the nanometer-to-micrometer range Auger-electrons emitted by ^{111}In-NLS-trastuzumab can reach nuclear DNA and manifest their radiotoxic effects only when internalized by cells through HER2-mediated processes (*90*). In human, normal hematopoietic stem cells express very low levels of HER2 (*170,17*), and therefore ^{111}In-NLS-trastuzumab should not have significant adverse effects on these tissues. However, the radiopharmaceutical might be radiotoxic to normal organs that exhibit minimal-to-moderate levels of HER2, such as the liver, spleen and kidneys (*17*). Uptake of ^{111}In-NLS-trastuzumab by these tissues may also occur through Fc_{γ}-receptor mediated processes in the liver and spleen, and charge interactions in the kidneys (*27*). Loss of ^{111}In from the DTPA chelate and its *in vivo* redistribution is also a possibility (*174*). However, these processes would not promote the internalization and nuclear uptake of ^{111}In that is required for its toxicity. Indeed, in previous studies examining the normal tissue distribution of ^{111}In-NLS-trastuzumab, an appreciable amount of radioactivity was found to accumulate in the liver, spleen and kidney (11-12 %ID/g, 6-7 %ID/g and 7-8 %ID/g at 72 h p.i., respectively) (*152*). However, in the current study there were no significant increases in the concentrations of ALT or CR in serum (Fig. 4.3), suggesting no evidence of acute liver or renal toxicities from the radiopharmaceutical. Moreover, histopathologic examination confirmed that there were no morphologic changes to the spleen, or changes characteristic of hepatotoxicity or renal toxicity (changes in renal tubular structure) (Fig. 4.4). These results are consistent with the previous finding that extremely high doses of ^{111}In-mAbs (up to 118 MBq per mouse, made possible by bone marrow transplantation) can be safely administered to mice with no signs of acute or chronic organ toxicity other than myelosuppression (*119*).

Cardiotoxicity is also a concern since prolonged trastuzumab therapy is associated with some risk for clinical cardiac dysfunction, especially when combined with chemotherapy regimens incorporating anthracyclines (*35*). Previously, we reported that the nuclear accumulation of ^{111}In-NLS-trastuzumab in cardiac tissue was very low (~0.1 %ID/g), suggesting

that the radiopharmaceutical should have a negligible toxic effect on heart function (*152*). Extrapolating these data to the human situation is complicated, however, due to the specificity of trastuzumab for only human HER2 and not the murine, c-erbB2 homologue (*21*). Nevertheless, HER2 receptor tyrosine kinases have been found only at minimal levels in the myocardium of breast cancer patients (*17*), and it has been suggested that the cardiotoxicity of trastuzumab-anthracycline combinations may in fact be related to myocardial injury caused by the anthracycline rather than by trastuzumab itself (*177-179*).

4.5 Conclusion

The results of this study demonstrated that the Auger electron-emitting radiopharmaceutical ^{111}In-NLS-trastuzumab had potent and selective tumor growth-inhibitory effects against HER2-overexpressing breast cancer xenografts *in vivo*. At the MTD previously determined in non-tumor bearing BALB/c mice, the radiopharmaceutical was well tolerated in treated tumor-bearing athymic mice. Taken together, these findings are encouraging for further development of this radiopharmaceutical for the treatment of HER2-positive breast cancer metastases in humans.

CHAPTER 5:

SUMMARY AND FUTURE DIRECTIONS

5.1 Thesis conclusions and summary of findings

This thesis has concentrated on the concept of molecular targeting of HER2 overexpressing tumors with ^{111}In-radiolabeled forms of trastuzumab (Herceptin) mAbs for treatment of HER2-positive breast cancer. The overall conclusions of the research described in this thesis are:

I. Conjugation of NLS-containing peptides to trastuzumab labeled with the Auger electron-emitter ^{111}In enhances its toxicity in HER2-positive breast cancer cells through routing of the radioimmunoconjugates to the cell nucleus.

II. NLS-peptides do not substantially interfere with the receptor-binding affinity of ^{111}In-trastuzumab, but enhance its ability to specifically accumulate *in vivo* into the nucleus of tumor cells.

III. ^{111}In-NLS-trastuzumab can kill trastuzumab-resistant breast cancer cells, and low-concentrations of methotrexate can potently enhance the sensitivity of these cells to the lethal Auger electrons emitted by this radiopharmaceutical.

IV. ^{111}In-NLS-trastuzumab exhibits potent and selective tumor-growth inhibitory effects against HER2-overexpressing breast cancer xenografts *in vivo*, and treatment with this radiopharmaceutical is associated with minimal normal tissue toxicity at the doses examined.

In Chapter 2, a novel radiotherapeutic agent capable of targeting the nucleus of HER2-overexpressing breast cancer cells was developed by conjugating ^{111}In-trastuzumab to NLS-peptides (CGYG*PKKKRKV*GG) derived from the SV-40 large T-antigen (*italicized*). ^{111}In-trastuzumab modified with 3 or 6 NLS peptides exhibited preserved binding affinity for HER2 on SK-BR-3 cells (K_d 3.1-5.9 $\times$ 10^{-9} moles/L), and its internalization was enhanced 2-5 fold. A similar phenomenon has been reported for ^{111}In-NLS-octreotide analogues in pancreatic tumor cells expressing somatostatin receptors (*126*). Hu et al. (*138*) similarly reported that mouse IgG

and anti-p21$^{WAF-1/Cip-1}$ mAbs conjugated to cationic peptides [GRKKRRQRRRPPQGYGC] derived from HIV-1 transactivator of transcription (TAT) protein exhibited enhanced cellular and nuclear uptake in human breast cancer cells. The mechanism of this NLS-enhanced, but receptor-mediated internalization might be explained by the cationic residues (lysine or arginine) in the NLS since cationic macromolecules have been shown to facilitate endocytosis through an adsorptive-mediated process through binding to negatively charged cell-surface proteins (*145*). Although the SV-40 NLS-peptides employed in these studies contain several cationic lysine residues, the uptake of radioactivity by SK-BR-3 cells exposed to ^{111}In-NLS-trastuzumab was blocked by unlabeled trastuzumab, demonstrating that internalization was mainly HER2 receptor-mediated.

The internalization of trastuzumab in combination with its routing to the nucleus mediated by the NLS-peptides was able to deliver DNA-damaging doses of Auger electron radiation to the nucleus of HER2-positive breast cancer cells and significantly diminished their surviving fraction in clonogenic assays. ^{111}In-NLS-trastuzumab was also avidly and specifically taken up by MDA-MB-361 tumors in athymic mice following i.v. injection. More importantly, there was no significant difference in the tumor and normal tissue uptake of ^{111}In-NLS-trastuzumab at 72 hours post-intravenous injection in athymic mice implanted s.c. with MDA-MB-361 tumor xenografts, but HER2-specific nuclear uptake in these tumors was improved 2-fold.

In Chapter 3, it was shown that trastuzumab-resistant breast cancer cells remained susceptible to the lethal, DNA-damaging Auger electrons from ^{111}In-NLS-trastuzumab. These studies were performed using MDA-MB-231 cells (which are HER2 0^{+}), that when transfected with the HER2 gene (231-H2N) express moderate HER2 levels and become sensitive to trastuzumab, as well as two trastuzumab-resistant subclones of 231-H2N cells (TrR1 and TrR2) (*156*). TrR1 and TrR2 cells were isolated from 231-H2N tumors in athymic mice with acquired trastuzumab resistance (*156*). On a molar concentration basis, ^{111}In-NLS-trastuzumab was 9 to 12-fold more toxic to 231-H2N and TrR1 cells compared to ^{111}In-trastuzumab (EC_{50} ~0.1-0.2 μmol/L versus 1.2-1.8 μmol/L, respectively), and 16 to 77-fold more lethal compared to unlabeled trastuzumab (3.2-7.7 μmol/L). MDA-MB-231 and TrR2 cells were less sensitive to ^{111}In-NLS-trastuzumab due to a 10-fold lower HER2 density. Low-doses of MTX had a radiosensitizing effect on 231-H2N and TrR1 cells, and enhanced their susceptibility to ^{111}In-

NLS-trastuzumab. As described previously, trastuzumab resistance is a major challenge in the treatment of HER2-amplified breast cancer (*22,24*). Even in responding patients, the effectiveness of the drug is limited and the duration of response short (*22,24*). Achieving a synergistic interaction by combining MTX and targeted Auger electron radioimmunotherapy could dramatically improve the response compared to either of these therapies alone.

The potent and selective tumor growth-inhibitory effect of ^{111}In-NLS-trastuzumab against HER2-overexpressing breast cancer xenografts was revealed in Chapter 4. The radiopharmaceutical was selectively radiotoxic to MDA-MB-361 breast cancer xenografts which have high levels of HER2 compared to MDA-MB-231 breast cancer xenografts with a low level of HER2 expression. There was no evidence of radiotoxicity over a 7-week observation period against normal tissues that accumulated appreciable levels of the radiopharmaceutical, such as the liver and kidneys. Cardiac toxicity might still be a possibility because the murine c-erbB2 homologue is not targeted in the mouse heart with ^{111}In-NLS-trastuzumab (*21*). A transgenic animal model might be more appropriate for this purpose (*21*). Nevertheless, these results are encouraging for the application of ^{111}In-NLS-trastuzumab for targeted Auger electron radiotherapy of HER2-positive advanced forms of breast cancer in humans.

5.2 Thesis discussion

5.2.1. The promise and perils of radioimmunotherapy

In the early part of the 20th century, Paul Ehrlich prophesied the role of modern-day pharmaceutical research, predicting that chemists would soon be able to produce substances ("magic bullets") that would seek out specific disease-causing agents (*175*). It was not until the early 1950s that this idea was first explored with an antibody conjugated to a radionuclide (*71*). The possibility of directing tumoricidal radiation doses to tumor cells using antibodies labeled with radionuclides provided the chance to turn into reality Ehrlich's "magic bullet" idea. However, although potentially useful for slowing solid tumor growth, radioimmunotherapy has not been effective in curing aggressive tumors (*176*). This has been primarily due to the problem of achieving sufficiently high tumor doses since a very small portion (0.001% to 0.05%) of the

administered radiolabeled antibody localizes in tumor tissue (*176*). The most commonly used radionuclides in radioimmunotherapy to date are high energy β-particle emitters (*71*). Since β-particles have a relatively long path length in tissue (2-12 mm), these radionuclides possess the advantage of being able to deliver "crossfire" doses of radiation to neighboring tumor cells, addressing issues such as antigen heterogeneity and poor tumor penetration of large antibody molecules (*67*). However, hematopoietic toxicities usually become dose-limiting before sufficiently high tumor doses can be reached. This is because circulating radiolabeled antibodies in the blood also irradiate and destroy surrounding normal stem cells in the bone marrow (*67*).

As previously mentioned in Chapter 2, Auger electron-emitting radioisotopes represent an intriguing alternative to β-particle emitters for targeted radiotherapy of cancer. Short-ranged Auger electron-emitters may be better suited to the treatment of microscopic or small-volume disease *if* they can be selectively directed into the target cells (*177*). These radionuclides are unique in that the Auger electron-emissions are only radiotoxic to cells which are able to internalize the radionuclide, due to the extremely short, subcellular range of these electrons (*177,178,67*). In situations where the Auger electron-emitter is internalized into the cytoplasm of the cell or particularly when localized in the cell nucleus however, they deliver very high LET radiation to the DNA and cause radiotoxicity comparable to that of α-emitters (*67*). Michel et al. (*103*) for example, described a strategy to deliver high doses of radiation selectively to HER2-overexpressing SK-BR-3 breast and SK-OV-3.ip1 ovarian cancer cells using mAb 4D5 (murine parent of trastuzumab) radiolabeled with the Auger electron-emitting radionuclide, ^{111}In. Despite the relatively high HER2 density on these cells (2 x 10^6 HER2 receptors per cell), very high specific activities (1.5 - 2.6 GBq/mg) were required for ^{111}In-4D5 to deliver a lethal radiation dose (*103*). This was likely due to the predominantly membrane and cytoplasmic localization of the ^{111}In-labeled mAbs, where most of the Auger electrons would have insufficient range to cause DNA damage in the nucleus. I utilized a novel strategy to insert ^{111}In-labeled trastuzumab mAbs directly into the nucleus of HER2-amplified breast cancer cells by conjugating them to 13-mer synthetic peptides (CGYG*PKKKRKV*GG) harboring the NLS of SV-40 large T-antigen (*italicized*), where dramatically lower doses of Auger electron radiation were required for lethality. Indeed, at only 240 MBq/mg (approximately 10-fold lower compared to ^{111}In-4D5), sufficient ^{111}In-NLS-trastuzumab mAbs were internalized and imported

into the nucleus of HER2-overexpressing breast cancer cells to induce frequent DNA double strand breaks and strongly decrease their clonogenic survival (Chapter 2 and 3). Other studies have extended this promising approach to the treatment of acute myelogenous leukemia (AML) (*125*). For example NLS conjugation enhanced the nuclear uptake and cytotoxicity of anti CD-33 mAbs ^{111}In-HuM195 and ^{111}In-M195 toward HL-60 myeloid leukemia cells and primary AML specimens (*125*). Taken together, these studies demonstrate that antibodies internalized into tumor cells through receptor-mediated processes can be efficiently routed to the nucleus through their modification with NLS-containing peptides and that this strategy can be exploited for targeted radiotherapy of hematologic as well as solid tumors using nanometer-to-micrometer range Auger electron-emitters.

5.2.2. Transport of molecules into the nucleus

NLS-conjugated radiopharmaceuticals represent a new class of agents that are not only transported into the desired tumor cell, but are also further transported into the nucleus where Auger electrons are most lethal (*124*). NLS are short positively-charged basic peptides that actively transport large proteins across the nuclear membrane (*179*). The SV-40 NLS-motif (PKKKRKV), for example, has been synthetically introduced into several Auger electron-emitting biomolecules typically excluded from the nucleus such as peptide growth factors and IgGs that target overexpressed tumor receptors, as well as oligodeoxynucleotides that target amplified gene products (i.e. anti-gene radiotherapy) (*124*). Small molecules and chemotherapeutic agents such as carboplatin have also been modified with an NLS and labeled with other Auger electron-emitting radionuclides, such as ^{191}Pt, ^{193m}Pt or ^{195m}Pt (*124*). These molecules undergo efficient nuclear translocation following conjugation to NLS. Naturally occurring NLS are also found in peptide growth factors or their receptors, where they function to deliver internalized ligands to the nucleus (*124*). In particular, the N-terminus intracellular domain of HER2 encodes an NLS (^{676}KRRQQKIRKYTMRR^{689}) and has been shown to interact with importin-β1 that facilitates the nuclear import of the receptor where it can transactivate the cyclooxygenase-2 promoter (*196,197*). The endogenous NLS in the HER2 receptor was unable to deliver ^{111}In-trastuzumab to the nucleus without modification with the NLS-peptides, but previously, it has been shown that ^{111}In-EGF is transported to the nucleus by the NLS in the transmembrane domain of the EGFR (*124*). The nuclear importation of ^{111}In-NLS-trastuzumab

is also believed to be due to interaction of the appended NLS peptides with importin α/β transporters following its HER2-mediated endocytosis. One aspect that is currently not well understood, however, is the mechanism by which ^{111}In-NLS-trastuzumab and other NLS-containing bioconjugates escape endosomal compartments. Bulmus et al. (*180*), described a novel pH-responsive polymer (pyridyl disulfide acrylate [PDSA]) containing a mixture of hydrophobic and acidic amino acids that are in a hydrated random coil conformation at physiological pH. However, at low pH such as those encountered in the endosome, these amino acids are protonated and form hydrophobic helices that become membrane-disruptive. Modification of ^{111}In-NLS-trastuzumab with an endosomal membrane disruption-motif such as PDSA might further enhance nuclear importation by avoiding post-endosomal routing to lysosomes and subsequent proteolytic degradation (*181*). Other approaches, such as using bipartite instead of monopartite NLS, which may improve interaction with importins (*179*), could potentially increase the efficiency of nuclear transport of ^{111}In-NLS-trastuzumab in breast cancer cells, thereby further amplifying the cytotoxicity of the Auger electrons.

5.2.3. The mechanism of tumor cell death

The predominant mechanism by which radiation kills mammalian cells is believed to be the reproductive (clonogenic) mode of cell kill primarily due to DNA double-strand breaks (*182*). Although most radiation-induced DNA breaks are rapidly repaired, residual or incorrectly repaired breaks lead to genetic instability, increased mutation frequency and chromosomal aberrations which may lead to apoptosis usually after several mitotic divisions. Even one double strand break remaining unrepaired in a cell can potentially result in cell death (*182*). On average, ^{111}In emits 14.7 Auger electrons per decay with an energy of 6.75 keV (*141*), and it has been estimated that the local energy deposition of an Auger electron-emitter incorporated into DNA would hit both DNA stands with energy of 1.6 MGy or higher (*85*). This energy deposition is sufficiently large enough to disrupt both DNA helices over distances of several nucleotides. In contrast, the decay of an Auger electron-emitter affixed to the cell plasma membrane or located extracellularly causes no extraordinary DNA damaging effects because of the insufficient range of the electrons (*86*).

Phosphorylation of H2AX (γH2AX) in response to double-strand breaks plays a crucial role in the recruitment of DNA repair and signaling factors at the sites of damage (*137*). An

immunocytochemical assay recognizing γH2AX foci is accepted as being an extremely sensitive and specific indicator for the existence of double-strand breaks induced by radiation (*201,202,148,203*). Using this assay, high levels of γH2AX-foci in HER2-overexpressing breast cancer cells that incorporated ^{111}In-NLS-trastuzumab into the nucleus were detected. Therefore, the radiotoxic effects of Auger electrons in cells that internalize ^{111}In-NLS-trastuzumab are likely mediated through direct ionizations and damage to DNA, or indirectly via the production of free radicals that can cause further chromosomal aberrations. Another possibility is the "bystander effect", in which radiobiologically damaged cells induce cell death in non-irradiated cells through the release of cytokines and free radicals (*183*). Xue et al. (*184*) showed that cells preloaded with the Auger electron-emitting ^{125}I-IUdR and mixed with unlabeled cells exerted a damaging effect on neighboring unlabeled tumor cells growing subcutaneously in athymic mice, thus demonstrating the potential of internalized Auger electron-emitters to generate bystander effects *in vivo*. Therefore, it is also possible that the anti-tumor effects of ^{111}In-NLS-trastuzumab are a result of toxic bystander signals produced and released from cells that sustain nuclear DNA damage, and which amplify the toxicity of the radiopharmaceutical by killing neighboring non-targeted tumor cells. It is important to note that this effect is not exclusive to tumor cells since freely diffusible bystander signals could also cause non-specific toxicities to normal tissues (*183*). However, there were no hematological toxicities associated with the administration of ^{111}In-NLS-trastuzumab to female BALB/c mice at the MTD, and no evidence of major damage to normal tissues that accumulated large amounts of the radiopharmaceutical such as the liver, spleen or kidney. There were also no generalized toxicities from the radiopharmaceutical in MDA-MB-361 tumor-bearing mice. Nevertheless, the bystander effect associated with Auger electron-radiotherapy using ^{111}In-NLS-trastuzumab is an intriguing area that warrants further investigation.

5.2.4. The clinical role of HER2-targeted Auger electron radiotherapy in breast cancer

In a phase III trial in HER2-overexpressing metastatic breast cancer, the addition of trastuzumab to a cytotoxic chemotherapy regimen was associated with statistically significant benefits, including longer median duration of response (9.1 versus 6.1 months), higher overall response rate (50% versus 32%) and lower death rate at one year (22% versus 33%) (*36*). Therefore, the use of ^{111}In-NLS-trastuzumab in conjunction with chemotherapeutics is a natural

extension of this approach. Considerable attention has been given to combining radioimmunotherapy with drugs that are known to be radiosensitizers or have other potential additive or synergistic properties (*72,69*). In Chapter 3, the radiosensitization effect of combined treatment using MTX and ^{111}In-NLS-trastuzumab was shown *in vitro*. Antimetabolites such as MTX are among the most potent radiosensitizers, and are often active at concentrations below those necessary to cause cytotoxicity (*164*). Non-cytotoxic concentrations of gemcitabine, for example, have been shown to enhance the radiosensitivity of HT-29 human colon carcinoma cells to external beam γ-irradiation, and produce RER values in the range of 1.4 to 2.0 (*185*). This is consistent with the level of radiosensitization that was observed, where RER values of approximately 1.6 were achieved in trastuzumab-sensitive (231-H2N) and trastuzumab-resistant (TrR1) breast cancer cells by combining non-toxic concentrations of MTX with ^{111}In-NLS-trastuzumab. Paclitaxel, taxotere, gemcitabine, topotecan, 5-fluorouracil, doxorubicin, tirapazamine or halogenated pyrimidines have also been combined with targeted radioimmunotherapeutics, suggesting that other chemotherapeutic drugs could be potential radiosensitizers if combined with ^{111}In-NLS-trastuzumab (*83*). It is likely that targeted Auger electron radiotherapy of HER2-positive breast cancer with ^{111}In-NLS-trastuzumab would ultimately be used in combination with other therapeutic agents including radiosensitizing chemotherapy in order to achieve a greater rate of response and more durable remissions.

Combination therapy may also be particularly necessary in order to overcome challenges associated with the inadequate delivery of the radiopharmaceutical to all cancer cells. HER2 heterogeneity, for example, has been observed in primary human breast cancer and metastases (*186*) and these low antigen-expressing regions may not be eradicated with a radiolabeled antibody targeted to one particular tumor-associated antigen. Antibody mixtures ("cocktails") that combine two or more radiolabeled antibodies recognizing several antigens may therefore be a useful strategy at circumventing the problems of non-uniform antibody delivery and antigen heterogeneity (*90*). Michel et al. (*103*) demonstrated that two non-competing ^{111}In-labeled mAbs to HER2 (21.1 and 4D5) used together resulted in increased binding of radioactivity on the surface of SK-BR-3 breast and SK-OV-3.ip1 ovarian cancer cells, and enhanced cytotoxicity compared to either mAb alone. Alternatively, one might predict further dramatic improvements through combining an Auger electron emitting agent such as ^{111}In-NLS-trastuzumab with a low-

energy beta emitter such as ^{177}Lu. The mean range of the emitted β-particles from ^{177}Lu is about 300 μm, which is long enough to give local crossfire irradiation and to allow for exposure of the cell nucleus even if the radionuclide is localized mainly on the cell surface, but also short enough not to irradiate large volumes of normal tissues (*90*).

5.3 Future Directions

To translate ^{111}In-NLS-trastuzumab from preclinical investigation to a phase I clinical trial, it will be necessary to create a pharmaceutical quality formulation manufactured under current Good Manufacturing Practices (cGMP) and obtain regulatory approval from Health Canada in the form of a Clinical Trial Application (CTA) (*187*). Thus, future research in this project will be to design and manufacture a kit under GMP conditions for the preparation of ^{111}In-NLS-trastuzumab Injection suitable for administration to patients. The formulation and quality control specifications and tests will be based on those that have previously been reported for analogous kits that have been approved by Health Canada for preparation of ^{111}In-DTPA-hEGF, an Auger electron-emitting radiotherapeutic agent for EGFR-overexpressing breast cancer (*187*).

Another area of future research interest is to elucidate the mechanisms of chemotherapy induced-radiosensitization of HER2-positive breast cancer cells to ^{111}In-NLS-trastuzumab. MTX, for example, has also been shown to radiosensitize normal and malignant cells to γ-radiation by causing these cells to arrest in the relatively radiosensitive G_1-S transition of the cell-cycle (*209,210,142,211*). Flow cytometric analysis of nuclear DNA content could therefore be used to determine if MTX-induced G_1/S-phase arrest also sensitizes breast cancer cells to Auger electron radiotherapy. Alternatively, trastuzumab can enhance radiation-induced apoptosis in breast cancer cells in a HER2-dependent manner (*188*). Therefore, the ability of combination treatment using ^{111}In-NLS-trastuzumab and MTX to induce apoptosis in breast cancer cells could be evaluated by probing for annexin V which has high affinity for externalized phosphatidylserine on the membrane of apoptotic cells (*189*). The results of *in vivo* testing will also need to be assessed before the combination of radiosensitizing chemotherapy and HER2-targeted Auger electron radiotherapy is evaluated in future phase I clinical trials.

Finally, micro-PET imaging studies using [^{18}F]-2-fluorodeoxyglucose (^{18}F-FDG) could potentially be used to assess early tumor response after therapy with ^{111}In-NLS-trasuzumab in mice bearing tumor xenografts. PET is a noninvasive imaging technique that permits the detection of annihilation photons produced by the disintegration of positron-emitting radioisotopes (*190*). Micro-PET is a dedicated PET scanner designed for high resolution imaging of small laboratory animals. ^{18}F-FDG is the most commonly available PET radiopharmaceutical, and its biological uptake is substantially increased in most types of cancer as compared with its uptake in most normal organs or tissues (*190*). ^{18}F-FDG-PET is used in clinical oncology for the staging and restaging of established disease, for the detection of occult tumors and for monitoring response to treatment with the ultimate goal of tailoring therapy according to the information provided (*190*). Studies performed in patients with breast cancer, for example, demonstrated a relatively rapid decline in the standardized uptake value (SUV) of ^{18}F-FDG in responding tumors after just one cycle of chemotherapy, whereas nonresponding tumors showed an increase, no change, or only a small decline in radiopharmaceutical uptake (*195,196*). Thus, patients who demonstrated an early response on PET can continue treatment, whereas a change in treatment would be indicated for those whom lack such a response (*190,191*). Although this technique is exquisitely sensitive for detecting response in breast cancer to chemotherapy, there has been only a single report examining the role of ^{18}F-FDG-PET in monitoring the effectiveness of therapy with targeted radiotherapeutics (*192*). Thus micro-PET studies in mice will provide insight into implementing PET into future clinical trials to monitor patient response to HER2-targeted Auger electron radioimmunotherapy.

REFERENCES

1. Breast cancer stats. 17 August 2008; http://www.cancer.ca.
2. Jemal A, Siegel R, Ward E, et al. Cancer statistics, 2008. *CA: a cancer journal for clinicians.*2008;58:71-96.
3. Russo J, Russo IH. Breast development, hormones and cancer. *Advances in experimental medicine and biology.*2008;630:52-56.
4. Polyak K. Breast cancer: origins and evolution. *The Journal of clinical investigation.*2007;117:3155-3163.
5. Page DL, Kidd TE, Jr., Dupont WD, Simpson JF, Rogers LW. Lobular neoplasia of the breast: higher risk for subsequent invasive cancer predicted by more extensive disease. *Human pathology.*1991;22:1232-1239.
6. Moulder S, Hortobagyi GN. Advances in the treatment of breast cancer. *Clinical pharmacology and therapeutics.*2008;83:26-36.
7. Black MM, Opler SR, Speer FD. Survival in breast cancer cases in relation to the structure of the primary tumor and regional lymph nodes. *Surgery, gynecology & obstetrics.*1955;100:543-551.
8. Ellis IO, Galea M, Broughton N, Locker A, Blamey RW, Elston CW. Pathological prognostic factors in breast cancer. II. Histological type. Relationship with survival in a large study with long-term follow-up. *Histopathology.*1992;20:479-489.
9. Fisher ER, Costantino J, Fisher B, Palekar AS, Redmond C, Mamounas E. Pathologic findings from the National Surgical Adjuvant Breast Project (NSABP) Protocol B-17. Intraductal carcinoma (ductal carcinoma in situ). The National Surgical Adjuvant Breast and Bowel Project Collaborating Investigators. *Cancer.*1995;75:1310-1319.
10. Morrow M, Strom EA, Bassett LW, et al. Standard for breast conservation therapy in the management of invasive breast carcinoma. *CA: a cancer journal for clinicians.*2002;52:277-300.
11. Hortobagyi GN, Buzdar AU, Strom EA, Ames FC, Singletary SE. Primary chemotherapy for early and advanced breast cancer. *Cancer Lett.*1995;90:103-109.

12. Costa A, Zurrida S, Gatti G, et al. Less aggressive surgery and radiotherapy is the way forward. *Current opinion in oncology.*2004;16:523-528.
13. Isaac N, Panzarella T, Lau A, et al. Concurrent cyclophosphamide, methotrexate, and 5-fluorouracil chemotherapy and radiotherapy for breast carcinoma: a well tolerated adjuvant regimen. *Cancer.*2002;95:696-703.
14. Morandi P, Rouzier R, Altundag K, Buzdar AU, Theriault RL, Hortobagyi G. The role of aromatase inhibitors in the adjuvant treatment of breast carcinoma: the M. D. Anderson Cancer Center evidence-based approach. *Cancer.*2004;101:1482-1489.
15. Slamon D, Eiermann W, Robert N, Pienkowski T. Phase III randomized trial comparing doxorubicin and cyclophosphamide followed by docetaxel (ACT) with doxorubicin and cyclophosphamide followed by docetaxel and trastuzumab (ACTH) with docetaxel, carboplatin and trastuzumab (TCH) in HER2 positive early breast cancer patients: BCIRG 006 study. *Breast Cancer Res Treat.*2005;94(Suppl 1):S5.
16. Cooke T. What is HER2? *Eur J Oncol Nurs.*2000;4:2-9.
17. Press MF, Cordon-Cardo C, Slamon DJ. Expression of the HER-2/neu proto-oncogene in normal human adult and fetal tissues. *Oncogene.*1990;5:953-962.
18. Yarden Y, Sliwkowski MX. Untangling the ErbB signalling network. *Nat Rev Mol Cell Biol.*2001;2:127-137.
19. Olayioye MA. Update on HER-2 as a target for cancer therapy: intracellular signaling pathways of ErbB2/HER-2 and family members. *Breast Cancer Res.*2001;3:385-389.
20. Ursini-Siegel J, Schade B, Cardiff RD, Muller WJ. Insights from transgenic mouse models of ERBB2-induced breast cancer. *Nature reviews.*2007;7:389-397.
21. Pegram M, Ngo D. Application and potential limitations of animal models utilized in the development of trastuzumab (Herceptin): a case study. *Adv Drug Deliv Rev.*2006;58:723-734.
22. Nahta R, Esteva FJ. Herceptin: mechanisms of action and resistance. *Cancer Lett.*2006;232:123-138.
23. Slamon DJ, Godolphin W, Jones LA, et al. Studies of the HER-2/neu proto-oncogene in human breast and ovarian cancer. *Science (New York, NY.*1989;244:707-712.

24. Nahta R, Yu D, Hung MC, Hortobagyi GN, Esteva FJ. Mechanisms of disease: understanding resistance to HER2-targeted therapy in human breast cancer. *Nat Clin Pract Oncol.*2006;3:269-280.
25. Slamon DJ, Clark GM, Wong SG, Levin WJ, Ullrich A, McGuire WL. Human breast cancer: correlation of relapse and survival with amplification of the HER-2/neu oncogene. *Science (New York, NY.*1987;235:177-182.
26. Roque AC, Lowe CR, Taipa MA. Antibodies and genetically engineered related molecules: production and purification. *Biotechnology progress.*2004;20:639-654.
27. Lobo ED, Hansen RJ, Balthasar JP. Antibody pharmacokinetics and pharmacodynamics. *Journal of pharmaceutical sciences.*2004;93:2645-2668.
28. Reilly RM, Sandhu J, Alvarez-Diez TM, Gallinger S, Kirsh J, Stern H. Problems of delivery of monoclonal antibodies. Pharmaceutical and pharmacokinetic solutions. *Clinical pharmacokinetics.*1995;28:126-142.
29. Wu AM, Senter PD. Arming antibodies: prospects and challenges for immunoconjugates. *Nat Biotechnol.*2005;23:1137-1146.
30. Cho HS, Mason K, Ramyar KX, et al. Structure of the extracellular region of HER2 alone and in complex with the Herceptin Fab. *Nature.*2003;421:756-760.
31. Carter P, Presta L, Gorman CM, et al. Humanization of an anti-p185HER2 antibody for human cancer therapy. *Proc Natl Acad Sci U S A.*1992;89:4285-4289.
32. Baselga J, Tripathy D, Mendelsohn J, et al. Phase II study of weekly intravenous recombinant humanized anti-p185HER2 monoclonal antibody in patients with HER2/neu-overexpressing metastatic breast cancer. *J Clin Oncol.*1996;14:737-744.
33. Cobleigh MA, Vogel CL, Tripathy D, et al. Multinational study of the efficacy and safety of humanized anti-HER2 monoclonal antibody in women who have HER2-overexpressing metastatic breast cancer that has progressed after chemotherapy for metastatic disease. *J Clin Oncol.*1999;17:2639-2648.
34. Vogel CL, Cobleigh MA, Tripathy D, et al. Efficacy and safety of trastuzumab as a single agent in first-line treatment of HER2-overexpressing metastatic breast cancer. *J Clin Oncol.*2002;20:719-726.

35. Tokunaga E, Oki E, Nishida K, et al. Trastuzumab and breast cancer: developments and current status. *Int J Clin Oncol.*2006;11:199-208.

36. Slamon DJ, Leyland-Jones B, Shak S, et al. Use of chemotherapy plus a monoclonal antibody against HER2 for metastatic breast cancer that overexpresses HER2. *N Engl J Med.*2001;344:783-792.

37. Romond EH, Perez EA, Bryant J, et al. Trastuzumab plus adjuvant chemotherapy for operable HER2-positive breast cancer. *N Engl J Med.*2005;353:1673-1684.

38. Buzdar AU, Ibrahim NK, Francis D, et al. Significantly higher pathologic complete remission rate after neoadjuvant therapy with trastuzumab, paclitaxel, and epirubicin chemotherapy: results of a randomized trial in human epidermal growth factor receptor 2-positive operable breast cancer. *J Clin Oncol.*2005;23:3676-3685.

39. Clynes RA, Towers TL, Presta LG, Ravetch JV. Inhibitory Fc receptors modulate in vivo cytoxicity against tumor targets. *Nat Med.*2000;6:443-446.

40. Gennari R, Menard S, Fagnoni F, et al. Pilot study of the mechanism of action of preoperative trastuzumab in patients with primary operable breast tumors overexpressing HER2. *Clin Cancer Res.*2004;10:5650-5655.

41. Lipponen P, Ji H, Aaltomaa S, Syrjanen K. Tumour vascularity and basement membrane structure in breast cancer as related to tumour histology and prognosis. *J Cancer Res Clin Oncol.*1994;120:645-650.

42. Izumi Y, Xu L, di Tomaso E, Fukumura D, Jain RK. Tumour biology: herceptin acts as an anti-angiogenic cocktail. *Nature.*2002;416:279-280.

43. Klos KS, Zhou X, Lee S, et al. Combined trastuzumab and paclitaxel treatment better inhibits ErbB-2-mediated angiogenesis in breast carcinoma through a more effective inhibition of Akt than either treatment alone. *Cancer.*2003;98:1377-1385.

44. Wen XF, Yang G, Mao W, et al. HER2 signaling modulates the equilibrium between pro- and antiangiogenic factors via distinct pathways: implications for HER2-targeted antibody therapy. *Oncogene.*2006;25:6986-6996.

45. Baselga J. Is circulating HER-2 more than just a tumor marker? *Clin Cancer Res.*2001;7:2605-2607.

46. Molina MA, Codony-Servat J, Albanell J, Rojo F, Arribas J, Baselga J. Trastuzumab (herceptin), a humanized anti-Her2 receptor monoclonal antibody, inhibits basal and activated Her2 ectodomain cleavage in breast cancer cells. *Cancer Res.*2001;61:4744-4749.

47. Fornier MN, Seidman AD, Schwartz MK, et al. Serum HER2 extracellular domain in metastatic breast cancer patients treated with weekly trastuzumab and paclitaxel: association with HER2 status by immunohistochemistry and fluorescence in situ hybridization and with response rate. *Ann Oncol.*2005;16:234-239.

48. Kostler WJ, Schwab B, Singer CF, et al. Monitoring of serum Her-2/neu predicts response and progression-free survival to trastuzumab-based treatment in patients with metastatic breast cancer. *Clin Cancer Res.*2004;10:1618-1624.

49. Valabrega G, Montemurro F, Aglietta M. Trastuzumab: mechanism of action, resistance and future perspectives in HER2-overexpressing breast cancer. *Ann Oncol.*2007;18:977-984.

50. Lan KH, Lu CH, Yu D. Mechanisms of trastuzumab resistance and their clinical implications. *Ann N Y Acad Sci.*2005;1059:70-75.

51. Sherr CJ, Roberts JM. CDK inhibitors: positive and negative regulators of G1-phase progression. *Genes Dev.*1999;13:1501-1512.

52. Lane HA, Beuvink I, Motoyama AB, Daly JM, Neve RM, Hynes NE. ErbB2 potentiates breast tumor proliferation through modulation of p27(Kip1)-Cdk2 complex formation: receptor overexpression does not determine growth dependency. *Mol Cell Biol.*2000;20:3210-3223.

53. Le XF, Claret FX, Lammayot A, et al. The role of cyclin-dependent kinase inhibitor p27Kip1 in anti-HER2 antibody-induced G1 cell cycle arrest and tumor growth inhibition. *J Biol Chem.*2003;278:23441-23450.

54. Anido J, Scaltriti M, Bech Serra JJ, et al. Biosynthesis of tumorigenic HER2 C-terminal fragments by alternative initiation of translation. *Embo J.*2006;25:3234-3244.

55. Nagy P, Friedlander E, Tanner M, et al. Decreased accessibility and lack of activation of ErbB2 in JIMT-1, a herceptin-resistant, MUC4-expressing breast cancer cell line. *Cancer Res.*2005;65:473-482.

56. Zabrecky JR, Lam T, McKenzie SJ, Carney W. The extracellular domain of p185/neu is released from the surface of human breast carcinoma cells, SK-BR-3. *J Biol Chem.*1991;266:1716-1720.

57. Esteva FJ, Cheli CD, Fritsche H, et al. Clinical utility of serum HER2/neu in monitoring and prediction of progression-free survival in metastatic breast cancer patients treated with trastuzumab-based therapies. *Breast Cancer Res.*2005;7:R436-443.

58. Diermeier S, Horvath G, Knuechel-Clarke R, Hofstaedter F, Szollosi J, Brockhoff G. Epidermal growth factor receptor coexpression modulates susceptibility to Herceptin in HER2/neu overexpressing breast cancer cells via specific erbB-receptor interaction and activation. *Exp Cell Res.*2005;304:604-619.

59. Motoyama AB, Hynes NE, Lane HA. The efficacy of ErbB receptor-targeted anticancer therapeutics is influenced by the availability of epidermal growth factor-related peptides. *Cancer Res.*2002;62:3151-3158.

60. Valabrega G, Montemurro F, Sarotto I, et al. TGFalpha expression impairs Trastuzumab-induced HER2 downregulation. *Oncogene.*2005;24:3002-3010.

61. Ritter CA, Perez-Torres M, Rinehart C, et al. Human breast cancer cells selected for resistance to trastuzumab in vivo overexpress epidermal growth factor receptor and ErbB ligands and remain dependent on the ErbB receptor network. *Clin Cancer Res.*2007;13:4909-4919.

62. Smith BL, Chin D, Maltzman W, Crosby K, Hortobagyi GN, Bacus SS. The efficacy of Herceptin therapies is influenced by the expression of other erbB receptors, their ligands and the activation of downstream signalling proteins. *Br J Cancer.*2004;91:1190-1194.

63. Frasca F, Pandini G, Sciacca L, et al. The role of insulin receptors and IGF-I receptors in cancer and other diseases. *Archives of physiology and biochemistry.*2008;114:23-37.

64. Lu Y, Zi X, Zhao Y, Mascarenhas D, Pollak M. Insulin-like growth factor-I receptor signaling and resistance to trastuzumab (Herceptin). *J Natl Cancer Inst.*2001;93:1852-1857.

65. Nahta R, Yuan LX, Zhang B, Kobayashi R, Esteva FJ. Insulin-like growth factor-I receptor/human epidermal growth factor receptor 2 heterodimerization contributes to trastuzumab resistance of breast cancer cells. *Cancer Res.*2005;65:11118-11128.

66. Lu Y, Zi X, Pollak M. Molecular mechanisms underlying IGF-I-induced attenuation of the growth-inhibitory activity of trastuzumab (Herceptin) on SKBR3 breast cancer cells. *Int J Cancer.*2004;108:334-341.

67. Reilly RM. Biopharmaceuticals as targeting vehicles for in situ radiotherapy of malignancies. In: Knäblein J, ed. *Modern Biopharmaceuticals*. Weinheim: Wiley-VCH Verlag GmbH & Co; 2005:497-535.

68. Sharkey RM, Goldenberg DM. Targeted therapy of cancer: new prospects for antibodies and immunoconjugates. *CA: a cancer journal for clinicians.*2006;56:226-243.

69. Stern M, Herrmann R. Overview of monoclonal antibodies in cancer therapy: present and promise. *Crit Rev Oncol Hematol.*2005;54:11-29.

70. DeNardo GL. Treatment of non-Hodgkin's lymphoma (NHL) with radiolabeled antibodies (mAbs). *Semin Nucl Med.*2005;35:202-211.

71. Sharkey RM, Goldenberg DM. Perspectives on cancer therapy with radiolabeled monoclonal antibodies. *J Nucl Med.*2005;46 Suppl 1:115S-127S.

72. Burke JM, Jurcic JG, Scheinberg DA. Radioimmunotherapy for acute leukemia. *Cancer Control.*2002;9:106-113.

73. Brechbiel MW, Waldmann TA. Anti-HER2 radioimmunotherapy. *Breast disease.*2000;11:125-132.

74. Tsai SW, Sun Y, Williams LE, Raubitschek AA, Wu AM, Shively JE. Biodistribution and radioimmunotherapy of human breast cancer xenografts with radiometal-labeled DOTA conjugated anti-HER2/neu antibody 4D5. *Bioconjug Chem.*2000;11:327-334.

75. Zhang DY, Li Y, Rizvi SM, Qu C, Kearsley J, Allen BJ. Cytotoxicity of breast cancer cells overexpressing HER2/neu by (213)Bi-Herceptin radioimmunoconjugate. *Cancer Lett.*2005;218:181-190.

76. Akabani G, Carlin S, Welsh P, Zalutsky MR. In vitro cytotoxicity of 211At-labeled trastuzumab in human breast cancer cell lines: effect of specific activity and HER2 receptor heterogeneity on survival fraction. *Nucl Med Biol.*2006;33:333-347.

77. Li Y, Cozzi PJ, Qu CF, et al. Cytotoxicity of human prostate cancer cell lines in vitro and induction of apoptosis using 213Bi-Herceptin alpha-conjugate. *Cancer Lett.*2004;205:161-171.

78. Ballangrud AM, Yang WH, Palm S, et al. Alpha-particle emitting atomic generator (Actinium-225)-labeled trastuzumab (herceptin) targeting of breast cancer spheroids: efficacy versus HER2/neu expression. *Clin Cancer Res.*2004;10:4489-4497.

79. Horak E, Hartmann F, Garmestani K, et al. Radioimmunotherapy targeting of HER2/neu oncoprotein on ovarian tumor using lead-212-DOTA-AE1. *J Nucl Med.*1997;38:1944-1950.

80. Milenic DE, Garmestani K, Brady ED, et al. Potentiation of high-LET radiation by gemcitabine: targeting HER2 with trastuzumab to treat disseminated peritoneal disease. *Clin Cancer Res.*2007;13:1926-1935.

81. Milenic DE, Garmestani K, Brady ED, et al. Alpha-particle radioimmunotherapy of disseminated peritoneal disease using a (212)Pb-labeled radioimmunoconjugate targeting HER2. *Cancer Biother Radiopharm.*2005;20:557-568.

82. Milenic DE, Garmestani K, Brady ED, et al. Multimodality therapy: potentiation of high linear energy transfer radiation with paclitaxel for the treatment of disseminated peritoneal disease. *Clin Cancer Res.*2008;14:5108-5115.

83. DeNardo SJ, Denardo GL. Targeted radionuclide therapy for solid tumors: an overview. *Int J Radiat Oncol Biol Phys.*2006;66:S89-95.

84. DeNardo SJ. Radioimmunodetection and therapy of breast cancer. *Semin Nucl Med.*2005;35:143-151.

85. Buchegger F, Perillo-Adamer F, Dupertuis YM, Bischof Delaloye A. Auger radiation targeted into DNA: a therapy perspective. *Eur J Nucl Med Mol Imaging.*2006.

86. Kassis AI. The amazing world of auger electrons. *Int J Radiat Biol.*2004;80:789-803.

87. Reilly RM, Kiarash R, Cameron RG, et al. 111In-labeled EGF is selectively radiotoxic to human breast cancer cells overexpressing EGFR. *J Nucl Med.*2000;41:429-438.

88. Walicka MA, Adelstein SJ, Kassis AI. Indirect mechanisms contribute to biological effects produced by decay of DNA-incorporated iodine-125 in mammalian cells in vitro: double-strand breaks. *Radiat Res.*1998;149:134-141.

89. Walicka MA, Adelstein SJ, Kassis AI. Indirect mechanisms contribute to biological effects produced by decay of DNA-incorporated iodine-125 in mammalian cells in vitro: clonogenic survival. *Radiat Res.*1998;149:142-146.

90. Boswell CA, Brechbiel MW. Auger electrons: lethal, low energy, and coming soon to a tumor cell nucleus near you. *J Nucl Med.*2005;46:1946-1947.

91. Bodei L, Kassis AI, Adelstein SJ, Mariani G. Radionuclide therapy with iodine-125 and other auger-electron-emitting radionuclides: experimental models and clinical applications. *Cancer Biother Radiopharm.*2003;18:861-877.

92. Kassis AI, Wen PY, Van den Abbeele AD, et al. 5-[125I]iodo-2'-deoxyuridine in the radiotherapy of brain tumors in rats. *J Nucl Med.*1998;39:1148-1154.

93. Kassis AI, Kirichian AM, Wang K, Semnani ES, Adelstein SJ. Therapeutic potential of 5-[125I]iodo-2'-deoxyuridine and methotrexate in the treatment of advanced neoplastic meningitis. *Int J Radiat Biol.*2004;80:941-946.

94. Krenning EP, Kwekkeboom DJ, Bakker WH, et al. Somatostatin receptor scintigraphy with [111In-DTPA-D-Phe1]- and [123I-Tyr3]-octreotide: the Rotterdam experience with more than 1000 patients. *European journal of nuclear medicine.*1993;20:716-731.

95. de Jong M, Kwekkeboom D, Valkema R, Krenning EP. Radiolabelled peptides for tumour therapy: current status and future directions. Plenary lecture at the EANM 2002. *Eur J Nucl Med Mol Imaging.*2003;30:463-469.

96. Andersson P, Forssell-Aronsson E, Johanson V, et al. Internalization of indium-111 into human neuroendocrine tumor cells after incubation with indium-111-DTPA-D-Phe1-octreotide. *J Nucl Med.*1996;37:2002-2006.

97. Janson ET, Westlin JE, Ohrvall U, Oberg K, Lukinius A. Nuclear localization of 111In after intravenous injection of [111In-DTPA-D-Phe1]-octreotide in patients with neuroendocrine tumors. *J Nucl Med.*2000;41:1514-1518.

98. Slooter GD, Aalbers AG, Breeman WA, et al. The inhibitory effect of (111)In-DTPA(0)-octreotide on intrahepatic tumor growth after partial hepatectomy. *J Nucl Med.*2002;43:1681-1687.

99. Anthony LB, Woltering EA, Espenan GD, Cronin MD, Maloney TJ, McCarthy KE. Indium-111-pentetreotide prolongs survival in gastroenteropancreatic malignancies. *Semin Nucl Med.*2002;32:123-132.

100. Valkema R, De Jong M, Bakker WH, et al. Phase I study of peptide receptor radionuclide therapy with [In-DTPA]octreotide: the Rotterdam experience. *Semin Nucl Med.*2002;32:110-122.

101. Chen P, Cameron R, Wang J, Vallis KA, Reilly RM. Antitumor effects and normal tissue toxicity of 111In-labeled epidermal growth factor administered to athymic mice bearing epidermal growth factor receptor-positive human breast cancer xenografts. *J Nucl Med.*2003;44:1469-1478.

102. Chen P, Mrkobrada M, Vallis KA, et al. Comparative antiproliferative effects of (111)In-DTPA-hEGF, chemotherapeutic agents and gamma-radiation on EGFR-positive breast cancer cells. *Nucl Med Biol.*2002;29:693-699.

103. Michel RB, Andrews PM, Castillo ME, Mattes MJ. In vitro cytotoxicity of carcinoma cells with 111In-labeled antibodies to HER-2. *Mol Cancer Ther.*2005;4:927-937.

104. Mattes MJ, Goldenberg DM. Therapy of human carcinoma xenografts with antibodies to EGFr and HER-2 conjugated to radionuclides emitting low-energy electrons. *Eur J Nucl Med Mol Imaging.*2008;35:1249-1258.

105. Ylikomi T, Bocquel MT, Berry M, Gronemeyer H, Chambon P. Cooperation of proto-signals for nuclear accumulation of estrogen and progesterone receptors. *Embo J.*1992;11:3681-3694.

106. Beckmann MW, Scharl A, Rosinsky BJ, Holt JA. Breaks in DNA accompany estrogen-receptor-mediated cytotoxicity from 16 alpha[125I]iodo-17 beta-estradiol. *J Cancer Res Clin Oncol.*1993;119:207-214.

107. Bloomer WD, McLaughlin WH, Weichselbaum RR, et al. Iodine-125-labelled tamoxifen is differentially cytoxic to cells containing oestrogen receptors. *Int J Radiat Biol Relat Stud Phys Chem Med.*1980;38:197-202.

108. DeSombre ER, Mease RC, Hughes A, Harper PV, DeJesus OT, Friedman AM. Bromine-80m-labeled estrogens: Auger electron-emitting, estrogen receptor-directed ligands with potential for therapy of estrogen receptor-positive cancers. *Cancer Res.*1988;48:899-906.

109. McLaughlin WH, Milius RA, Pillai KM, Edasery JP, Blumenthal RD, Bloomer WD. Cytotoxicity of receptor-mediated 16 alpha-[125I]iodoestradiol in cultured MCF-7 human breast cancer cells. *J Natl Cancer Inst.*1989;81:437-440.

110. Yasui L, Hughes A, DeSombre E. Relative biological effectiveness of accumulated 125IdU and 125I-estrogen decays in estrogen receptor-expressing MCF-7 human breast cancer cells. *Radiat Res.*2001;155:328-334.

111. DeSombre ER, Hughes A, Hanson RN, Kearney T. Therapy of estrogen receptor-positive micrometastases in the peritoneal cavity with Auger electron-emitting estrogens--theoretical and practical considerations. *Acta oncologica (Stockholm, Sweden).*2000;39:659-666.

112. Barendswaard EC, Humm JL, O'Donoghue JA, et al. Relative therapeutic efficacy of (125)I- and (131)I-labeled monoclonal antibody A33 in a human colon cancer xenograft. *J Nucl Med.*2001;42:1251-1256.

113. Behr TM, Sgouros G, Vougiokas V, et al. Therapeutic efficacy and dose-limiting toxicity of Auger-electron vs. beta emitters in radioimmunotherapy with internalizing antibodies: evaluation of 125I- vs. 131I-labeled CO17-1A in a human colorectal cancer model. *Int J Cancer.*1998;76:738-748.

114. Daghighian F, Barendswaard E, Welt S, et al. Enhancement of radiation dose to the nucleus by vesicular internalization of iodine-125-labeled A33 monoclonal antibody. *J Nucl Med.*1996;37:1052-1057.

115. Woo DV, Li D, Mattis JA, Steplewski Z. Selective chromosomal damage and cytotoxicity of 125I-labeled monoclonal antibody 17-1a in human cancer cells. *Cancer Res.*1989;49:2952-2958.

116. Behr TM, Behe M, Lohr M, et al. Therapeutic advantages of Auger electron- over beta-emitting radiometals or radioiodine when conjugated to internalizing antibodies. *European journal of nuclear medicine.*2000;27:753-765.

117. Welt S, Scott AM, Divgi CR, et al. Phase I/II study of iodine 125-labeled monoclonal antibody A33 in patients with advanced colon cancer. *J Clin Oncol.*1996;14:1787-1797.

118. Meredith RF, Khazaeli MB, Plott WE, et al. Initial clinical evaluation of iodine-125-labeled chimeric 17-1A for metastatic colon cancer. *J Nucl Med.*1995;36:2229-2233.

119. Karamychev VN, Panyutin IG, Kim MK, et al. DNA cleavage by 111In-labeled oligodeoxyribonucleotides. *J Nucl Med.*2000;41:1093-1101.

120. Sedelnikova OA, Luu AN, Karamychev VN, Panyutin IG, Neumann RD. Development of DNA-based radiopharmaceuticals carrying Auger-electron emitters for antigene radiotherapy. *Int J Radiat Oncol Biol Phys.*2001;49:391-396.

121. Goldfarb DS, Gariepy J, Schoolnik G, Kornberg RD. Synthetic peptides as nuclear localization signals. *Nature.*1986;322:641-644.

122. Yoneda Y, Arioka T, Imamoto-Sonobe N, Sugawa H, Shimonishi Y, Uchida T. Synthetic peptides containing a region of SV 40 large T-antigen involved in nuclear localization direct the transport of proteins into the nucleus. *Exp Cell Res.*1987;170:439-452.

123. Yoneda Y, Semba T, Kaneda Y, et al. A long synthetic peptide containing a nuclear localization signal and its flanking sequences of SV40 T-antigen directs the transport of IgM into the nucleus efficiently. *Exp Cell Res.*1992;201:313-320.

124. Costantini DL, Hu M, Reilly RM. Peptide motifs for insertion of radiolabeled biomolecules into cells and routing to the nucleus for cancer imaging or radiotherapeutic applications. *Cancer Biother Radiopharm.*2008;23:3-24.

125. Chen P, Wang J, Hope K, et al. Nuclear localizing sequences promote nuclear translocation and enhance the radiotoxicity of the anti-CD33 monoclonal antibody HuM195 labeled with 111In in human myeloid leukemia cells. *J Nucl Med.*2006;47:827-836.

126. Ginj M, Hinni K, Tschumi S, Schulz S, Maecke HR. Trifunctional somatostatin-based derivatives designed for targeted radiotherapy using auger electron emitters. *J Nucl Med.*2005;46:2097-2103.

127. Poon GM, Gariepy J. Cell-surface proteoglycans as molecular portals for cationic peptide and polymer entry into cells. *Biochemical Society transactions.*2007;35:788-793.

128. Jones SW, Christison R, Bundell K, et al. Characterisation of cell-penetrating peptide-mediated peptide delivery. *Br J Pharmacol.*2005;145:1093-1102.

129. Reubi JC, Macke HR, Krenning EP. Candidates for peptide receptor radiotherapy today and in the future. *J Nucl Med.*2005;46 Suppl 1:67S-75S.

130. Sedelnikova OA, Karamychev VN, Panyutin IG, Neumann RD. Sequence-specific gene cleavage in intact mammalian cells by 125I-labeled triplex-forming oligonucleotides conjugated with nuclear localization signal peptide. *Antisense Nucleic Acid Drug Dev.*2002;12:43-49.

131. Haefliger P, Agorastos N, Renard A, Giambonini-Brugnoli G, Marty C, Alberto R. Cell uptake and radiotoxicity studies of an nuclear localization signal peptide-intercalator conjugate labeled with [99mTc(CO)3]+. *Bioconjug Chem.*2005;16:582-587.

132. Buchsbaum DJ. Experimental radioimmunotherapy. *Semin Radiat Oncol.*2000;10:156-167.

133. Lawrence TS, Blackstock AW, McGinn C. The mechanism of action of radiosensitization of conventional chemotherapeutic agents. *Semin Radiat Oncol.*2003;13:13-21.

134. Guarneri V, Conte PF. The curability of breast cancer and the treatment of advanced disease. *Eur J Nucl Med Mol Imaging.*2004;31 Suppl 1:S149-161.

135. Tang Y, Wang J, Scollard DA, et al. Imaging of HER2/neu-positive BT-474 human breast cancer xenografts in athymic mice using (111)In-trastuzumab (Herceptin) Fab fragments. *Nucl Med Biol.*2005;32:51-58.

136. Konecny G, Pauletti G, Pegram M, et al. Quantitative association between HER-2/neu and steroid hormone receptors in hormone receptor-positive primary breast cancer. *J Natl Cancer Inst.*2003;95:142-153.

137. Peng M, Litman R, Jin Z, Fong G, Cantor SB. BACH1 is a DNA repair protein supporting BRCA1 damage response. *Oncogene.*2006;25:2245-2253.

138. Hu M, Chen P, Wang J, Chan C, Scollard DA, Reilly RM. Site-specific conjugation of HIV-1 tat peptides to IgG: a potential route to construct radioimmunoconjugates for targeting intracellular and nuclear epitopes in cancer. *Eur J Nucl Med Mol Imaging.*2006;33:301-310.

139. Hnatowich DJ, Childs RL, Lanteigne D, Najafi A. The preparation of DTPA-coupled antibodies radiolabeled with metallic radionuclides: an improved method. *J Immunol Methods.*1983;65:147-157.

140. Cardoso F, Piccart MJ, Durbecq V, Di Leo A. Resistance to trastuzumab: a necessary evil or a temporary challenge? *Clin Breast Cancer.*2002;3:247-257; discussion 258-249.

141. Howell RW. Radiation spectra for Auger-electron emitting radionuclides: report No. 2 of AAPM Nuclear Medicine Task Group No. 6. *Med Phys.*1992;19:1371-1383.

142. Wasielewski M, Elstrodt F, Klijn JG, Berns EM, Schutte M. Thirteen new p53 gene mutants identified among 41 human breast cancer cell lines. *Breast Cancer Res Treat.*2006;99:97-101.

143. Austin CD, De Maziere AM, Pisacane PI, et al. Endocytosis and sorting of ErbB2 and the site of action of cancer therapeutics trastuzumab and geldanamycin. *Mol Biol Cell.*2004;15:5268-5282.

144. Ong GL, Mattes MJ. Limitations in the use of low pH extraction to distinguish internalized from cell surface-bound radiolabeled antibody. *Nucl Med Biol.*2000;27:571-575.

145. Pardridge WM, Buciak J, Yang J, Wu D. Enhanced endocytosis in cultured human breast carcinoma cells and in vivo biodistribution in rats of a humanized monoclonal antibody after cationization of the protein. *J Pharmacol Exp Ther.*1998;286:548-554.

146. Lub-de Hooge MN, Kosterink JG, Perik PJ, et al. Preclinical characterisation of 111In-DTPA-trastuzumab. *Br J Pharmacol.*2004;143:99-106.

147. Goddu SM, Howell RW, Rao DV. Cellular dosimetry: absorbed fractions for monoenergetic electron and alpha particle sources and S-values for radionuclides uniformly distributed in different cell compartments. *J Nucl Med.*1994;35:303-316.

148. Kolar Z, Murray PG, Zapletalova J. Expression of c-erbB-2 in node negative breast cancer does not correlate with estrogen receptor status, predictors of hormone responsiveness, or PCNA expression. *Neoplasma.*2002;49:110-113.

149. Love RR, Duc NB, Havighurst TC, et al. Her-2/neu overexpression and response to oophorectomy plus tamoxifen adjuvant therapy in estrogen receptor-positive premenopausal women with operable breast cancer. *J Clin Oncol.*2003;21:453-457.

150. Nahta R, Hortobagyi GN, Esteva FJ. Growth factor receptors in breast cancer: potential for therapeutic intervention. *Oncologist.*2003;8:5-17.

151. Wolff AC, Hammond EH, Schwartz JN, Hagerty KI, DC A. American Society of Clinical Oncology/College of American Pathologists guideline recommendations for human epidermal growth factor receptor 2 testing in breast cancer. *J Clin Oncol.*2007;25.:118-145.

152. Costantini DL, Chan C, Cai Z, Vallis KA, Reilly RM. (111)In-labeled trastuzumab (Herceptin) modified with nuclear localization sequences (NLS): an Auger electron-emitting radiotherapeutic agent for HER2/neu-amplified breast cancer. *J Nucl Med.*2007;48:1357-1368.

153. O'Donoghue JA, Wheldon TE. Targeted radiotherapy using Auger electron emitters. *Phys Med Biol.*1996;41:1973-1992.

154. Spittle MF. Methotrexate and radiation. *Int J Radiat Oncol Biol Phys.*1978;4:103-107.

155. Allen BG, Johnson M, Marsh AE, Dornfeld KJ. Base excision repair of both uracil and oxidatively damaged bases contribute to thymidine deprivation-induced radiosensitization. *Int J Radiat Oncol Biol Phys.*2006;65:1544-1552.

156. du Manoir JM, Francia G, Man S, et al. Strategies for delaying or treating in vivo acquired resistance to trastuzumab in human breast cancer xenografts. *Clin Cancer Res.*2006;12:904-916.

157. Li JC, Kaminskas E. Accumulation of DNA strand breaks and methotrexate cytotoxicity. *Proc Natl Acad Sci U S A.*1984;81:5694-5698.

158. Lawrence TS, Chang EY, Hahn TM, Hertel LW, Shewach DS. Radiosensitization of pancreatic cancer cells by 2',2'-difluoro-2'-deoxycytidine. *Int J Radiat Oncol Biol Phys.*1996;34:867-872.

159. Worm J, Kirkin AF, Dzhandzhugazyan KN, Guldberg P. Methylation-dependent silencing of the reduced folate carrier gene in inherently methotrexate-resistant human breast cancer cells. *J Biol Chem.*2001;276:39990-40000.

160. Nahta R, Takahashi T, Ueno NT, Hung MC, Esteva FJ. P27(kip1) down-regulation is associated with trastuzumab resistance in breast cancer cells. *Cancer Res.*2004;64:3981-3986.

161. Yu D, Liu B, Jing T, et al. Overexpression of both p185c-erbB2 and p170mdr-1 renders breast cancer cells highly resistant to taxol. *Oncogene.*1998;16:2087-2094.

162. Kersemans V, Cornelissen B, Minden MD, Brandwein J, RM R. Drug-resistant acute myeloid leukemia (AML) cells and primary AML specimens are killed by 111In-anti-CD33 monoclonal antibodies modified with nuclear localizing sequences. *J Nucl Med.*2007:in press.

163. Orlando L, Cardillo A, Ghisini R, et al. Trastuzumab in combination with metronomic cyclophosphamide and methotrexate in patients with HER-2 positive metastatic breast cancer. *BMC Cancer.*2006;6:225.

164. Shewach DS, Lawrence TS. Antimetabolite radiosensitizers. *J Clin Oncol.*2007;25:4043-4050.

165. Wong JY. Systemic targeted radionuclide therapy: potential new areas. *Int J Radiat Oncol Biol Phys.*2006;66:S74-82.

166. Costantini DL, Bateman K, McLarty K, Vallis KA, Reilly RM. Trastuzumab-Resistant Breast Cancer Cells Remain Sensitive to the Auger Electron-Emitting Radiotherapeutic Agent 111In-NLS-Trastuzumab and Are Radiosensitized by Methotrexate. *J Nucl Med.*2008;49:1498-1505.

167. Rao DV, Howell RW. Time-dose-fractionation in radioimmunotherapy: implications for selecting radionuclides. *J Nucl Med.*1993;34:1801-1810.

168. Buhring HJ, Sures I, Jallal B, et al. The receptor tyrosine kinase p185HER2 is expressed on a subset of B-lymphoid blasts from patients with acute lymphoblastic leukemia and chronic myelogenous leukemia. *Blood.*1995;86:1916-1923.

169. McLarty K, Cornelissen B, Scollard DA, Done SJ, Chun K, Reilly RM. Associations between the uptake of (111)In-DTPA-trastuzumab, HER2 density and response to trastuzumab (Herceptin) in athymic mice bearing subcutaneous human tumour xenografts. *Eur J Nucl Med Mol Imaging.*2008.

170. Giaccone G, Linn SC, Pinedo HM. Multidrug resistance in breast cancer: mechanisms, strategies. *Eur J Cancer.*1995;31A Suppl 7:S15-17.

171. Pauletti G, Dandekar S, Rong H, et al. Assessment of methods for tissue-based detection of the HER-2/neu alteration in human breast cancer: a direct comparison of fluorescence in situ hybridization and immunohistochemistry. *J Clin Oncol.*2000;18:3651-3664.

172. Olfert ED, Cross BM, McWilliam AA, eds. *Guide to the Care and Use of Experimental Animals*. Canadian Council on Animal Care; 1993:173-176.

173. Herceptin ® (trastuzumab) [package insert]. South San Francisco, CA: Genentec, Inc.; 2000.

174. Goodwin DA, Meares CF, McTigue M, McCall MJ, Chaovapong W. Metal decomposition rates of 111In-DTPA and EDTA conjugates of monoclonal antibodies in vivo. *Nuclear medicine communications.*1986;7:831-838.

175. Mello AM, Pauwels EK, Cleton FJ. Radioimmunotherapy: no news from the newcomer. *J Cancer Res Clin Oncol.*1994;120:121-130.

176. Wilson AM, Bianco JA, Stallman DJ. Tumor. In: Wilson AM, ed. *Textbook of Nuclear Medicine*. Philadelphia: Lippincott-Raven Publishers; 1998:211-238.

177. Adelstein SJ. Merrill C. Sosman Lecture. The Auger process: a therapeutic promise? *AJR Am J Roentgenol.*1993;160:707-713.

178. Kassis AI. Cancer therapy with Auger electrons: are we almost there? *J Nucl Med.*2003;44:1479-1481.

179. Stewart M. Molecular mechanism of the nuclear protein import cycle. *Nat Rev Mol Cell Biol.*2007;8:195-208.

180. Bulmus V, Woodward M, Lin L, Murthy N, Stayton P, Hoffman A. A new pH-responsive and glutathione-reactive, endosomal membrane-disruptive polymeric carrier for intracellular delivery of biomolecular drugs. *J Control Release.*2003;93:105-120.

181. Gilyazova DG, Rosenkranz AA, Gulak PV, et al. Targeting cancer cells by novel engineered modular transporters. *Cancer Res.*2006;66:10534-10540.

182. Takahashi A, Matsumoto H, Nagayama K, et al. Evidence for the involvement of double-strand breaks in heat-induced cell killing. *Cancer Res.*2004;64:8839-8845.

183. Boyd M, Ross SC, Dorrens J, et al. Radiation-induced biologic bystander effect elicited in vitro by targeted radiopharmaceuticals labeled with alpha-, beta-, and auger electron-emitting radionuclides. *J Nucl Med.*2006;47:1007-1015.

184. Xue LY, Butler NJ, Makrigiorgos GM, Adelstein SJ, Kassis AI. Bystander effect produced by radiolabeled tumor cells in vivo. *Proc Natl Acad Sci U S A.*2002;99:13765-13770.

185. Shewach DS, Hahn TM, Chang E, Hertel LW, Lawrence TS. Metabolism of 2',2'-difluoro-2'-deoxycytidine and radiation sensitization of human colon carcinoma cells. *Cancer Res.*1994;54:3218-3223.

186. Tapia C, Savic S, Wagner U, et al. HER2 gene status in primary breast cancers and matched distant metastases. *Breast Cancer Res.*2007;9:R31.

187. Reilly RM, Scollard DA, Wang J, et al. A kit formulated under good manufacturing practices for labeling human epidermal growth factor with 111In for radiotherapeutic applications. *J Nucl Med.*2004;45:701-708.

188. Liang K, Lu Y, Jin W, Ang KK, Milas L, Fan Z. Sensitization of breast cancer cells to radiation by trastuzumab. *Mol Cancer Ther.*2003;2:1113-1120.

189. Vermes I, Haanen C, Steffens-Nakken H, Reutelingsperger C. A novel assay for apoptosis. Flow cytometric detection of phosphatidylserine expression on early apoptotic cells using fluorescein labelled Annexin V. *J Immunol Methods.*1995;184:39-51.

190. Juweid ME, Cheson BD. Positron-emission tomography and assessment of cancer therapy. *N Engl J Med.*2006;354:496-507.

191. Lavayssiere R, Cabee AE, Filmont JE. Positron Emission Tomography (PET) and breast cancer in clinical practice. *European journal of radiology.*2008.

192. Joyce JM, Degirmenci B, Jacobs S, McCook B, Avril N. FDG PET CT assessment of treatment response after yttrium-90 ibritumomab tiuxetan radioimmunotherapy. *Clinical nuclear medicine.*2005;30:564-568.